AGGREGATION INHIBITION OF PARKINSON'S RELATED ALPHA-SYNUCLEIN THROUGH INTERACTIONS WITH ITS HOMOLOG BETA-SYNUCLEIN.

By

MARIA K. JANOWSKA

A dissertation submitted to the

Graduate School of New Brunswick

Rutgers, the State University of New Jersey

In partial fulfillment of the requirements

For the degree of

Doctor of Philosophy

Graduate Program in Chemistry and Chemical Biology

And

Graduate Program in Computational Biology and Molecular Biophysics

Written under the direction of

Prof. Jean Baum

And approved by

_____

_____

_____

_____

New Brunswick, New Jersey

October, 2015

ABSTRACT OF THE DISSERTATION

AGGREGATION INHIBITION OF PARKINSON'S RELATED ALPHA-SYNUCLEIN THROUGH INTERACTIONS WITH ITS HOMOLOG BETA-SYNUCLEIN.

by MARIA K. JANOWSKA

Dissertation Director:

Jean Baum Ph.D

Alpha-synuclein (αS) and beta-synuclein (βS) are small pre-synaptic, neuronal proteins, which have high sequence similarity, co-localize and very likely play a similar function in cells. However, αS and βS differ significantly in terms of their involvement in Parkinson's disease: while αS aggregation is believed to be a centerpiece and main hallmark of the disease, non-fibrillar βS is held to be a negative regulator of αS toxicity. In my research I focused on uncovering the basis for the non-aggregating properties of βS and understanding the basis of inhibition of αS aggregation by βS.

In my research I used integrated biophysical approach primarily focusing on NMR with compliments from CD, DLS, ESI-MS, aggregation assays, cell toxicity assays, chromatography and TEM. Using paramagnetic relaxation enhancement (PRE) I was able to obtain the first ever contact maps for alpha synuclein transient dimers. A similar approach enabled me to discriminate between interactions of alpha synuclein homo-dimers and alpha/beta hetero-dimers which shed light on the

interactivity profiles of alpha and beta synuclein. PRE titrations further revealed additional differences in the interactive propensities of these two proteins, that possibly give rise to the differences in aggregation rates. Thus, I was able to provide an initial answer to the first question: beta synuclein can inhibit alpha synuclein aggregation through specific weak interactions that can slow down formation of the aggregation prone complexes. I also sought to extend the knowledge about the inhibition of αS aggregation by βS by characterizing inhibition events at the later stages of aggregation that involve higher order species such as oligomers.

I further investigated the molecular determinants of P123H, a beta synuclein mutant that switches beta synuclein from being a non-toxic to a toxic species. I discovered that the mutation in the C-terminus induces a conformational change in the P123H ensemble that leads to a collapse of the C-terminus. It is especially interesting that this one mutation can exacerbate the effect of alpha synuclein aggregation, suggesting again that the extension of the synuclein C-terminus plays an important regulatory role in aggregation and inhibition. Coupled together these facts suggest that beta-synuclein's conformational characteristics make it particularly well-suited to inhibit alpha synuclein aggregation, which in turn provides a good candidate platform for developing inhibitors of alpha synuclein aggregation.

Acknowledgements

I am very grateful to many people without whom I would not be who I am today and who helped me get to the point in life I am at right now. The Ph.D. and events that brought me here constitute an amazing mixture of coincidences and small everyday miracles coupled with the wonderful people who God put on my path that helped shape the person I am now.

First of all I would like to thank my Parents for theirs love and theirs support, for letting me learn from my own mistakes and for teaching me responsibility and honesty, for believing in me and also sometimes doubting that I could fight hard enough to get what I wanted. I would like to thank my siblings Krystian, Magda, Andrzej, Michal, Krzysiek and Faustyna: you are the best teachers of life one could imagine. I still recall the adventures we had together, and the way everything was new and fun. I would like also to thank all my family: my grandparents, uncles, aunts, cousins for being there for me and for giving me the support I needed.

I would like to deeply thank my acquired family: my second Mother and Father, for accepting me without reservation, for the time you took to create a friendship with me and for always being there for me if I needed something, for the support you gave me when I arrived to in a foreign land. I am touched to the core that I was so blessed to have you here.

The next round of gratitude goes to my girlfriends Basia Kwiecien and Dominika Slowak. Girls, because of you I know what friendship is about. We can be apart for a long, long time, but we never stop being kindred spirits.

I would like to thank my teachers from the middle school and high school who helped me to understand the basics and much more! Special thanks to Mrs. Szymanska, Mrs. Kaminska, Mr. Mazurkiewicz, Mrs. Czarnecka: you were great science and math teachers but that was not all that you tought me.

I also want to express my gratitude to the Biophysics program at the Faculty of Biochemistry, Biophysics and Biotechnology at Jagiellonian University in Krakow, which together

with the Faculties of Physics, of Mathematics and of Chemistry provided me with an excellent basis for my Ph.D. studies. My thanks go to all the professors who taught me biophysics, who enkindled in me a fascination with the subject and complexity of the systems in the living cell , who thought us that it is not possible to understand Life without a thorough and broad understanding of all Science. Special thanks go to the excellent professors: Ewa Gudowska-Nowak, Malgorzata Dutka, Hubert Harańczyk, Halina Gabryś, Marta Pasenkiewicz-Gierula, Marta Dziedzicka-Wasylewska, Krzysztof Lewiński and Grzegorz Lewicki. Thanks to the Faculty of Biophysics would not be complete without thanking the wonderful secretaries who made studying much easier and bearable: Mrs. Janina Mrugalska, Mrs. Malgorzata Calikowska and Mrs. Dorota Zołnierczyk.

To my friends who majored in biophysics with me: who was not there, will never understand, as the degree was very demanding. For the friendships forged in those hard times ☺ Thank you all with special thanks to Kasia Pogoda and Dominika Żurek.

My Master thesis advisor Prof. Jerzy Dobrucki and his laboratory provided me with knowledge about cell cultures, microscopy and many other things. I would like to thank Dr. Dobrucki for being an excellent example of scientific integrity and hard work that leads to a profound understanding of the subject of study. I would like to thank also the members of the Cellular Biophysics lab Mirek Zarębski, Dominika Trembecka-Lucas, Kasia Kędziora, Mateusz Kuzak, and all the great people in the lab!

I would like to thank my Master thesis co-advisor Dr. Bojan Zagrovic for allowing me to work on a project I chose for myself. Working on molecular dynamics in your laboratory was great fun! Even despite the fact that we were in Split,Croatia where we could just jump in the sea whenever we got overwhelmed with work. Thank you for your enthusiasm that started my fascination with research. I would like to also thank all the people I met working in Bojan's lab that made it great not only from the scientific point of view but also for the great and fun working environment to be in. Thank you Rita, Antonija, Anton, Drazen, Ruben, Mario and Daniela.

Over the course of the last 5 years I learned many new things, and I am grateful to the many people who walked this path with me. Teachers of science, lab mates and coworkers: Dr. Seho Kim, Dr. Nagarajan Murali (NMR), Dr. Lijuan Kang (synuclein handling), Dr. Run Yan (cell toxicity), Dr. Avanish Parmar and Kenneth McGuinness (CD and DLS), Gina Moriarty (lab awareness and chemical thinking), Ana Monica Nunes (lab work). I also thank Mike Olson, Snow Yang and Neha Sikka on whom I could practice my mentoring skills! I hope you survived, and that it was not so bad. I thank also all the other members of the Baum lab that I had the pleasure to work with.

I thank my committee members, for their advice and helpfulness throughout my Ph.D. program: Prof. Maral Mouradian, Prof. David Case, Prof. Stephen Burley and Prof. Darrin York. It is an honor for me to have you on my committee.

Special thanks go to my advisor, Prof. Jean Baum, for mentoring me throughout these years. For teaching me how to express science in more basic terms, for allowing me to work on the projects of my own choosing, and for supporting me in them, which helped me , at least to some extent, answer the question of why βS does not aggregate and inhibits αS aggregation.

Lastly I thank my husband. Paweł, I do not have the words to express my gratitude for supporting me throughout these years, for believing in me and for constantly trying to convince me that I should not work too much! It was great journey. I am very happy we walked it together.

Table of Contents

List of Figures

List of tables

Abbreviations

AD, Alzheimer Disease;

αS, α-synuclein;

Ac-αS, Acetylated α-synuclein;

βS, β-synuclein

Ac- βS, Acetylated β-synuclein;

γS, gamma synuclein;

BOG, beta-octyl glucopyranoside;

CD, circular dichroism;

CN-PAGE, clear native PAGE;

DLB, Diffuse Lewy Body Disease, or Dementia with Lewy Bodies;

DLS, dynamic light scattering

DTT,,Dithiothreitol;

ELISA, enzyme-linked immunosorbent assay;

ESI-MS, Electrospray ionization mass spectrometry;

GST, glutathione S-transferase;

HSQC, Heteronuclear single quantum coherence spectroscopy;

HX, hydrogen exchange

IDP, intrinsically disordered protein;

KO, knock-out;

LB, Luria broth

MTSL, S-(1-oxyl-2,2,5,5-tetramethyl-2,5-dihydro-1H-pyrrol-3-yl)methyl methanesulfonothioate);

mRNA, messenger RNA;

NAC, non-amyloid component region;

Nat, N-acetyltransferase;

NatB, N-acetyltransferase B;

NMR, nuclear magnetic resonance;

NOE, Nuclear Overhauser effect

PTM, post-translational modifications;

PBS, Phosphate buffer saline;

PD, Parkinson's disease;

PFA, Paraformaldehyde

PPII, Polyproline II;

PRE, paramagnetic relaxation enhancement;

RBC, red blood cells;

RDC, Residual dipolar coupling;

SE-AUC, sedimentation equilibrium-analytical ultracentrifugation; ;

SEC, Size exclusion chromatography;

SLS, static light scattering;

SSP, secondary structure propensities;

ThT, Thioflavin T

tg, transgenic;

wt, wild type;;

Chapter 1. Introduction

My PhD research has focused on uncovering the basis for the inhibition of alpha synuclein (αS) aggregation by its homolog beta synuclein (βS). Alpha synuclein is an abundant neuronal protein whose aggregation constitutes the hallmark of Parkinson's disease. Despite high sequence similarity between alpha and beta synuclein, only alpha synuclein aggregates readily, while beta synuclein is fibrillation resistant and able to inhibit aggregation of alpha synuclein both *in vivo* and *in vitro*. Both proteins belong to the class of intrinsically disordered proteins. Thus, previous efforts to uncover their aggregation tendencies had proved challenging. In my research I aimed to answer two main questions:

1. How is beta synuclein able to inhibit alpha synuclein aggregation?
2. What are the molecular determinants of beta synuclein that contribute to its non-fibrillogenic nature?

As the problem is highly complex I will focus on its various aspects in the introduction. This background section is divided into two main parts: the first part focuses on the importance of αS and its involvement in Parkinson's disease, and the second part characterizes βS and its influence on αS aggregation.

1.1. Background: Role of alpha synuclein conformations in disease

1.1.1. Paper citation information

Chapter 1.1 was published as review paper in the special issue "The Many faces of proteins" of the FEBS Journal.[2] I was a second author on the paper, and I partially wrote and edited the paper. Paper

citation: Moriarty, G. M., Janowska, M. K., Kang, L. J. & Baum, J. (2013). Exploring the accessible conformations of N-terminal acetylated alpha-synuclein. *Febs Letters* **587**, 1128-1138; PMC Journal.

1.1.2. General considerations about αS.

Alpha synuclein (αS) fibrils are found in the Lewy Bodies of patients with Parkinson's disease (PD). It is believed that the transition from the native state to the highly ordered fibrils can be one of the causes of PD. Recently, the view of the native state of αS as a monomeric ensemble was challenged by a report suggesting that αS exists in its native state as a helical tetramer. This review reports on our current understanding of αS within the context of these recent developments and describes the work performed by a number of groups to address the monomer/tetramer debate. A number of in depth studies have subsequently shown that both non-acetylated and acetylated αS purified under mild conditions are primarily monomer. A description of the accessible states of acetylated αS monomer and the ability of αS to self-associate is explored.

Parkinson's disease (PD) research has sought to answer questions of alpha synuclein (αS) function and the mechanism of aggregation surrounding disease pathology. Both remain to be fully articulated today, but several observations have been established and a range of neurodegenerative diseases termed the "synucleinopathies" have been identified[3,4]. PD in particular is the synucleinopathy characterized by the loss of dopaminergic neurons and is largely considered to be an age-related disease, accompanied in part by age-related deposition of αS[5]. αS, a major protein component of Lewy Bodies[6,7] in patients with Parkinson's, is a small primarily neuronal protein that is known to make a structural transition to amyloid fibrils[8-10]. αS is expressed abundantly in the nervous system and localizes near presynaptic nerve terminals[11-15]. It is also expressed at high levels in erythrocytes and platelets[16]. αS's function is unknown, but there is strong evidence that it exhibits lipid binding in vesicles and synaptic membranes[17] and may somehow exert its pathology through this behavior[18]. There is evidence that αS functions in assembly of the SNARE complex involved in

vesicle transport[19], that it may more generally be involved in synaptic vesicle trafficking and regulation and/or may play a key role in neuronal cell survival[20-24].

The deposition of αS has largely been thought to originate from an intrinsically disordered monomer ensemble that under fibril promoting conditions forms amyloid [9,25,26], but recently the position was challenged[27]. Selkoe and colleagues pushed the biophysical community's long-held view of the native intrinsic disorder of αS by suggesting that the protein exists in its native state as a fibril resistant helical tetramer. They purified the sample from human erythrocytes, opting to exclude a potentially "harsh" and commonly used boiling step from the purification. Based on this work several questions presented themselves. Do bacterial systems that are commonly used to obtain sample for biophysical characterization not possess the necessary machinery for tetramer assembly? Could the commonly used boiling step during purification denature some key native structure that promoted a helical tetramer of αS? Aside from these assembly and purification issues, there was also one molecular difference between the purified samples of Selkoe and colleagues and previous studies, indicative of modification to the monomer by an acetyl group (Ac-αS).

This review reports on our current understanding of αS within the context of these recent developments and describes the work performed by a number of groups to address the monomer/tetramer debate[27-35] (Figure 1). Numerous studies have addressed these issues and indicate that αS, both acetylated and non-acetylated, exists as intrinsically disordered monomer conformational ensemble under mild purification conditions. We highlight that the ensemble of monomers can develop into a wide range of accessible conformations upon changes of environmental conditions, that it can populate many soluble oligomeric states of varying morphologies and toxicities, and settle into various insoluble fibril or amorphous aggregate morphologies[25], that have largely been studied in the context of PD-related pathology (Figure 1). We discuss the suggestion of a soluble fibril resistant helical tetramer that may have to dissociate before fibril formation can proceed through the monomer (Figure 1). The potential that established methods might disrupt native-stabilizing interactions of a fibril-resistant helical tetramer of αS have

heightened awareness to cell machinery, to αS purification methods, and to the difficulties in choosing appropriate methods of characterization. The extent to which N-terminal acetylation

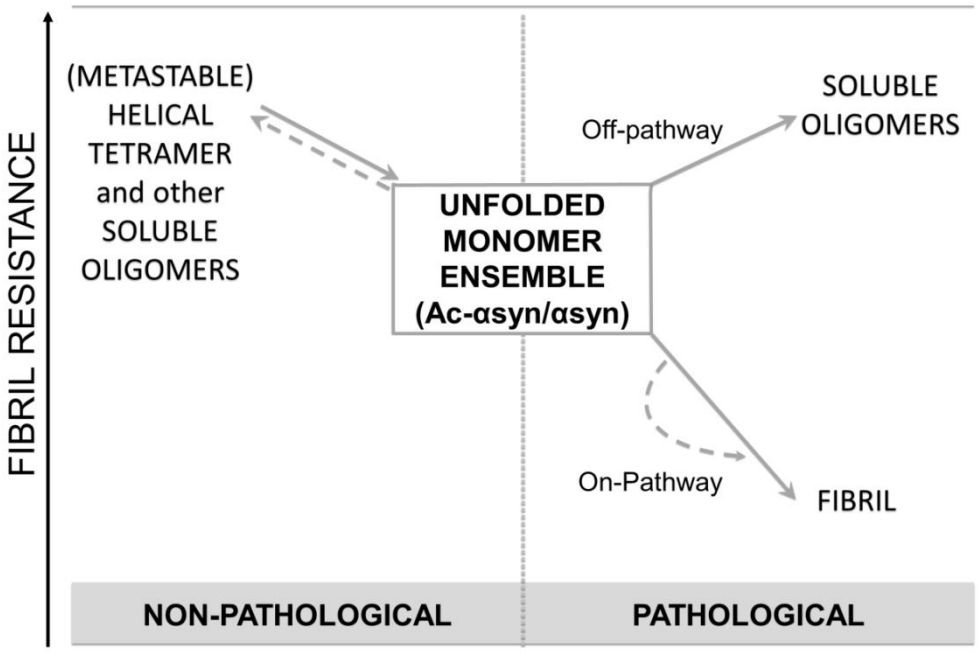

Figure 1 A schematic diagram of the possible accessible states of non-acetylated and acetylated αsyn. The right side represents two possible pathological aggregation pathways from the unfolded monomeric ensemble to 1) insoluble fibrils through on-pathway transient oligomeric intermediates and 2) to off-pathway soluble oligomers. Off-pathway soluble oligomers represent non-fibrillar end products of aggregation. The left side presents 1) the recent proposal that αsyn can exist as a soluble fibril resistant helical tetramer which is acetylated, and 2) other known oligomers that are not toxic such as methionine oxidized oligomers. It is proposed that the non-pathological tetramer needs to dissociate to the monomeric ensemble before pathological aggregation can occur (dark arrow).

impacts upon the conformation and aggregation behavior of αS is discussed separately and it is shown that the acetyl group does not promote the formation of the helical tetramer under mild purification conditions.

1.1.3. Overview of non-acetylated αS ensemble: monomers and dimers

Biophysical characterization of the non-acetylated monomer ensemble.

The native state of non-acetylated αS has been thought to originate from an ensemble of intrinsically disordered monomeric forms, with recognition that the monomers therein are capable of adopting a wide range of accessible conformations depending on solution and environmental conditions [36-40]. Uversky first spoke of αS as the "protein chameleon"[25] due to its ability to respond to its environment and binding partners by varying its foldedness and aggregation state. αS is often described as a 140 residue intrinsically disordered protein (IDP) characterized by three distinct regions of the protein: an N-terminal lipid binding repeat region that houses the mutations A30P, E46K, and A53T linked to early onset disease, a hydrophobic non-amyloid component (NAC) region implicated in fibril formation, and an acidic more proline-rich C-terminus suggested to have chaperone activity and possess some key role in modulating structure in the N-terminus[8,41,42]. As it is summarized in Table 1, to study PD related aggregation, αS has typically been obtained from overexpression in bacteria, yielding a non-acetylated IDP, as bacteria typically do not modify their proteins by acetylation (Figure 2A)[43-45]. Additionally, while boiling as part of the purification protocol would typically be considered to be harsh for a globular protein, IDP's are in general characterized by thermostability[36]. Because of this heat stability, αS has often been boiled to achieve purity. In addition, IDP's like αS are generally characterized by a highly charged sequence, a lack of stable secondary structure, and a larger than expected Stokes radius compared to spherical and folded proteins of the corresponding molecular weight[36,46,47].

The αS monomer is both unfolded and extended, as it was first reported to have a larger Stokes radius than expected for globular protein of similar molecular weight and a primarily random coil circular dichroism (CD) spectrum (Table 1) [36,38,48]. However, the protein is not fully extended for a protein of its size, implying a slight compaction of the monomeric ensemble[38,49]. Evidence for contact between the C-terminus and both the NAC and N-terminal regions of the protein from nuclear magnetic resonance (NMR) [40,50-57], electron paramagnetic resonance[58] and molecular dynamic studies[54,59] indicates a possible source of this compaction, as well as some transient secondary structure[57,60-62]. The compaction may be at least be partially driven by hydrophobic patches located in

the C-terminal (residues 115-119, and 125-129) associating with and shielding both the hydrophobic N-terminal and NAC regions[52,63]. It should be emphasized that evidence for contact between the N- and C- termini does not imply a static closed picture of αS as an IDP[61,64]. Rather, this is a dynamic interaction, and observation of slight compaction is the result of observations on a highly averaged bulk ensemble[50].

Under conditions promoting pathological aggregation of αS, conformational shifts in the ensemble are observed. There is evidence that these interactions may keep the N-terminus from pathological misfolding[41,65], as their release is associated with increased fibril formation [40,52,54,66,67]. For example, when the solution pH is lowered, there is a structural rearrangement of the monomer ensemble with enhanced contacts between the NAC region and the C-terminus resulting from charge neutralization and compaction of the C-terminal region[40,56,60,68]. Environmental or experimental shifts that reduce the net charge or increase hydrophobicity of the protein [69-71], or interaction with small molecules or metal ions[72-74] can change subtly, but significantly, both the long-range and short range contacts and conformations sampled in the monomeric ensemble (Figure 1).

Therefore, small changes to the αS monomer can potentiate big effects on aggregation behavior, yet only small differences to the monomer ensemble. For example, the familial mutations (A30P, E46K,A53T) of αS are structurally comparable, as they are similarly unfolded and have similar radii of gyration, but they have distinct kinetics of fibril formation[57,75-81]. NMR spectroscopy has revealed that mutations affect chemical shifts surrounding the mutation site and that we can correlate these shifts to region-specific shifts in the population of transient secondary structure. These relatively small shifts in transient secondary structure populations can explain bulk differences in fibril formation rates[61,82,83].

The N-terminal region is also known to adopt helical structure upon binding lipids, representing a more dramatic conformational shift of the monomer ensemble[84-86]. NMR groups have demonstrated that αS displays chemical shifts characteristic of a mostly unfolded peptide, but that the first 100 residues transiently populate helical structure. When bound to lipids or micelles,

however, chemical shifts of these residues indicate a structured helical environment.[87,88]. Bax characterized the structure of the micelle bound form of the protein, and the fact that αS adopts helical structure at its N-termini through its repeat region upon binding lipids membranes and micelles has become a well-known fact[84]. Because αS localizes near synaptic nerve termini[11], its lipid-induced helical structure[37,89-91] may be crucial in understanding the protein's function at the membrane, yet it is still unknown how this N-terminally helical monomer conformation is related to the trigger of fibril formation.

Dimers: equilibrium species and pathological intermediates.

Dimers can exist in pseudo-equilibrium within the monomer ensemble and also as on-pathway intermediates to the fibril. Within the monomeric conformational ensemble of non-acetylated αS, there exists some small population of dimer. The Baum lab demonstrated that indeed antiparallel transient inter-chain contacts between the C-terminal hydrophobic patches and the N-terminal region (residues: 3-15 and 35-50) could be detected by using NMR paramagnetic relaxation enhancement experiments[56]. Electrospray ionization mass spectrometry (ESI-MS) obtained under similar conditions has shown that the predominant oligomeric form we observe in αS is the dimer. This soft ionization technique has revealed the "conformational heterogeneity" of αS, where the monomers and dimers themselves exist in both extended and compact conformations[32,92,93], suggesting that the ensemble view of αS also extends into its higher oligomeric states.

It is unknown whether this pseudo-equilibrium anti-parallel dimer is on pathway to the fibril formation. It is reasonable to assume that inter-chain N-N species, which adopts the same parallel orientation as monomer units as in the core of the fibril, lies further along the pathway to fibril formation than anti-parallel oriented monomers[94]. This would imply reorientation of monomer units as an obligatory step before formation of the fibril. However, at least one report demonstrates that toxic prefibrillar amyloid aggregates adopt an antiparallel orientation[95], and in this sense we cannot draw any analogy to this pseudo-equilibrium dimer population that exists in the fibril accessible monomer ensemble.

As the monomeric ensemble is shifted towards more fibril prone conditions, previously described conformational changes, as well as changes in population of oligomeric species occurs. Incubation at high temperature is one external factor inducing this shift[96]. Under these conditions, soluble oligomers of αS spontaneously associate and a dimer is the predominant oligomeric species of αS to appear alongside formation of the fibril, along with smaller populations of higher-order oligomers. Biophysical characterization of this partially folded intermediate is consistent with a partially folded monomer and pre-molten globule like dimer, that is slightly less ordered and has more hydrophobic patches exposed than the native monomer[38]. This on-pathway dimer that appears at the time of fibril formation may be conformationally dissimilar from the equilibrium dimer population previously described, which is not necessarily correlated with fibril formation. There is some evidence that formation of at least one species of dimer is the rate limiting step of fibril formation[97] and cysteine mutants have shown that particular dimer linkages accelerate fibril formation *in vivo* and *in vitro*[97]. This implies accessibility of many distinct conformations for the dimer, in the same way as the monomer. Additionally, dimers are not the sole on-pathway oligomeric species that appear during events of PD pathology. Observations of higher order oligomers, that occur alongside fibril formation and in response to other events appear to include a large slew of different species, which we address in the upcoming section.

1.1.4. Heterogeneity of the αS oligomeric structures and their pathogenicity.

The role of oligomers in *in vivo* pathology.

The motivation to understand whether there is a helical tetramer of Ac-αS lies not only in desire to accurately portray the protein *in vivo*, but also to understand how oligomers in particular function in disease-related pathology of PD. There is ample evidence that soluble oligomers are the real pathogenic species of neurodegenerative disease, whereas fibrils serve as reservoirs of misfolded, irreversibly modified deposited protein better-off removed from solution[98-105]. Because amyloid deposits were first detected in brains of sick individuals, it was assumed that they were the neurotoxic

species, but because amyloid is such a common structural motif, the ability to form amyloid is now considered a general property of a polypeptide in solution[106]. Over and over, conversion of IDPs into amyloid aggregates has not been observed to be a simple two-state transition. Oligomer formation has been established as an important mechanistic step in fibril formation, for example as in Alzheimer's disease[104,107]. As briefly described in αS, soluble oligomeric intermediates commonly appear as insoluble fibrils form[108-110] and the situation may be quite similar to that established for AD.

What determines if a protein will form soluble oligomeric species, or if an amyloid fibril will form? It seems that a polypeptide will sample many parallel or antiparallel conformations before a final structural state is preferred[111]. This arises from a competition between hydrophobic forces and side chain interactions, versus the propensity of the polypeptide chain to form β-sheet like hydrogen bonds[112]. The prefibrillar oligomer is thought to be the cytotoxic species, as toxic inter-chain associations are sampled that a monomer alone could not support. The fluorescent probe 8-anilinonaphthalene-1-sulfonic acid binds to exposed hydrophobic patches. Its binding demonstrates that the most toxic species are associated with greater overall surface hydrophobicity[96,113-115]. In fact, overall greater hydrophobicity is associated with increased chance for exposed hydrophobic portions of the sequence to exhibit toxicity through interaction with the membrane. This may as well be the case for αS [114,116].

Oligomeric PD pathology may be rooted in membrane association, where oligomers of αS can perturb membrane integrity and cause cell death by altering transport across the membrane [117-120]. At least one report demonstrates that *in vivo* membrane associated αS oligomers correlate with toxicity rather than inclusion formation[121] but also that the degree of oligomer toxicity is related to an array of structurally diverse morphologies that can form. Interestingly, of the familial mutants implicated in PD, A30P and A53T have different kinetics of fibril formation relative to the wild type monomer, but both share the property of an accelerated oligomerization[122,123]. These mutants may

exert their pathology through the formation of pore-like oligomers that form alongside fibril formation[124].

Oligomers on the aggregation pathway are highly heterogeneous.

Early "prefibrillar" oligomers and "late" soluble oligomers, not a part of the fibril have been observed of αS[109,125] Their isolation and structural characterization has been of great interest, and some shared features of fibril accelerating or inhibiting species have been characterized. It was postulated that an on-pathway amyloidogenic transition occurs through partially folded oligomeric species originating in the dimer[38]. Soluble aggregates first appear that maintain the helical character of the monomer, but lose some disorder in favor of β-rich structure. β-rich intermediates build as fibril formation proceeds and begin to get consumed at the end of the lag phase[109,113]. This may describe the formation of initial aggregates and their conversion into amyloid-like aggregates, described by Dobson and colleagues using FRET[108]. AFM has been used to observe β-rich spherical and annular oligomer morphologies prior to fibril formation of αS. The initial aggregates appear to be spherical aggregates. They have been shown to convert to more spherical compact species, and then into annular species upon further incubation[126]. Annular species of αS are known to induce membrane leakage[105,127], but spheroidal species can bind brain-derived membranes quite tightly, as well[126]. Spherical morphologies seem to disappear once the fibril has formed, whereas annular species may sometimes coexist with the fibril[126]. Oligomer induced toxicity is relevant to the entire fibril process.

Many times stable oligomers are observed after the fibril has formed, or are instead preferred. "Late" stage distinct oligomeric species appear once fibrils have formed and they are also β-rich [110,113,125,128]. Some suggest they occur from dissociation of the fibril or that they represent end-products of a fibril resistant-soluble oligomerization pathway and may not be converted into fibril. At the end of fibril formation 10-20% of protein exists as such a non-fibrillar oligomer.

There are many pathways refer to soluble species. Organic solvents have been used to model membranes, and it has been shown that a helical rich monomer will eventually associate into a

helical rich oligomer that also appears stable [129]. Covalently cross-linked non-fibrillar oligomers are also well known to form under oxidative or nitrative stresses. Nitration, for example, inhibits fibril formation through the formation of inhibitory higher-order oligomers than the dimer [130]. This mix of species only further describes the range of the secondary structures, morphologies and pathologies that oligomers of αS are capable of populating[94,96,131-133]. Increased oxidative stresses and increased metal levels have been correlated with PD, so this class of stable non-fibrillar oligomers that form under stresses are potentially important players in the mechanism of aggregation as well[134].

Various pathways available to soluble oligomer, not surprisingly results in a very heterogeneous population of possible oligomers. Oligomer morphology has been shown to be highly dependent on solution conditions, including the presence of lipids[126,135-138]. Also, incubation with different types of metals generates partially folded structures[139-141] that go on to form a variety of oligomeric structures. Whereas incubation with $Cu^{2+}/Fe^{3+}/Ni^{2+}$ produce spherical particles of 0.8-4 nm particles, incubation with Co^{2+}/Ca^{2+} produces pore-like annular rings 70-90 nm in diameter[142].

Stabilization of non-fibrillar oligomers that appear to be non-pathogenic.

In previous paragraphs our focus was on oligomers more closely linked to pathology, but as mentioned, some oligomers can be stabilized in non-fibrillar forms not capable of adopting cross-β structure on their own and may not necessarily be linked to cytotoxicity (Figure 1). The αS monomer that has been modified by methionine oxidation of the αS monomer to the sulfoxides is one example of these non-toxic non-fibrillar species. This modification at methionine residues promotes the stabilization of an oligomer that appears slightly more unfolded than monomeric αS. While probably not covalently cross-linked, these oligomers exhibit stability and do not go on to form fibrils[143-145]. Furthermore, these oligomers do not exhibit toxicity toward dopaminergic neurons, suggesting that particular conformational features are indeed necessary to exert pathology as an oligomer (Figure 1)[145]. Interaction with small molecules like the flavonoid baicalein can also prevent formation of the fibril by stabilizing soluble oligomeric end products and these oligomers also do not disrupt membranes[146]. Structurally these species are spherical, have a well developed secondary structure, are

relatively globular with a packing density intermediate between globular protein and pre-molten globule and very high thermodynamic stability. In contrast oligomers stabilized by modification of the monomer with 4-hydroxy-nonenal are non-fibrillar, but are also toxic[146]. Could a helical tetramer be similarly stabilized, such that the stabilization in the oligomer conformation is more favorable than in amyloid, and could it also share conformational features of non-pathology with aforementioned species? For example, in amyloid-β two oligomers of similar size but dissimilar toxicity have been identified, where more toxic species adopts a conformation that hydrophobic regions to remain more exposed(Ladiwala2012).

1.1.5. αS is N-terminally acetylated in vivo.

Before attention was drawn to the possible role of the acetyl group by the recent report[27] of tetramer formation of αS, αS was studied from a variety of sources, some of which were mammalian and were likely to be N-terminally acetylated. Although the acetyl group had not previously warranted an explicit examination, drawing comparisons between in-cell work *and in vitro* work could be challenging. Therefore, the report suggested that co- or post-translational modifications (PTM's), namely acetylation, may have significant influence on αS structure and aggregation properties (Table 1). PTM's to αS are known to regulate/modify αS's propensity to aggregate[133,143,147]. It has been known for some time that αS in human tissues is acetylated, but the role of N-terminal acetylation is unclear, as it is seen in both healthy and individuals sick with synucleinopathies. Two mass spectrometry (MS) studies of αS from human tissues, both report that the base mass of the protein before any other modifications is the acetylated form -- consistent with that reported by Selkoe and colleagues from red blood cells (RBCs)[27,148,149]. The report indicated that acetylation of αS was not limited to neuronal tissue; however, the site of acetylation was not identified.

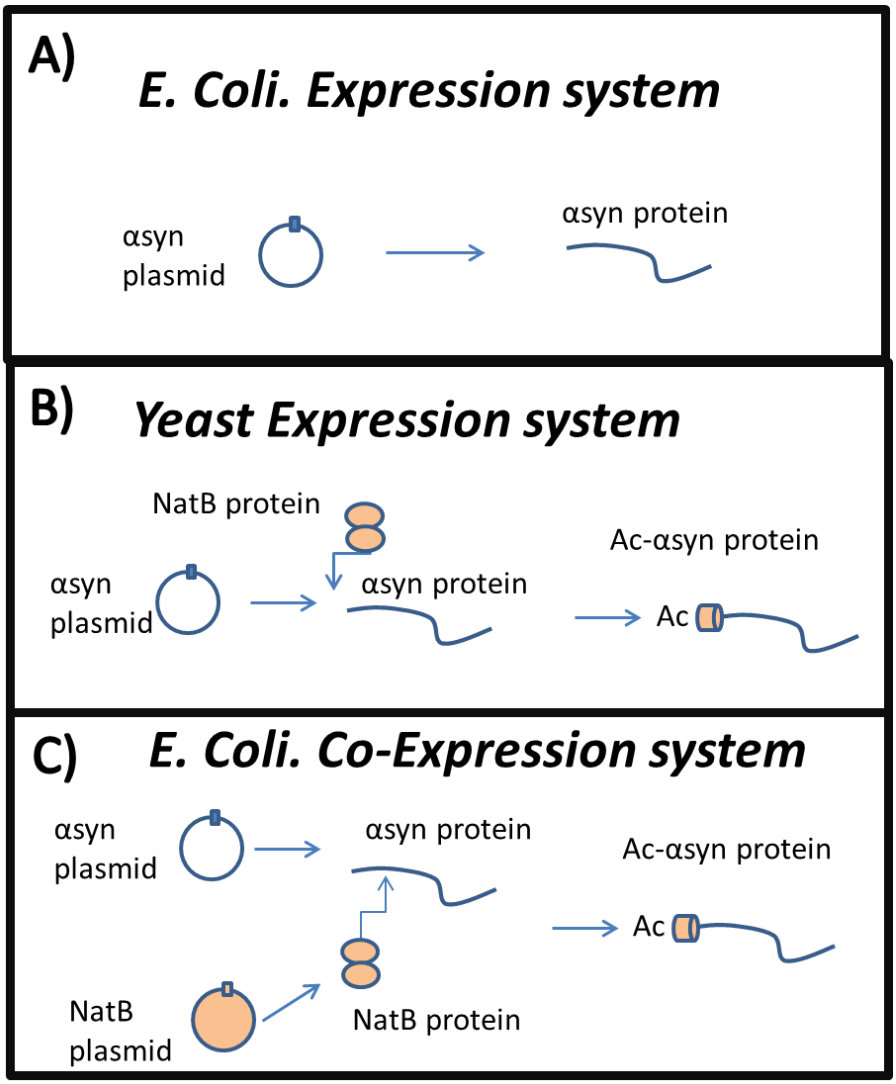

Figure 2 A pictoral representation of the co-expression system designed to generate Ac-αsyn in bacteria. In this figure: ring-like circles represent plasmids, lines represent the αsyn protein, and two ellipses represent the NatB protein. A) Bacteria, lacking NatB, express non-acetylated protein. B) Yeast house yeast-NatB which acts upon αsyn and generates Ac-αsyn. C) To obtain Ac-αsyn within a bacterial expression system, plasmids encoding yeast-NatB can be co-expressed with the plasmid encoding for αsyn so that Ac-αsyn is obtained[1].

Bacteria lack the machinery for N-terminal acetylation.

Mammals modify the proteins they produce with many more PTM's than yeast and bacteria, as these may play a role in more complex signaling pathways[150,151]. N-terminal acetylation is a well-known modification in eukaryotic cells. Up to 80% of proteins are modified by N-terminal acetylation in mammals, whereas bacteria rarely acetylate their N-termini and if they do, by distinctly different mechanisms [45]. The aforementioned MS studies[148,149] indicated that acetylation occurs at the N-terminus, where an acetyl group has removed the α-amino charge of the initiating amino acid by covalent modification at that site.

N-terminal acetylation is carried out mostly co-translationally by a group of enzymes known as N-acetyltransferases (Nat) in eukaryotes[152,153]. Mammalian cells have these complexes, and yeast an analogous enzyme complex, but bacteria do not. Nat's catalyze the transfer of an N-acetyl group from acetyl-coenzyme A to the N-termini of proteins with sequence specificity. Different Nat's (types A-F in eukaryotes) work upon different initiating amino acid substrates, dependent upon the identity of the first two to three amino acids of the protein polypeptide[154]. Therefore, depending on the type of cell to synthesize αS, the protein may or may not be acetylated (Figure 2A, 2B). Specifically, N-acetyltransferase B (NatB) has αS as a substrate, producing acetylated αS (Ac-αS). NatB targets proteins beginning with Met-Asn-, Met-Glu- or as in the case of αS, Met-Asp-. Substrates of NatB are acetylated nearly 100% of the time, as the acidic amino acids in the second position are thought to stimulate the transfer of the acetyl group[151].

Possible roles of N-terminal acetylation *in vivo*

Recognizing that αS acetylation does indeed occur, one study prior to Bartels' *et al.* investigated the role of NatB activity in a yeast model by disrupting NatB activity[155]. They found NatB activity to be essential for proper membrane targeting of αS. Without NatB activity, non-acetylated αS is produced, and a much more diffuse cytoplasmic localization of αS compared to those with whole NatB activity (producing Ac-αS) was observed. While this *in vivo* effect was observed in this one instance for Ac-αS, the role of N-terminal acetylation is not generally well understood[156]. One study suggests that N-terminal acetylation represents an early sorting step, where acetylated

proteins are targeted toward the endoplasmic reticulum, unless they remain non-acetylated and are kept localized to the cytosol instead[157]. N-terminal acetylation may also regulate degradation pathways[158] or be responsible for structural effects at the N-terminus[159]. Levels of acetylation may be related to regulation of other post translational modifications, NatB, specifically, has been shown to induce elevated phosphorylation levels in yeast[160] consistent with the aforementioned yeast study of αS, where decreased levels of phosphorylation are observed when the protein remains non-acetylated and localized in the cytosol[155]. Acetylation may not be necessary at all for proteins, but some examples do point to a necessity. For example, tropomyosin requires N-terminal acetylation so that it may bind to actin[161].

1.1.6. αS is proposed to be a helical tetramer in its native state.

Selkoe and colleagues strived to isolate αS under physiological conditions and have challenged the existence of the αS monomeric ensemble[27] by proposing a fibril resistant helical tetramer form of the protein (Table 1). In contrast to the typical protocol in which αS has been derived from bacterial systems, overexpressed and denatured, they purified αS from gently-treated RBCs known to have a high endogenous expression level of human Ac-αS. From both RBC lysate and endogenously expressed αS from neuronal and non-neuronal cells lines, Selkoe and colleagues showed on Clear Native PAGE (CN-PAGE), that αS migrates near the tetramer position against folded, globular protein standards. The unusual migration of an IDP against globular standards was not unfamiliar. Native gels are unreliable objective determinants of molecular weight as protein migration depends strongly on protein charge and interaction with the acrylamide matrix depending on the shape of the protein. IDP's typically display a Stokes radius of a much higher molecular weight species, and this has previously been attributed to enhanced interactions with the matrix[38], so that *E. coli* derived boiled αS, too, will migrate near the position of the tetramer at 58 kDa on a native gel[27].

Selkoe and colleagues' report also stated that they obtained a CD spectrum that indicated largely helical structure that was sensitive to irreversible heat denaturation. Isolation from human cell

line 3D5 (which are M17D cells stable expressing αS) yielded similar results to RBC derived αS, and they showed that αS derived from *E. coli* was random coil even after non-denaturing purification, consistent with previous reports[43]. Therefore Selkoe and colleagues implied that expression in human cell lines and a non-denaturing purification are necessary to "preserve" this native tetramer structure. If this is indeed the native form of αS, non-denaturing methods of purification and mammalian machinery may be necessary to observe it. When denatured, RBC αS became random coil, and migrated more similarly to *E. coli* derived αS on a native gel, rather than the mildly purified helical sample.

Helical structure of αS can be induced by its interaction with membranes. Therefore, it might logically follow that the milder purification did not fully remove helix inducing lipids. However, treatment with Lipidex and subsequent phosphate analysis indicated the sample was relatively pure in that regard (0.25 mol phosphate/αS monomer). They also employed some unbiased methods of MW determination including sedimentation equilibrium-analytical ultracentrifugation (SE-AUC) and scanning transmission electron microscopy both indicating a tetramer. A higher lipid binding capacity for this native αS was demonstrated with surface plasmon resonance. Bartels *et al.* also observed one other unprecedented trait of the sample – that under standard fibril assay conditions, ThioflavinT (ThT) fluorescence did not indicate that RBC ac-αS formed any fibrils *in vitro* – clearly also in contrast to previously observed results and the *in vivo* condition (Table 1).

Not too long after, Wang *et al.*[136] similarly reported a dynamic tetramer form of the protein. The protein was obtained by recombinant expression methods and was modified by a 10 residue N-terminal tag left over from a glutathione S-transferase (GST) construct, making it difficult to compare directly with the tetramer obtained from RBCs. The purification method was 'non-denaturing' but included the non-physiological detergent beta-octyl glucopyranoside (BOG) typically used to purify membrane bound protein. Perhaps N-terminal acetylation was somehow mimicked by the cleaved GST-tag and would prove to be important in the context of a non-denaturing purification. Researchers now would interpret data in light of a greater possibility of the tetramer,

and more carefully consider their assumption that their expression and purification methods did not preclude an accurate representation of the protein *in vivo*.

Table 1 Historical description of shifts in αS purification approaches and conformational properties

	1996- Dec. 2011	> Dec 2011	> May 2012
Source	**Mostly Bacterial**	**Mammalian**	**Bacterial / Mammalian**
N-terminal acetylation	No	Yes	Yes
Purification protocol	Often denaturing	Non-denaturing	Denaturing and non-denaturing
Average secondary structure	Primarily random coil	Primarily helical	Primarily random coil
Transient initiating N-terminal helix	No	---	Yes
Primary native state	Monomer	Tetramer	Primarily monomer
Fibril Prone	Yes	No	Yes
Referring section within text	2-3	5, 7*	6, 8

* In the more recent report by the same group it was suggested, that the tetramer is conditions dependent (some monomer population was identified).

Subsequent studies indicate that αS exists as a primarily unfolded monomer

A rapid period of overlapping work began to determine the oligomeric state of αS from various cell sources, under non-denaturing conditions and to investigate the role of the acetyl group modification. Lashuel and colleagues examined αS from mouse, rat and human brains and addressed

the issue of the source, the purification and the characterization methods of the protein and their impact on the oligomerization state (Table 1)[31].

In response to report by Bartels *et al.*, Lashuel and colleagues determine that αS exists as an unfolded monomer within neuronal sources. Lashuel *et al.*[31] examined bacterial lysates under denaturing and non-denaturing conditions (with and without a boiling purification step respectively) against a range of non-globular standards: including 1) *E. coli* derived unfolded monomeric αS 2) disulfide linked A140C αS including some dimer and 3) Ac-αS. Regardless of purification, samples from bacterial lysates elute and migrate at identical positions on a size exclusion chromatography (SEC) column or CN-PAGE. This indicated that the various samples are either all unfolded monomers, all more compact tetramers, or that coincidentally these structures migrate at identical positions. Coupled now with a far UV spectrum of a primarily random coil protein, rather than a helical spectrum observed by CD, however, Lashuel's bacterial αS appears to be unfolded regardless of whether it has been boiled and it resembles unfolded monomeric αS. A random coil spectrum is not necessarily synonymous with a monomeric protein. Static light scattering (SLS) was used as a more unbiased molecular weight determinant alongside elution from SEC[162]. While data from size exclusion chromatography (SEC), indicated a Stokes radius close to a globular standard at 64 kDa, SLS indicates a protein of 14 kDa. Therefore bacteria, consistent with Selkoe and colleagues' observations, do not assemble into a helical tetramer, even without boiling.

Lashuel and coworkers[31] demonstrated a sensitivity of CN-PAGE to small differences in the protein composition and went on to use CN-PAGE to explore the role of mammalian machinery and denaturation by boiling. Whether endogenous or overexpressed, whether boiled or not, whether isolated from bacteria or present in mouse, rat samples or HEK293,HeLa,SH-SY5Y,CHO,and COS-7 mammalian cell lines -- identical CN-page migration and sometimes SEC-SLS, repeatedly indicated the unfolded monomer. Across research groups, acrylamide percentages, purification protocols and the source, the samples of αS co-migrate with recombinant αS. To test whether factors present in cell could promote tetramerization, they examined fresh or aged samples, since aged samples are

expected to be more oligomer-rich, along with a control of exogenously added recombinant protein. *In vivo* oligomer-specific enzyme-linked immunosorbent assay (ELISA) could not detect any other oligomers in the samples, confirming that purification has not disturbed this observation[31,163]. In addition, the report explored the possibility that the tetramer population could be dynamic and unstable, so that if the protein for some fraction of the time populates a tetrameric state, it would have a different cross-linking profile than a protein that populates primarily the monomer state. They observed that no significant amount of oligomers beyond the dimer are observed, indicating that DSS could not effectively capture a tetramer either. This report additionally repeated the RBC purification procedure[31]. Unable to replicate the tetramer, it was still concluded that disordered monomer is isolated from RBC's. It is not clear what Selkoe and colleagues[27] did differently, but Fauvet *et al.*[31] does note that samples of sufficient quantity and purity could not be obtained using this purification, even with another hydrophobic interaction chromatography (HIC) step, suggesting some complicating interactions in either sample. Fauvet *et al.* also attempted the GST-constructed αS protocol and cannot replicate the dynamic tetramer observations of Wang and colleagues.

Concurrently, Rhoades and colleagues sought to determine if the nature of the purification method[34] or N-terminal acetylation had enough biophysical consequence to promote the fibril resistant tetramer. They examined samples purified with and without BOG and the N-terminal acetyl-group. Rhoades is the first to use a bacterial co-expression system to generate Ac-αS (Figure 2C). In this co-expression system developed by Mulvihill et a[1], the yeast analog to NatB is cloned into a bacterial plasmid, allowing overexpression of αS into more unsophisticated expression systems. The yeast NatB is shown to function in bacteria to produce N-terminally acetylated proteins, and it seems to acetylate αS close to 100% of the time in *E.coli*. Rhoades finds that N-terminal acetylation and non-physiological purification including BOG were necessary for observation of helical oligomeric αS. Non-acetylated or BOG free αS was disordered and presumably monomeric, but the CD spectrum of Ac-αS purified in the presence of BOG was helical. Rhoades also encounters the complication that disordered monomer and helical tetramer have similar hydrodynamic radii, but

coupled with SE-AUC, which is "independent" of molecular shape, Ac-αS(BOG) was shown to have a sedimentation curve that exchanged with an oligomer. That the sample was specifically tetrameric is not clear. While the report by Trexler et. al, does not exclude the possibility that N-terminally acetylated αS has a higher affinity for membranes and/or BOG itself, the work was further provocative towards the role of acetylation in helicity and oligomerization.

Continued discussion on the oligomerization state of αS.

In response to the studies that indicate that cellular αS is an unfolded monomer[29,31], Selkoe and coworkers[35],with an even further heightened awareness to experimental conditions, recently reported that endogenous αS is predominantly tetramer. Using *in* vivo cross-linking as their primary tool, they identify several factors which might matter in terms of isolating the tetramer. During overexpression, particularly in protein derived from IPTG induction, more monomer is found. More monomer is also isolated when cross-linking is done at 4C° as opposed to 37C°. The tetramer is "preserved" in a concentration dependent manner at the time of lysis, where a higher concentration at the time of lysis favors the tetramer. This suggests that macromolecular crowding in cell may favor folding and stabilization of the native non-pathological tetramer. For this reason and for the fact that the Ac-αS level is endogenously high in erythrocytes, Selkoe and colleagues' considers RBC's an ideal system to obtain Ac-αS. These results may reflect sensitivity of the experiments themselves, or may reflect the preference of the monomer to associate with itself, even in the presence of other binding partners, but that it is also stabilized in the monomeric form.

N-terminal acetylation of monomeric αS induces helix formation and affects lipid binding.

Because Ac-αS is now recognized to be the physiologically relevant species in the brain, its biophysical characterization has been pursued. Questions that have been raised include the monomer or oligomeric preference of the Ac-αS species, its conformation, interactions with membranes and ability to form fibrils. Kang *et al.*[32], show that recombinant 100% acetylated Ac-αS purified under mild physiological conditions exists primarily as a monomeric protein. Electrospray ionization-ion

mobility spectrometry-mass spectrometry (ESI-IMS-MS) experiments indicate a small population (5-10%) of dimer that is consistent with previous observations of dimer species in solution. Lashuel and colleagues[30] use similar techniques as in their first report and again do not observe any higher-order oligomers, now in the acetylated protein. This suggests that acetylation by itself is not sufficient to favor a helical tetramer. Selenko and colleagues [29] show by in-cell NMR that non-acetylated αS is a disordered monomer in the macromolecular environment of the cell. Lashuel[30] additionally compares Ac-αS and αS with in-cell NMR and draws similar conclusions. Although the possibility of exchange with higher-order oligomers cannot be ruled out, the predominant cellular form indicated by these experiments of Ac-αS is unfolded monomer.

The conformational properties of Ac-αS have also thus far been investigated and it is shown that there is minimal change in the hydrodynamic radius and intra-chain long-range interactions[30,33]. However, the N-terminal acetyl group affects the transient secondary structure as observed by NMR[30,32,33]. Residue-specific NMR chemical shift analysis shows that there is an increase in the transient helical propensity at the initiating N-terminus[30,32,33] that may arise as the acetyl group masks the alpha-amino positive charge and interacts favorably with the helix dipole moment. Additionally, the acetyl group itself is a good N-cap, favoring hydrogen bonding for an N-terminal alpha helix at the initiating residues[164,165] .

At least one report suggests the membrane binding properties of Ac-αS are strongly altered by acetylation and indicates a two- fold higher lipid affinity. It is suggested that the increase in N-terminal transient helix may be critical to initiating membrane binding. Preformed transient helix at the N-terminus may therefore play an important role in the recognition of binding partners, may be important for membrane recognition, or may imply that lipid mediated association of the hydrophobic surfaces of helices may relevant to routes of self-association of the monomer.

Fibril formation of Ac-αS was investigated by measuring the fibrillation kinetics using ThT fluorescence. While groups of Lashuel[30] and Bax[33] found no significant differences in fibril formation rate, Kang *et al.*[32] found that N-terminal acetylation slows the rates of fibril formation by

approximately a factor of two. Clearly the acetyl group alone cannot inhibit fibril formation, but it does impart a small inhibitory effect, which may arise from a redistribution of the monomeric protein ensemble.

1.1.7. Conclusions

Recent studies that suggested that αS exists as a soluble, tetrameric, fibril-resistant form of αS were provocative, and a monomer/tetramer debate followed. The discussions about the accessible states of αS have raised many important questions related to cellular machinery, αS purification methods and the extent to which acetylation impacts on a monomer-oligomer equilibrium. A number of in depth studies have subsequently revealed that both non-acetylated and acetylated αS purified under mild or harsh conditions is primarily a monomer.

Despite the controversy surrounding the notion of a helical non-pathological tetramer, the concept of a soluble, non-pathological αS oligomer was perhaps not new. Biophysical studies have shown that αS can be induced to self-associate into a heterogeneous variety of soluble oligomers, some of which may be beneficial, or non-pathological. For example, methionine oxidation, arising from conditions of oxidative stress, stabilizes a fibril resistant oligomer of αS that is non-toxic to dopaminergic cells[145]. This may be consistent with the regulatory role methionine oxidation is suggested to have, sometimes being beneficial.

In order to understand the interplay between aggregation prone and aggregation resistant kinetic pathways from the unfolded monomer, the initial interchain associations between monomers within the starting ensemble and associations present in already-isolated stable soluble oligomers may need to be considered further. Defining the properties that drive these different species may lend to our understanding of how to enhance fibril resistant, fibril prone and/or non-toxic pathways *in vivo*. Because of the great ability of αS to adopt many conformations in a variety of oligomeric states, working from the monomer ensemble of Ac-αS we may (again) isolate stabilizing interactions of a helical oligomeric species that does not tend toward fibril and we may begin to better elucidate

shared features of non-pathology and fibril resistance amidst the entirety of the currently known heterogeneous oligomer population of αS

1.2. Background: alpha synuclein and beta synuclein characterization. The inhibitory role of beta synuclein.

1.2.1. The synuclein family

αS belongs to the superfamily of synucleins. They are small lipoproteins expressed abundantly in the brain. There are three members of the synuclein family: alpha synuclein (αS), beta synuclein (βS) and gamma synuclein (γS).[166] αS and βS are expressed abundantly in the brain, and they are mostly located in close proximity to the neuronal ends where they are believed to regulate presynaptic vesicle recycling. γS, on the other hand, is mostly expressed in peripheral neurons, though it was first detected as a breast cancer specific gene.[166] Since only αS and βS colocalize in the brain we decided to focus on the possible interactions between these two proteins. In light of the fact that αS and βS have different fibrillation propensities[167] and that βS was implicated in the mitigation of αS toxicity in *in vivo* models, we decided to examine this matter more closely.

1.2.2. Beta synuclein as an alpha synuclein regulator

Regulation of αS expression

βS shares high sequence similarity with αS, but they differ in aggregation propensities.[167] αS aggregates readily to both oligomers and fibrils while βS does not form fibrils and is not prone to form oligomers. However, as it was shown by *in vivo* studies, βS can mitigate αS toxicity, and coincubation of αS with βS decreases the number of inclusion bodies formed in mice brains.[168] Interestingly, it has been shown that there are changes in expression levels of αS and βS in Diffuse Lewy Bodies Disease (DLB) and Alzheimer's disease (AD). Levels of the βS are diminished and levels of αS are elevated in DLB, and in AD βS levels are also diminished. [169] Expression levels of βS mRNA also decreases in the cortical brain regions in patients with Levy Body dementia.[170] In PD βS mRNA is overexpressed in the caudate nucleus, and in PD-associated dementia the levels of αS

mRNA are diminished (post-mortem studies).[171] This data suggests that misregulation of synuclein expression levels is an important factor in the development of disease.

Regulation of αS aggregation on the protein level

βS has the ability to ameliorate the influence of αS toxicity and aggregation in the doubly transfected mice. Doubly transfected mice exhibit a smaller number of inclusion bodies and have significantly better motor assessment than only αS transfected mice.[172] These facts point to the protective nature of βS against αS toxicity, possibly through direct interactions as there is evidence of the co-immunoprecipitation of αS with βS.[172] The effect of βS on αS is also detectable in the case of αS mutant A53T: overexpression of βS can mitigate the impact of A53T αS in mouse models. Interestingly, tg mice overexpressing βS have reduced levels of αS expression but not of RNA, again suggesting complex regulation mechanisms.[173] Additional studies have also shown that injection of lenti-βS reduced the formation of αS inclusions in tg mice.[174] Again there was evidence of the co-immunoprecipitation of αS and βS in tg mice and in B103 cells, as well as the increased activity of neuroprotective pAkt in tg mice.[174] In vitro studies also pointed out that βS inhibits the formation of αS protofibrils, which are thought to be toxic species involved in PD.[175] βS coincubation with the disease-linked mutant of αS A53T also showed the formation of fewer protofibrils as detected by measuring oligomer concentration using SEC.[175] In addition βS can mediate membrane linked toxicity of αS: βS does not oligomerize on its own upon exposure to polyunsaturated fatty acids (PUFA; cell line MES 23), but can inhibit PUFA-induced oligomerization of αS.[176] All the data mentioned in this section suggests a multilevel involvement of βS in the regulation of αS toxicity. However no direct experimental information about the inhibition mechanism has been found until now. There are indications from molecular dynamics experiments that suggest antiparallel dimeric interactions between αS and βS on membranes retard the formation of αS oligomers.[177]

βS as a neuroprotector

αS overexpression is thought to be one of the causes leading to its toxicity.[178] Studies show that overexpression of αS suppresses signaling through, ERK,[179] and can regulate Bcl-2 expression through PI3-K/Akt pathways.[180] The serine threonine kinase Akt (known also as protease B) is involved in neuroprotection. Studies addressed the effect of the neurotoxic drug rotenone on cells expressing αS, βS and control cells (empty vector). It was shown that the βS cells up-regulated pAkt both in the presence and absence of rotenone, suggesting that βS plays a neuroprotective role through the activation of neuroprotective protein pathways. On the other hand αS-transfected cells and control cells were susceptible to rotenone toxicity.[181] The protective role of βS can be also carried out by regulation of the protein clearance mechanism. Studies showed that αS and γS are able to inhibit the proteasome (the proteasome is responsible for the degradation of oxidized proteins), while βS can act as a negative regulator of the αS inhibition of the proteasome, which suggests that βS can help in cell clearance.[182] βS additionally protects against isoaspartate damage of αS as less oligomers of αS are formed in the presence of βS.[183] βS is also able to protect against staurosporine (an apoptotic effector) and the dopamine derived toxin 6-hydroxydopamine.[184] Cells treated with these toxins displayed an anti-apoptotic phenotype. βS lowers p53 expression levels (p53 plays a role in cell regulation, apoptosis and genomic stability). [184] Finally, βS protects against heat-induced aggregation of adolase and alcohol dehydrogenase, citrate synthase and the aggregation of αS and $A\beta_{1-40}$ in vitro.[168]

1.2.3. Synuclein function as analyzed by mice knock-outs (KO).

To determine the effect of the synucleins on synapse plasticity and function, the groups of Chandra and Buchman prepared double αS and βS mice knock-outs (KO), and triple αS, βS and γS mice KO.[185-187] The effect of the double KO on mice was not significant as it seemed that the phenotype was rescued by the increased expression of γS (50%), complexins (complexins are localized in presynaptic nerves and are responsible for calcium dependent neurotransmitter release), and the 14-3-3 proteins (14-3-3 are signaling protein for kinase phosphateses and transmembrane

receptors). The main difference in the double KO mice compared to control mice was a 20% lower dopamine level.[185]

Triple mice KO lacking αS, βS and γS displayed changes in the phenotype, mostly manifested in the alteration of synaptic functions and transmission, age dependent dysfunction and survival. The size of the excitory synapse was diminished by 30% in triple KO mice.[187] Additionally, triple synuclein KO had lower dopamine levels in the dorsal stratium but dopamine metabolites were less affected by the lack of synucleins. Even though the dopamine levels were diminished, the mice behaved like hyperdopaminergic animals. This could be linked to a two-fold increase in the rate of dopamine release despite the 30% decrease in dopamine levels. These studies show that in the absence of the synucleins dopamine axons release more vesicles (or their content).[186] The characterization of double and triple synuclein KO in mice showed that synucleins play a role in the synaptic vesicle release and dopamine circuit, thus suggesting that theirs role in the brain is similar, as the knock out of even two synucleins was not able to induce a highly noticable effect in the cells. One question still remains: why are there two synucleins mostly expressed in the same cellular locus? Do the synucleins interplay with each other to modulate the release of synaptic vesicles in a sophisticated manner? The answer to this question is out of the scope of this thesis, but hopefully we will be able to give some suggestions about the cooperation between synucleins *in vitro*.

1.2.4. Toxicity of βS

Despite its evident neuroprotective nature, βS was also implicated in the axon pathology of the hippocampus in DLB and in some sporadic cases of PD.[188,189] Recent studies also shown that βS can cause toxicity in cultured primary neurons and can form digestion resistant aggregates in rat models *in vivo* and when overexpressed. βS was also shown to accumulate with αS in the lysosomal vacuoles of fibroblast cells from KO mice of the presenilin-1 protein, mutations of which are implicated in Alzheimer's disease. Furthermore, two βS mutations were found in the respectively sporadic and familiar cases of DLB: V70M and P123H.[190] However the fact that βS is not

incorporated into Lewy Bodies suggests that the origin of the pathology might be diverse in the case of αS and βS

The influence of the mutants of βS on cell lines was investigated, and in case of P123H mice models were also produced. Both of the mutants (V70M and P123H) formed lysosomal inclusions in B103 cell lines. Interestingly, the number of lysosomal inclusions increased upon co-expression of βS mutants with αS. Therefore the toxicity of βS is exacerbated by αS. A53T αS mutant coexpression with P123H βS mutant caused an increase in the number of inclusions, while other familiar αS mutants, A30P and E46K, had inclusion levels similar to the wild type αS with P123H. On the other hand wild type βS with the addition of αS mutants exhibited only a small amount of inclusions.[191] Similar conclusions were drawn from tg mice models of the P123H βS mutants where mice brains exhibited extensive neuritic pathology including swelling of the striatum and globus pallidus, which consists of small spheroidal inclusions. However no Lewy Body inclusions were found in the cells. The neuropathy of P123H βS was not abolished in the αS KO mice, but was enhanced in the P123H βS/αS doubly tg mice, suggesting that the pathology of βS can be increased by the presence of αS but that P123H-βS is toxic on its own.[192] Facts described here suggest that βS can mediate neuronal toxicity. However it seems plausible that the mechanism followed in different pathologies are not the same. Thus, again, close investigation of the αS and βS models must be performed, as both proteins can possibly carry out both protective and degenerative functions, and depending on the external factors, they can be performed with results that are distinct.

1.2.5. Characterization of βS

βS is a 134 residue long protein in which three regions can be distinguished: N-terminus (residues 1-60), NAC (61-84) and C-terminus (85-134). Similarly to other members of synuclein family, βS is an intrinsically unfolded protein, which means that it does not have one defined structure but interconverts between multiple conformations. All the members of the synuclein family can interact with membranes through the N-terminus and the NAC, which can fold into a helices

upon membrane binding. The C-terminus is implicated to be a regulatory domain and display chaperone activity. The βS N-terminus is slightly helical up to residue 65 (residues with high helical propensities are 20-35 and 55-65). The NAC does not exhibit any structure, and the C-terminus exhibits extensive polyproline II secondary structure. R_2 values indicate higher mobility at the NAC terminus residues 70-80.[193,194] There are no significant interactions within βS (PRE data), which is consistent with the hydrodynamic radius of βS that shows that βS is highly extended (compaction of 20%). The difference between the hydrodynamic radius of βS in solution and and its fully extended form is 3Å. [190,191]

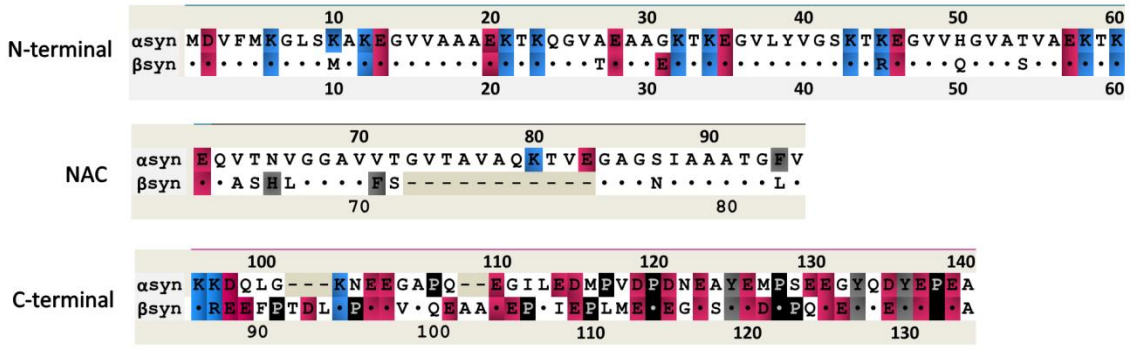

Figure 3 Aligned sequences of aS and bS for the three regions of synucleins: N-terminal, NAC and the C-terminal. Identical residues are shown by dots in the bS sequence and deletions are shown by dashes. Residues are color-coded according to the scheme: blue – positive charge, red negative charge, black-prolines, grey-aromatic residues.

alpha and beta synuclein sequence comparison

βS is a homolog of αS with which it shares 62% sequence identity. αS and βS have extremely well conserved N-termini with only 6 residues being different. In βS there is a deletion of 11 NAC residues (73-83) which form part of the core of the fibril in the case of αS. The least conserved region of the the synuclein sequence is the C-terminus which highly charged and extended. In the case of βS the C-terminus is 5 residues longer, has a greater negative charge and contains 3 more prolines. All of these factors can contribute to a more extended conformation and extensive polyproline II secondary structure in the βS sequence. All the single mutations in αS which are linked

to Parkinson's disease are located in the N-terminus (A18T, A29T, A30P, E46K, H50Q, G51E, A53T[2,195-197]). Therefore it seems that the N-terminus of the synucleins is highly sensitive to changes in secondary structure and even the small number of mutations in the N-terminus combined with the deletion of part of the NAC and C-terminus may contribute to the delayed aggregation-prone nature of βS.

Basis for βS non-fibrillogenic properties

The comparison of the sequences of αS and βS provides us with important information about αS aggregation determinants. Studies on αS revealed that residues 71-82 of αS are necessary for αS aggregation. Interestingly, βS lacks residues 73-83. Furthermore, deletion of residues 71-82 in the αS abolishes its aggregation behavior. However insertion of the deleted NAC region back into the βS sequence does not fully recover the fibrillogenic phenotype. The peptide consisting of residues 71-82 can self-assemble and seed αS.[198] αS with a deletion of residues 73-83 aggregates much slower than wild type αS, and a deletion of residues 71-83 almost completely abolishes aggregation. βS with an insertion of αS residues 73-83 and 71-83, does not recover the aggregation-prone behavior. This suggests an important role of the NAC in aggregation, but also points to additional factors that can contribute to the aggregation of the αS sequence.[199] Another study which carried out a 6 residue swap from NAC region (residues 63-66 and 71-72) predicted by computational methods showed that βS with αS has increased tendencies to aggregate in SDS and αS aggregation rates for the swap were decreased.[200] Another study pointed out the N-terminus residues that can also contribute to aggregation rates: mutations in residues 45-46 caused βS to aggregate.[201] One of the regions that is thought to be inhibitory of αS aggregation is the C-terminus, deletions of which hasten aggregation of αS. The βS C-terminus is a better inhibitor of αS aggregation, but it is not only reason why βS is not fibrillogenic. These facts suggest delicate balance between aggregating and non-aggregating forms of the synucleins, indicating that aggregation-prone and aggregation-resistant behavior is the outcome of multiple contributing factors.

Factors that can promote aggregation of βS

βS is by itself mostly non-amyloidogenic. However there are some factors that can induce βS fibrillization. A study by Munishkina *et al*,[202] showed that βS can aggregate upon addition of metal ions such as Zn^{2+}, Pb^{2+} and Cu^{2+}. Other metal ions such as Al^{3+}, Hg^{2+}, Fe^{2+} induced oligomerization of βS. Because metals induce the formation of secondary structure in βS, this was thought to be a main reason for the conversion from a non-aggregating to aggregating form of the protein. There are also different factors that contribute to enhancing or inducing aggregation of βS in presence of metals including molecular crowding, pesticides (rotenone, paraquat, dieldrin), and glicosaminoglicans.[202] Detergent such as sodium dodecyl sulfate, which is often times used to mimic the behavior of the synucleins on membrane, as it induces formation of similar helical conformation in synucleins as the one on the micelles;in the case of βS residues 1-83 exhibits helical secondary structure. However, low concentrations of the SDS (0.25-0.77 mM) induce formation of the typical amyloid fibril topology in βS which can be rationalized by the induction of partial secondary structure which destabilizes the non-fibrillogenic conformations of βS and prompts it to form fibrils.[193]

1.2.6. beta synuclein as an inhibitor of alpha synuclein aggregation

In vitro βS is able to inhibit αS aggregation rates. The complete inhibition of αS aggregation occurs at a molar ratio of 4:1 βS to αS. [167] Studies *in vivo* suggested that αS and βS interact directly. However studies *in vitro* have not been able to confirm this hypothesis so far. The aggregation process can be divided into three stages: nucleation, elongation and mature oligomers phase. In the nucleation phase nuclei (seeds for the future aggregation process) are formed. A nucleus or seed is some form of the monomer or oligomer that has an ability to recruit monomeric chains of αS and to propagate to higher order oligomers and finally to fibrils. In the elongation stage the fibrils formed in grow on nucleus forming elongated protofibrils.[203] Sometimes the protofibrils break, and secondary nucleation sites are being formed. In the last stage mature fibrils are formed, which means that the fibrils have rearranged into their final architecture and are no longer changing their conformation but

exist in equilibrium with the remaining monomers. Therefore there are many stages at which βS might inhibit αS aggregation. It is possible that βS prevents αS from misfolding and formation of the aggregation nucleus. Another option is that the βS interacts with monomers and retards transition to the toxic oligomers. βS could also disrupt the propagating nature of the nuclei by forming hetero-oligomers off the aggregation pathway. It could also delay the addition of monomers to the nuclei by interfering with the interactive surface of the nucleus. Finally βS, could lead to disaggregation of the αS fibrils through interactions with their termini. All of these scenarios are possible and are illustrated in the Fig. 4.

Several studies attempted to discriminate between these options, but were neither able to pinpoint specific interactions that contribute to aggregation inhibition nor to clearly determine at which stage aggregation inhibition occurs. Studies by Eliezer and co-workers showed that at the monomer level there is no evident change of HSQC chemical shifts in 5 molar excess βS in an αS

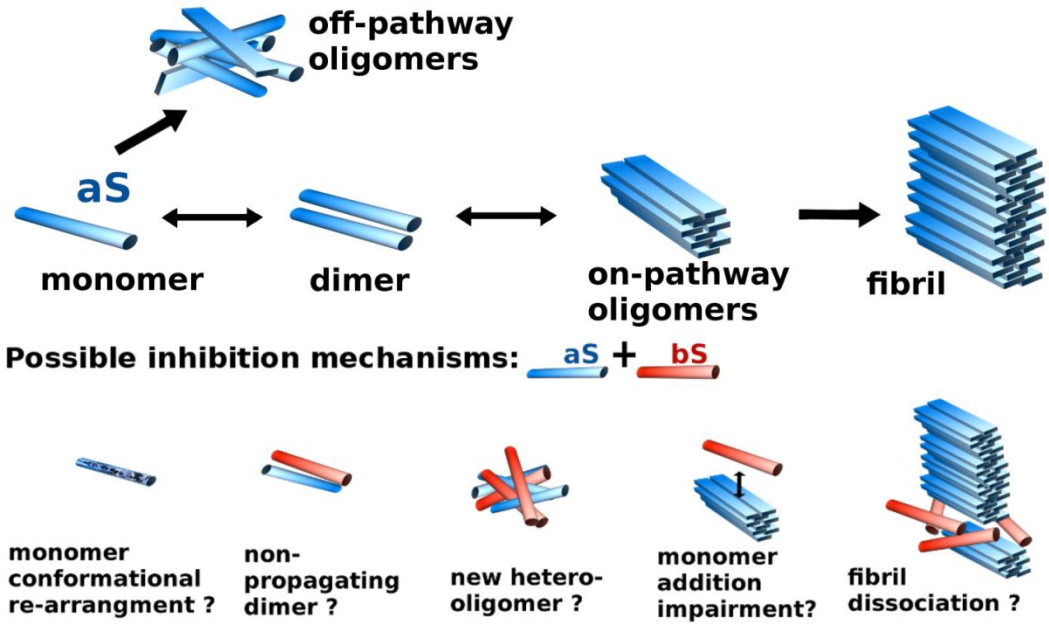

Figure 4. Possible mechanisms of the αS aggregation pathway and inhibition of αS aggregation by βS.

sample.[194] However, the unfolded nature of the synuclein and possibly low population might account for no interactions being detected rather than the lack of interactions in them. Studies by Lansbury[175]

showed that βS decreases the number of oligomers formed by αS. However it is not known what the mechanism behind this change is. In my work I attempted build on these approaches and identify the residue specific information about the interactions.

Inhibition of αS aggregation by many factors

Studies of the inhibitors of αS revealed interactions of inhibitors such as phthalocyanine tetrasulfate (PcTs) with residues 3-9 and 35-41 and of the phthalocyanine[204-206] tetrasulfate-copper (II) complex PcTS-Cu^{2+} with residues 3-18 and 38-51. Similarly the beta-wrapping protein that contains an αS fragment encompassing residues 37-54 was able to inhibit aggregation of αS at multiple time points during aggregation.[207] A library of peptides based on αS residues 45-54 was developed, and based on that aggregation inhibitory peptide for αS was proposed which can inhibit in ratio 1:1 (peptide:αS).[208] Different inhibitors of αS (EGCG, dopamine) [209,210] have been suggested to interact not with the N-terminus but with the C-terminus. Also peptides generated from fragments of the αS NAC region, which is found in the core of the fibril (residues 68-72 and 77-82), were shown to inhibit αS aggregation. Similarly to the work with αS-based peptide fragments, the sequence of βS was fragmented in search of a suitable inhibitor. It turned out that peptides made of residues 1-15 and 36-46 of βS interacted with αS, inhibited its aggregation and decreased αS amyloid formation and oligomerization. Interactions between the peptides from βS and αS have been confirmed by NMR. The peptide fragment consisting of residues 36-46 of βS was able to recover the behavioral abnormalities of Drosophila flies expressing αS A53T.[211] These facts suggests that there are specific regions in αS that are responsible for aggregation and that targeting these fragments is a valid and important strategy toward drug development.

1.2.7. Seeding and cross-seeding in neurodegenerative diseases

In the conformational disorder diseases such as PD, AD, Huntington, frontotemporal lobal degeneration, amyotrophic lateral sclerosis are diseases associated with the misfolding of proteins and

their accumulation in the nervous system. Interestingly, the misfolded nature of the diseases can be transmitted to hitherto unaffected proteins in a prion-like manner, meaning that misfolded proteins can spread to new cells and even regions of the brain and induce accumulation of the misfolded proteins.[212-219] It is postulated that the disease spreads through oligomeric species of the misfolded species as they are able not only to induce disease but also to induce toxicity in the cells, which can be an important factor in the progression of the neurodegenerative diseases. One of the concepts emerging from studying various neurodegenerative diseases is the idea of cross-seeding between the species in diseases such as AD, PD and Huntington disease. The main idea of this concept states that proteins involved in these neurodegenerative diseases can induce aggregation of proteins involved in other neurodegenerative disorders. For example αS involved in PD can cross-seed tau leading to Huntington disease and Abeta leading to AD. Literature suggests that such events contribute to increased toxicity and more pronounced symptoms.[220-222] The mechanism by which cross-seeding occurs is unknown. It is thought that similarity between the sequences may induce seeding effects and that the beta sheet secondary structure of the seed may be important in inducing misfolding in the other chain. This is interesting in light of the inability of βS to be seeded with the αS fibril seeds as measured by the concentration of the soluble fraction of βS.[223] βS is highly similar to αS which suggests that βS on its own does not exhibit the tendency to exist in the beta sheet structure. Furthermore, the first 15 residues of βS have the ability to protect cells (chick embryonic cortical neurons) against Abeta toxicity and oxidation stress.I In contrast αS oligomers can induce seeding of Abeta , and Abeta fibrils can cross-seed αS.[224,225] Similarly in the case of tau, co-incubation of αS with tau induces increased aggregation while co-incubation of tau with βS or with αS that has a deletion of the NAC residues 71-82 does not, which suggests that the formation of the beta-sheet structure is very important in the seeding event.[226] The data described in this paragraph suggest that βS has unique oligomerization properties and is unable to exist in aggregating conformations even when prompted with seeding.

2. Methods

In this chapter I will describe the experimental methods used in my research. These procedures include: in section 2.1: protein preparation (mutagenesis, protein expression and purification, spin labeling), preparation of samples specific to the different techniques used, experimental design, Nuclear Magnetic Resonance (NMR), circular dichroism (CD), dynamic light scattering (DLS), SDS-page gel, native gel, size exclusion column (SEC) chromatography, electrospray ionization mass spectrometry (ESI-MS), Thioflavin T aggregation assays (ThT), transmission electron microscopy (TEM); in section 2.2: a detailed description of the paramagnetic relaxation exchange (PRE) experiment; in section 2.3:) biological methods and procedures including cell culture maintenance, cell toxicity assay, immunostaining and fluorescence microscopy; in section 2.4: oligomer preparation.

2.1. Expression, purification and biophysical methods.

2.1.1. Mutagenesis, expression and purification

Mutants of αS and βS, were prepared by site-directed mutagenesis using AccuPrime pfx from Invitrogen. To obtain N-terminal acetylated forms of proteins co-expression with NatB plasmid cloning N-Acetylotransferase B was performed, αS described previously for αS, same approach was used for βS.[227] Protein purification was performed according to the previous protocols.[228]

2.1.2. NMR experiments

2.1.2.1. PRE experiments/controls

For all PRE experiments we used following buffer: 10mM MES, pH 6, without salt addition and with 10% D_2O required for NMR experiments. As we shown before charged residues have effect on formation of the transient complexes, so according to our previous finding we decided not to use salt.[56] Samples were prepared αS follow: lyophilized samples of ^{14}N-MTSL-cysteine mutants or ^{15}N non-modified proteins (αS or βS) were separately dissolved. First, samples were passed through

100kDa filter to remove higher order oligomers, then they were concentrated using 3kDa filters to be able to dilute sample to final concentration of 250uM of each protein. Usage of this relatively low concentration of the spin-label sample was chosen to minimize the non-specific interactions. Final sample volume was 350uL, which is volume of the Shigemi tube in which experiments were performed. Total sample concentration used was 500uM, where 250uM was non-modified ^{15}N protein and the other 250 was ^{14}N-MTSL labeled, cysteine mutant. We mixed non-modified ^{15}N-αS with αS-cysteine and βS cysteine mutants, similarly we mixed non-modified ^{15}N βS with αS-cysteine and βS-cysteine mutants, and thus detection was on non-modified proteins. Diamagnetic samples were prepared by reducing samples with 10x excess of Ascorbic Acid and later 5x buffer exchange using 3kDa cutoff filters from Millipore Inc. Changes in the samples concentration did not have significant effect on the changes in diamagnetic control. All the controls have similar pattern and are in range of the experimental error (data not shown).

All ^{1}H-R_2 of paramagnetic and diamagnetic (reduced) sample were acquired on 600 Varian at 15 °C using previously published pulse sequence and protocols.[56,229,230] Inter-chain paramagnetic relaxation enhancement rate (PRE rate – Γ_2) is residues specific difference of the ^{1}H-R_2 of paramagnetic and diamagnetic samples. Increased ^{1}H-R_2 relaxation rates on the ^{15}N visible chain indicates that the NMR blind ^{14}N -MTSL labeled protein is in the proximity of specific residues in the NMR ^{15}N labeled visible chain. Para- and diamagnetic ^{1}H-R_2 were analyzed and processed using nmrpipe[231] and sparky.[232] For all experiments 10 relaxation delays were used: 12, 32, 104, 12, 124, 64, 48, 94, 64, 20 ms. Two data points (12 ms, 64 ms) were repeated in the experiment for obtaining good statistics for the error analysis. Errors of Γ_2 were calculated using error propagation, errors were below 2 Hz. PRE experiments in the concentration used did not give rise to high background PRE values.

2.1.2.2. NMR PRE titration experiments.

For PRE titration experiments we used protocol described before.[233,234] After measuring spin label sample concentration we concentrated it to low volume > 32 uL and we were adding sample to the 350uL of 250uM ^{15}N sample of either αS or βS; the changes in the sample volume were less that 10% of the overall sample volume. We made following ratio of the ^{14}N-spin labeled samples to ^{15}N NMR visible samples for αS titration: 0, 0.25, 0.5, 0.75, 1, 1.5, in case of βS we went up to ratio 2. αS in this ratio exhibited shifts in the HSQC spectra, thus we removed this point from the analysis. We run 6 data points ranging from 12-125 msec with first point repeated twice for statistics. The PRE profiles for titration did not show significant contributions to the PRE values from the non-interactive regions.

PRE titration fitting and analysis. Increase in the $^{1}H_N$ Γ_2^{app} values due to paramagnetic relaxation enhancement, was fitted using equation:

$$^{1}H_N\Gamma_2^{app} = \frac{1}{1 + xK_d^{-1}}\Gamma_2^{free} + \frac{xK_d^{-1}}{1 + xK_d^{-1}}\Gamma_2^{bound}$$, where x is the concentration of ^{14}N-αS (T44C-MTSL) in solution, Γ_2^{free} – represents paramagnetic relaxation enhancement for unbound protein, and which values should be close to 0, and Γ_2^{bound} represents maximum saturation value. Fitting scheme was based on work of laboratiories of Bax[234] and Clore[233] The χ-squared statistic measuring the difference between the observed and predicted increase in ^{1}H-R_2 for residues whose 5th titration point exhibited PRE values higher that 15 Hz was optimized using the R statistics package minpack.lm, via Levenberg-Marquardt algorithm.[235] The resulting fit was robust to small changes in Γ_2^{free}, K_D, and Γ_2^{bound} and provided us with strengths of the interactions at the specific sites for αS/αS and αS/βS complexes (SI.table 1&2). Saturation of the titration profiles can be reached at high concentration of ligand, however usage of high concentrations of MTSL labeled samples causes artifacts arising from solvent-PRE effects[236]. To minimize artifacts we perform experiments at low ligand concentration, and to estimate K_d we use nonlinear regression model with three parameters $\Gamma_{2,free}$, Γ_2^{bound} and K_d.

We also fit the K_d values by modifying conventional equation for fitting chemical shifts changes to obtain K_d. We used following equation:

$$\Gamma_2 = \Gamma_2^0 + \Gamma_{2,\max} \frac{([P]+[L]+K_D) - \sqrt{([P]+[L]+K_D)^2 - 4[P][L]}}{2[P]}$$

Where [P] is total concentration of ^{15}N labeled protein, [L] is variable ligand concentration ^{14}N-MTSL labeled protein, $\Gamma_{2,max}$ is maximum PRE value that can be obtained in the experiment, and Γ_2^0 is the baseline PRE value, which was set to 0.5Hz when plotting. In general the K_d calculated with this methods are lower, so they overestimate binding for both homo- and hetero-complexes. However both methods results K_d values show that the αS/βS hetero-complex exhibit stronger binding than αS/αS homo-complexes.

2.1.2.3. NMR assignments

Assignments on βS and Ac-αS were performed using protocol described elsewhere.[228] Experiments were performed on 350uM ^{15}N and ^{13}C labeled sample with 10%D_2O in 10mM MES buffer pH 6 with 100mM NaCl. Secondary structure propensities were extracted using SSP program by Julie Forman-Kay.[237] If the values are positive then this region has helical propensities, if the values are negative then the beta-sheet propensities are more pronounced.

2.1.2.4. RDC experiments

For aligning medium we used C8E5-octanol bicelle aligning medium in 100mM NaCl, 10mM MES buffer pH 6.[238] Reagents: C8E5 and 1-octanol are purchased from Sigma. The quadrupolar deuterium splitting constants are measured prior to experiment to ensure correct medium obtained. Sample was prepared by dissolving lyophilized protein in buffer and passed through 100 kD and 3kD filters. Concentration of the protein was adjusted to 250 μM. Media splitting was added to final volume 5%. High resolution HSQC_IPAP spectra in the absence or in the presence of an alignment medium were collected.[239]

2.1.2.5. NMR relaxation experiments.

All NMR ^{15}N backbone relaxation data were recorded on Varian 600 MHz using pulse sequences including longitudinal relation rate R_1 [240], transverse relaxation rates R_2^{CPMG} [240] Dr. Seho Kim modified pulse sequences for R_1 and R_2 by adding steady state pulse at the beginning of the pulse sequence, to avoid the increase in the relaxation rates due to the protein solvent exchange. Individual FIDs were then processed by NMRPipe[231] and was analyzed by Sparky using a single exponential decaying function plugged in (Goddard and Kneller). The detailed fitting methods are described by Farrow *et al.*.[240]

2.1.3. Thioflavin T (ThT).

ThT assay is an assay to monitor formation of cross-beta structure, which is secondary structure found in fibril. 5-10 mg of lyophilized acetylated form of αS and βS was dissolved in Phosphate Buffer Saline, centrifuged for 10 min in 14000 rpm to remove big oligomers, and purified using size exclusion chromatography (Superdex 75 GL 10/300, from GE Healthcare Life Sciences), later protein was concentrated using 3kDa centrifugal units (Millipore Inc). Experiment set up was used αS previously described.[228]

2.1.4. Electrospray ionization mass spectroscopy (ESI-MS).

ESI-MS experiments were performed αS described previously.[241] Samples were prepared in 10mM Ammonium Acetate, pH 6 in final concentration 50uM, by using 100 kDa and 3kDa filters.

2.1.5. Dynamic light scattering (DLS).

DLS measurements were carried out using a Zetasizer Nano ZS (Malvern Instruments, UK). Data was collected using a 3 mW He-Ne laser light at a 633 nm wavelength back scattered light at an angle of 173°. Autocorrelation functions were determined from 6 correlation functions, with an acquisition time of 10 s per correlation function. Sample concentration was 200uM.

2.1.6. Negative straining TEM.

Fibrils were visualized using a JEM-100CXII manufactured by JEOL in electron imaging facility with assistance of Dr. Valentin Starovoytov. Negative staining TEM was performed using single droplet procedure[242] at ambient temperature. Micrographs were recorded at a magnification of 100,000. All of the chemicals are purchased from Sigma.

2.1.7. Circular dichroism (CD).

Experiments were performed on an AVIV Model 400 Spectrophotometer. Optically matched 0.1 cm path length quartz cuvettes (Model 110-OS, Hellma USA) were used. Wavelength scans were conducted from 190 to 260 nm at 15°C with 10 seconds averaging per time point. For all CD experiments 10mM phosphate buffer without addition of the salt, pH 6 was used. Low salt content ensures good CD spectra. Another important factor in acquiring good CD spectra is to know correct concentration of the protein, which can be ensured by measuring it with BCA assay.

2.2. Paramagnetic relaxation enhancement (PRE) experiments

2.2.1. Paper citation information.

Paper presents detailed description of the PRE methods, it provides insight on labeling methods. Paper was prepared as a book chapter for Methods in Molecular Biology, currently it is in the proof stage. Book will be available in 2016. Citation information: Maria K. Janowska & Jean Baum; *"Intermolecular Paramagnetic Relaxation Enhancement (PRE) Studies of Transient Complexes in Intrinsically Disordered Proteins"*; Protein Amyloid Aggregation; Methods in Molecular Biology, Editor: David Eliezer, vol(1345), copyright: Springer Science + Business Media New York

2.2.2. PRE experiment description

Many devastating neurodegenerative diseases are associated with proteins that convert from their normal soluble forms to amyloid fibrils that accumulate in the brain, and the mechanism by which

this occurs remains poorly understood. It is critically important to characterize the species formed during the very early stages of aggregation, as increasing evidence suggests that small protein oligomers may be more toxic than the final fibrillar aggregates. Atomic characterization of domain-domain interactions or inter-chain interactions at the earliest times is therefore key to understanding the structural transformation from monomer to fibril. Describing the dimer encounter complex is extremely challenging as these self-associated species are transient and exist at very low populations. In addition, proteins involved in neurodegenerative disease are often intrinsically disordered proteins (IDPs) such as α-synuclein, the primary protein in the Lewy bodies of patients with Parkinson's, or Aβ, the main component of amyloid plaques in Alzheimer's disease.

Inter-chain NMR paramagnetic relaxation enhancement (PRE) experiments allow the direct visualization and characterization of lowly populated transient encounter complexes in IDPs and establish the nature of the inter-chain interactions that may be present in the self-assembly process. ^{1}H inter-chain NMR PRE experiments are performed by making 1:1 mixtures of ^{15}N labeled protein and ^{14}N paramagnetic singly spin labeled protein and detecting broadened resonances on the ^{15}N labeled NMR visible sample that arise from the paramagnetic spin label on the ^{14}N chain. This experiment limits observation of PREs to inter-chain interactions only as the ^{14}N protein that contains the paramagnetic spin label is NMR blind, thereby making detection of intra-chain PREs impossible. The observed inter-chain transverse PRE rate on the ^{15}N labeled sample arises from the interaction of the paramagnetic center and the nucleus of interest, is proportional to $\langle r^{-6} \rangle$, and can provide distance information up to approximately 25Å with an MTSL spin label. Detection is very sensitive to lowly populated states and the transient dimer interactions can be detected under equilibrium monomer conditions established in the 1:1 ^{15}N labeled and paramagnetic spin labeled protein. The protocol for performing the inter-chain PRE experiments consists of six stages, including: (a) preparation of NMR ^{15}N labeled protein, (b) preparation of ^{14}N protein with single cysteine mutants, (c) preparation of paramagnetic NMR sample, (d) preparation of diamagnetic sample, (e) experimental acquisition, and (f) data analysis (Figure 5).

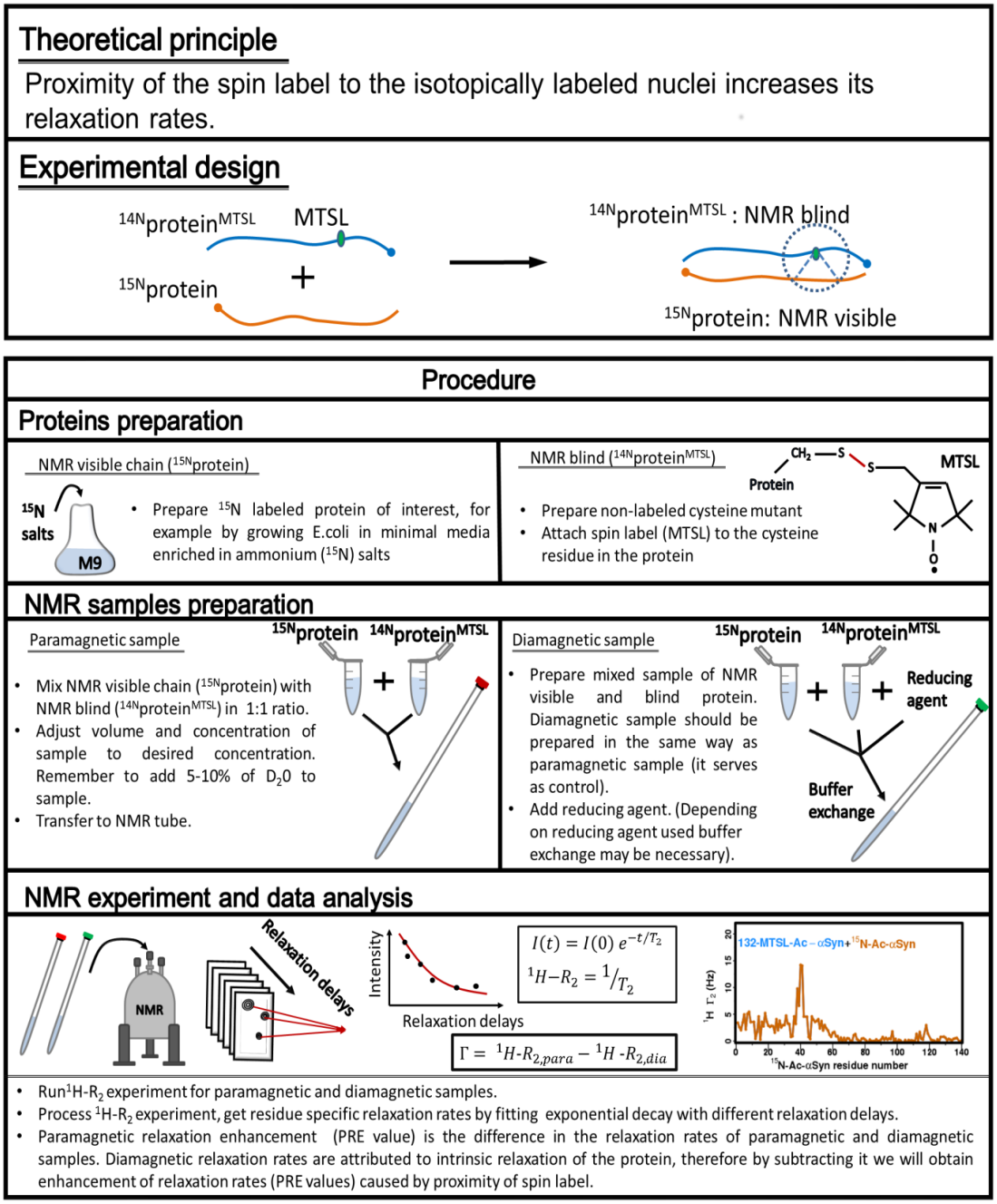

Figure 5 Procedure and basic theoretical principle behind the inter-chain paramagnetic relaxation enhancement experiments.

2.2.3. Materials

All solutions should be prepared using ultrapure water (prepared by purifying deionized water purifier with sensitivity of 18 MΩcm). Filter all the solutions through a 22 μm filter. All the buffers that will be used for HPLC/FPLC have to be filtered and degassed. Follow closely all the regulations for waste disposal.

Equipment: NMR spectrometer (field suitable for 2D experiments); FPLC or HPLC; desalting column; NMR tubes; protein preparation set-up; buffer exchange set-up.

Protein labeling scheme and purification components.

1. ^{15}N labeled protein (NMR visible chain). Grow cells, expressing protein of interest in M9 minimal media with addition of ^{15}N ammonium salt to ensure uniform ^{15}N labeling. Follow standard purification procedure for the protein of interest.
2. Unlabeled (^{14}N, NMR blind) – cysteine mutant. Grow single cysteine mutant in Luria Broth (LB) medium. Follow standard purification procedure for the protein of interest (*see* **Notes 1-3**).

Spin labeling of cysteine mutants.

1. Unlabeled (^{14}N, NMR blind) – cysteine mutant. Prepared as in point 2.1.2
2. Spin label. The most widely used spin label is MTSL (S-(1-oxyl-2,2,5,5-tetramethyl-2,5-dihydro-1H-pyrrol-3-yl)methyl methanesulfonothioate). The protocol described here assumes that MTSL will be used, but there are also different spin labels that can be used (*see* **Note 4**).
3. Acetone.
4. Standard buffers pH >7, (suggested buffers: PBS pH 7.4, Tris pH 7.7).
5. Reducing agent: dithiothreitol (DTT). Prepare stock of 1M DTT in water, filter through 22 μM filters. 1M DTT stock can be stored at -20°C (stable for ~1year).

Paramagnetic sample preparation.

1. Protein (as described above) solution in the desired buffer, with 10% D_2O in the final volume for NMR experiments (*see* **Notes 5-6**).

Diamagnetic sample preparation.

1. Use the same sample as the paramagnetic sample with the addition of a reducing agent, for example: dithiothreitol (DTT), β-mercaptoethanol (BME), ascorbate acid or sodium ascorbate (*see* **Note 7**).

2.2.4. Methods

Spin labeled protein preparation (MTSL-^{14}N labeled cysteine mutant).

1. Dissolve 5-10 mg of ^{14}N labeled single cysteine mutant in buffer with pH higher than 7 (suggested buffers: PBS pH 7.4, Tris pH 7.7).
2. Add 20 times molar ratio of DTT to solution.
3. Incubate for 4-6 hours in the cold room to remove cysteine disulfide bonds.
4. Inject sample into desalting column according to the manufacturer's specifications. Our laboratory uses GE™ Healthcare HiPrep™ 26/10, but other desalting columns can be used (*see* **Note 8**).
5. Immediately add 5 x excess of freshly prepared MTSL spin label solution (10 mg of MTSL in 400 uL of acetone).
6. Incubate in the dark overnight (4°C) on a shaking platform; the sample is light sensitive.
7. Remove excess spin label either by dialysis or buffer exchange (*see* **Note 9**).
8. Lyophilize the protein or concentrate it for immediate NMR sample preparation.

Paramagnetic sample preparation.

1. Mix ^{15}N labeled protein with ^{14}N MTSL labeled protein in a 1:1 ratio to the desired final concentration. Buffer should contain 10% D_2O for NMR experiments. NMR experiments require sample concentrations of at least 0.1 mM for a small, unfolded

protein. There are also upper limits to the concentration for the inter-chain PRE experiments (*see* **Note 6**).

Diamagnetic sample preparation.

1. Reduce the paramagnetic samples with 10 x excess of chosen reducing agent. Depending on the selection of reducing agent the sample may require buffer exchange (*see* **Note 7**).

NMR experiment acquisition - ^{1}H-R_2 experiments of para- and diamagnetic samples.

1. Two identical experiments will be performed, one with the paramagnetic sample and the second with the diamagnetic sample.
2. Contributions of the PRE effect to the relaxation rates are measured by detecting line broadening on the ^{15}N labeled NMR visible chain via standard $^{1}H_N$ transverse relaxation experiments (^{1}H-R_2). $^{1}H_N$ transverse relaxation experiments require acquisition of spectra with multiple time points (relaxation delays). eq. (1). For unfolded proteins optimal relaxation delay times are from 10 ms to at least 160ms. T2 is obtained by fitting data obtained at multiple relaxation delays to eq. 1.

$$I(t) = I(0)\, e^{-t/T_2} \text{ ; where } {}^{1}H{-}R_2 = {}^{1}/_{T_2} \quad (1)$$

For the calculation of error we measure duplicate time points (at least two) and use a standard error propagation routine.

PRE data analysis – obtaining paramagnetic relaxation enhancement rates (PRE rates, Γ).

1. Analyze the relaxation experiments using a standard processing procedure for relaxation experiments to obtain paramagnetic and diamagnetic relaxation rates (^{1}H-$R_{2,\,para}$ and ^{1}H-$R_{2,dia}$). Diamagnetic relaxation rates (^{1}H-$R_{2,dia}$) are attributed to the intrinsic relaxation of the nuclei, while the paramagnetic relaxation rates (^{1}H-$R_{2,para}$) are the sums of the intrinsic relaxation rates and the enhancement of relaxation caused by the proximity of the spin label. Thus, the paramagnetic relaxation enhancement rate (PRE rate - Γ) is the difference of the relaxation rates of the paramagnetic and diamagnetic samples (eq. 2).

$$\Gamma = {}^{1}H\text{-}R_{2,para} - {}^{1}H\text{-}R_{2,dia} \quad (2)$$

Direct correlation of PRE rates to distances is complicated due to the fact that the residue is experiencing a weighted average of all possible populations of the complex (*see* **Notes 10-11**). Due to the $\langle r^{-6} \rangle$ dependence, the populations that have closer distances are more heavily weighted.

2. To obtain a detailed analysis of transient interactions it is necessary to incorporate spin labels at many different positions. It is suggested that spin labels be placed at approximately every 10-30 residues for intra-chain PRE experiments, and inter-chain PRE require similar or even more extensive spacing of spin labels (*see* **Note 12**).

2.2.5. Notes

1. *Cysteine mutation requirements for PRE experiments.* Many of the spin labels that are used in the PRE experiments are thiol specific, which means that they interact specifically with cysteines to form disulfide bonds. For the interchain-PRE scheme to work successfully a single cysteine has to be present in the protein. Therefore site directed mutagenesis schemes may have to be applied to either remove intrinsic cysteines and/or to introduce single cysteine mutations into the protein..[243-246]
2. *Testing protein functionality upon mutation and spin labeling.* The PRE approach using site directed mutagenesis has many advantages, but introducing mutations and MTSL modifications could cause changes in the protein function and structure. Thus it is recommended that a functionality test be performed on the mutated and/or MTSL spin labeled proteins.
3. *Detection of distances in PRE experiments.* The positions of the spin labels should be chosen with care both to minimize the effect of the mutation on protein structure or function, as well as to optimize detection of the inter-chain PRE effect. Typically the spin label is able to enhance relaxation rates of the nuclei for distances up to approximately 25Å. Trial and error may be required for optimal selection of spin label positions. We recommend starting with

spin labels near the termini as well as central regions of the protein to obtain preliminary results and then fine tune around the interactive positions.

4. *Selection of the spin label.* Commonly used are cysteine specific and nitroxide derivatives (for example: MTSL, TEMPO - ((2,2,6,6-Tetramethylpiperidin-1-yl)oxy), PROXYL – (3-(2-Iodoacetamido)-2,2,5,5-tetramethyl-1-pyrrolidinyloxy)), or metal chelating groups (S-(2-pyridylthio)-cysteaminyl-EDTA, which in the paramagnetic form chelates Mn^{2+}, and the diamagnetic form chelates Ca^{2+}).[230,247,248] We use MTSL because it is small, generally stable and the reaction is highly cysteine specific and efficient.
5. *Optimize solution conditions to obtain maximum PRE effect.* PRE experiments are able to detect lowly populated interactions, even as low as 0.5-5%.[249] However, for weakly interactive species in IDPs it is extremely important to optimize buffer conditions and the experimental setup. For example many of the weak and transient interactions are stabilized through electrostatic interactions, so optimizing the ionic strength of the experiment will be important. Optimization includes selection of buffer concentration and type, ionic strength, ligand, and temperature.[250]
6. *Selection of sample concentration.* Sample concentration is another important variable in inter-chain PRE experiments. For weakly associating proteins, increasing the concentration of the spin labeled protein may lead to an increase in non-specific interactions driven by diffusion. We recommend using a low concentration of spin labeled sample on the order of 0.5 mM or less to avoid collisional non-specific interactions.[230] We mix 0.25 mM NMR visible chain with 0.25 mM NMR blind-spin labeled chain to be able to detect PRE and avoid non-specific interactions arising from collisional diffusion.
7. *Selection of paramagnetic sample reducing agent.* There are many reducing agents that can be used to reduce the paramagnetic form of the spin label to the diamagnetic form. Options include β-mercaptoethanol (BME), dithiothreitol (DTT), and ascorbate ions (either as ascorbic acid or sodium ascorbate). BME and DTT break disulfide bonds and thus they are able to cleave the

MTSL spin label attached to the cysteine. Ascorbate reduces the nitroxides to hydroxylamine with no cleavage of the MTSL.[251] Another option is to obtain the diamagnetic analogue of MTSL, MTS (1-Acetyl-2,2,5,5-tetramethyl-3-pyrroline-3-methyl)-methanethiosulfonate), and attach this compound to the cysteine using the protocol described above. The drawbacks of BME and DTT are that elimination of the spin label results in different para- and diamagnetic samples. Additionally, DTT is pH sensitive and the reaction needs to be performed at pH higher than 7. We recommend using ascorbate ions to obtain the diamagnetic form of the protein as the MTSL spin label will remain and the paramagnetic and diamagnetic samples will thus be more identical. Care needs to be taken as ascorbic acid changes the pH of the sample (pH changes vary depending on the buffer), while sodium ascorbate changes the ionic strength of the sample (by ~ 5mM). In order to readjust the pH or ionic strength buffer exchange may be necessary. Buffer exchange may change the sample concentration and para- and diamagnetic sample concentrations may not be identical.

8. *Preparation of the spin labeled sample –usage of desalting column.* To prepare for the paramagnetic spin labeling reaction there are two important steps. 1) First all disulfide bonds that may have been formed between the cysteine containing monomers need to be removed. This is achieved by incubating the sample with the reducing agent DTT for a few hours. 2) Second, after the reduction of disulfide bonds it is critical that all DTT be removed from solution before the spin label reaction is performed. Thus, for fast and complete removal of DTT from the protein solution a desalting column should be used. The spin labeling reaction will not work in the presence of DTT (see note 7 for preparation of diamagnetic sample), and there is a danger that the reaction will not go to 100% completion and the reaction product will be diamagnetic, not paramagnetic as desired.
9. *Completion of spin labeling reaction.* To test if the MTSL spin labeling is complete MALDI spectra of the sample can be acquired. Incomplete spin labeling, even at small percentages, will diminish the PRE values.[252]

10. *Comparison of ^{1}H-R_2 values of diamagnetic sample (with reduced spin label) and non-labeled sample.* Comparison of the diamagnetic sample with the wild type unlabeled ^{14}N sample is a further check that the diamagnetic sample has maintained its integrity and that the conformational ensemble of the diamagnetic protein is similar to the unlabeled protein as sampled by ^{1}H-R_2 values.[56] If there are big differences in the ^{1}H-R_2 values of the diamagnetic sample and the non-spin labeled control, it could mean that the sample is degrading or aggregating and should not be used.
11. *Interpretation of the PRE rates - protein and spin label flexibility.* Issues regarding the flexibility of spin labels and the effect on the PRE rates are thoroughly described in a highly recommended review by Iwahara and Clore.[230] If the protein belongs to the class of IDPs, or if the protein exists in more than one form, then the PRE rates are weighted averages over the interactions. PRE distances scale between the unpaired electron and the nucleus as $\langle r^{-6} \rangle$ and thus the fragments that have shorter distances will dominate the PRE rates.
12. *Spin label sampling for mapping of hetero-interactions.* To obtain a good sampling of protein contacts it is important to have an appropriate number of spin labels across the protein. Papers describing the density of spin labels for intra-chain PRE experiments suggest placing a spin label every 10-30 residues.[51,253-256] For inter-chain PRE experiments we suggest at least the same spacing of spin labels per chain.

2.3. Biological methods

All biological experiments were performed in the laboratory of Dr. M. Maral Mouradian with the assistance of Dr. Run Yan.

2.3.1. Cell culture maintenance

Two strains of human neuroblastoma undifferentiated SH-SY5Y cells were used in the research: a native strain and a strain stably transfected with αS. The cell culture was maintained using 10%

Fetal Bovine Serum (Life Sciences) with 90% of Dulbecco's modified Eagle's medium (DMEM) with L-Glutamine, sodium pervade and L-glucose (4.5 g/L) (Sigma or Corning). Cells stably expressing αS also required 250 μg/ml of G418 antibiotic (Sigma) for plasmid preservation. Cells were maintained in tissue-culture plates from Sigma or Corning, incubated at 37°C in in 5% CO_2 atmosphere. Cells were grown until 70-80% confluence between each pass. Cells stably expressing αS are more vulnerable and should not be in concentrations lower than 15% after passage as they would not recover. Cell passage was performed in sterile conditions ensured by: (a) 5 min. UV lamp prior to passage, (b) 2 min. hood blowerprior to passage, (c) careful sterilization of the work area and any items placed in the hood with 70% ethanol. The procedure for the cell passage (sub-culturing) was as follows:

1. Warm all solutions used in cell sub-culturing to 37°C.
2. Prepare new plates to which cells will be transferred. Label plates with the date, cell line name, dilution from the previous plate, and any additional information necessary for the experiment. In particular it should be noted if a different than usual percentage of FBS was used.
3. Check by optical microscopy that the concentration of the cells on the plate is 70-80%.
4. Remov medium using a vacuum device under the hood.
5. Wash cells with 10 mL of PBS. (5 sec)
6. Add of 1mL of 0.05% trypsin-EDTA solution for 1 min or until the cells start to deattach from the plate (large chunks of cells floating on the plate visible to the naked eye). It is helpful to tap the plate several times against the bench surface under the hood to help the cells to deattach.
7. Add 9 mL of 10% FBS+DMEM medium to a final volume 10 mL in order to halt the trypsin reaction. Break up cell clusters by by pipetting media up and down the plate; cells transferred to the new plate should be separate not in clumps.

8. Transfer the cells to the new plate. Eukaryotic cells usually divide every ~24h, so plan the experiment accordingly. Usually cells should not be split in dilution ratios higher than 1:20.
9. Monitor cells under the microscope. They should be round and spread out evenly not in clumps.

2.3.2. Cell toxicity assay – LDH assay.

The LDH assay is a commercially available calorimetric assay which measures the amount of released lactate dehydrogenase which is a cytosolic enzyme that is indicative of toxicity. The assay kits used were from Roche and Pierce. The cell toxicity assay was used to monitor the effect of different protein variants and oligomeric species on the cell lines.

The protocol used was as follows:

1. Sub-culture the cells into a 96 well plate. Treatment should be started when cells are at 40-60% confluence in the plate wells.. Calculate and plan accordingly, taking into account the reduced surface of the wells. Growth medium is DMEM+10% FBS. Cells need to be sub-cultured onto the well plate at least 12h before treatment to ensure their recovery.
2. Incubate cells in DMEM (100 uL) without any FBS for 2-16 hours before treatment to ensure that all the cells will be synchronized in the cell cycle. Incubating with DMEM also has the advantage of keeping cells at the desired density.
3. Add 100uL of DMEM+2% FBS to the wells. Thus the final concentration of FBS should be 1%. The FBS concentration can be lower for short treatments. FBS gives fluorescence signal so while using LDH assay, so too high concentrations of FBS are not recommended.
    - Note: Multiple washing removes cells from the plate and changes theirs morphology. This not healthy, so the number of washings should be reduced to a minimum. For this reason we add 100uM of DMEM+2%FBS to the cells without removing the old solution (100 uM DMEM without FBS) first.
4. Add treatment to the cells. Treatment in my case meant different species of αS or βS, but in general it could be anything including proteins, inhibitors or chemical compounds. The

concentration of the treatment should be adjusted by performing a concentration dependent assay. In the case of oligomers we varied the concentration from the nM to uM range. Each samples must be repeated at least 4 times for statistical accuracy.

5. Controls that need to be included in the assay include: (a) a background control: buffer, (b) a negative control: untreated cells, (c) a positive control: cells releasing 100% LDH by treatment with 10% triton or with lysis buffer. We used triton but was not satisfied with results, so we would recommend using the lysis buffer.
6. Incubate plate for desired amount of time. Monitor cells for signs of change in the morphology. We used times ranging from 24-72h of incubation.
7. Prepare assay solution according to the manufacturer's protocol. Protocols will vary depending which LDH kit is used.
8. Transfer 50 uL of the media from cells to a new well plate and add LDH assay mix.
9. Start time measurement. Maintain cells at 15-20°C. Maximum time used is 30 min. Protect from light. Stop solution can be used if necessary.
10. Obtain reading at 490 nm wavelength excitation. It is recommended to obtain readings at multiple time points.
11. Calculate the cell toxicity according to the equations provided in the assay protocol.

2.3.3. Immuno-staining and cell imaging

Preparation of the coverslips

1. Cells for imaging need to grow on coverslips. To prepare the coverslips incubate them at least overnight in 1% collagen at 37°C. Coverslips must be covered with collagen and cannot float on the surface. Using forceps place the coverslips on the bottom of the plate.
2. Remove collagen from the plate. Dry the coverslips. If the coverslips attach to the bottom of the plate add some PBS to facilitate their removal.

Cell considerations

1. For the treatment 2 coverslips will be used per experiments: one coverslip with be treated with 1% triton in PFA to extract soluble fractions from the cells; the other coverslip will be without extraction.
2. Controls. both extracted and non-extracted untreated cells are used. Cells treated with monomers were also correct controls in my case.
3. Native cells vs. cells stably expressing αS. It is preferable to obtain results usingnative cells rather than cells stably expressing αS, as they are more reliable and uniform. However if native cells are unavailable, cells stably expressing αS can also be used.
4. As the treatment here is long, the cells at the start of the treatment should be at a density of 25%.
5. Before starting the treatment cells should be given time to recover after subculturing. At least 12 h should be given to the cells to recover, but more time is better.
6. Transfer the cells and coverslips to a smaller dish before starting treatment.

Fixing and staining

Necessary materials

- 4% PFA refrigerated at 4°C
- PBS
- 0.5% triton in PBS
- 1% triton in PFA
- Stock 100% donkey serum in restriction enzyme stored in refrigerator
- 1' antibody (flag 1:300/myc 1:1000)
- 12' antibody in donkey serum
- 0.01% ThioS. (10mg in 10g and then dilute 10x)
- DAPI

Note: Caution needs to be applied when preparing the solution of triton, as it is highly viscous. It is helpful to cut the end of the pipette tip when pipetting in triton. Also when adding triton to the solution it needs to be pipetted in an out multiple times.

Protocol

Work with cells should be performed under hood until step 13.

1. Wash cells with PBS.
2. Stain with 0.01% ThioS for 8 min.
3. Wash with PBS
4. Select non-extracted and extracted cells.
    a. Extraction cells: Add 500uL of 4% PFA+1% triton.
    b. Normal cells: Add 500uL of 4% PFA.
    c. Incubate both samples at 37˚C for 13 min. From here both cells are treated in the same way.
5. Wash with PBS 10s.
6. Permeabilize with 250-500 uL of 0.5% triton x100 in PBS. Incubate for 10 min at 37˚C.
7. Block with 350 uL of 5% Donkey Serum at 37˚C for 20 min.
8. Add 1' antibody 350uL, cover with foil, incubate at 4˚C overnight.

    NOTE: Collect antibody to reuse it!
9. Wash with 500 ul PBS 3x, 5 min. at ambient temperature.
10. Add 350uL of 2' antibody (1:1000), cover with foil and incubate at 4˚C for 1h.
11. Wash with 500 uL PBS 3x, 5 min. at ambient temperature.
12. Add DAPI 1.5uL+1 mL of PBS, 1.5 min at ambient temperature
13. Now you can work on the bench.

14. Mount the coverslips onto the rectangular glass. As cells are growing on the coverslips. Cells from the coverslips should face the inside of the glass. Add 5-10uL of the mounting buffer (depending on how much time one has for drying).
15. Add dried coverslip on the top with cells facing the mounting buffer. Remove bubbles carefully, by pressing with forceps on the glass. Don't press too hard.
16. Dry in the cold room until coverslips are not moving anymore.

Comments:

- At the step with PFA cells will deattach. Be very gentle at all steps to avoid disturbance of the cells and to have something to look at.
- Maintain cells in PBS if solution has been removed so that they do not dry out.
- ThioS gives a strong and sometimes non-specific signal. That is why we stain with ThioS before fixing cells first, so that there are multiple washings before imaging.

Imaging

1. Turn on UV lamp in the microscope at least 20 min before usage of the microscope.
2. Turn microscope on.
3. Check if the objective lens is clean. Wash it using specific washing solution.
4. Wash coverslips using ethanol and kim wipes.
5. Turn on imaging program AxioVisionRels4.7
6. Turn on multidimensional acquisition. We use channels for DAPI (blue), αS (Red) and ThioS (green).
7. Go to settings on the top channel and pick objective 63x. Activate selection. Objective 63x is an oil objective. Read the labels on the objective to make sure that the correct objective has been selected.
8. Turn on the laser light.
9. Switch the colors of the laser using the screw below the objective.

10. Apply a drop of oil on top of the oil objective.
11. Secure the sample on the racks on top of the objective.
12. Moe the objective up and touch the sample with the drop of oil on the top of the objective. Be careful not to bump the sample with the objective. Observe the samples on the DAPI channel. If the picture is sharp, you are in the plane of the sample.
13. Start acquisition. For the ThioS and αS channels use the same gain for all the samples. It is better to use a slightly lowerbecause information on color intensity is lost at higher gains, as all the colors are saturated.
14. Save the pictures.
15. To clean up:
    a. Turn off the light.
    b. Wash oil off the objectivecarefully to avoid lens damage.
    c. Put objective in low position.
    d. Switch objective to no objective position
    e. Turn off microscope.
    f. Turn off UV lamp.

2.4. Oligomer preparation and methods used in their characterization

2.4.1. Oligomer preparation

1. Weigh lyophilized sample of αS or βS.
    a. Usually we used an overall concentration of 12 mg/mL of protein for αS and βS samples. For mixed αS/βS samples we used 6mg/mL of each protein for a final concentration 12 mg/mL

b. Samples of 6mg/mL of αS or βS or an overall concentration of 24 mg/mL for αS/βS mixture were used as controls.

2. Dissolve sample in PBS by leaving in room temperature or incubating at 37°C in oven.
3. Remove large order species by centrifugation at 14000rpm for at least half an hour.
4. Transfer sample to 96 well plate. Maximum volume of each well is 150uL. Do not exceed this volume; otherwise sample will spill.
5. Incubate with shaking for desired amount of time. We used a fluorimeter to shake the sample: 700rpm linear shaking at 37°C.
6. After incubation for the desired amount of time remove sample from the well plate.

2.4.2. Oligomer purification

1. The incubated mixture of the protein can contain monomers, oligomers, and fibrils. Thus it is necessary to separate the different species from the sample.
2. To remove fibrils from the sample spin the sample at 14000rpm for an hour. The fibril has high molecular weight so it is possible to remove fibrils from the sample using centrifugation.
3. Separation of the oligomers from monomers was performed using two methods: (a) size exclusion column and (b) filters.
    a. Superose 6 or superdex columns were used to separate monomers from oligomers. 1mL of a 12 mg/mL sample incubated as described in the previous paragraph was injected into a column equilibrated in PBS buffer. Oligomeric and monomeric samples were collected. If a superdex column was used, all oligomers were located in the void volume of the sample, while if a superose 6 column was used for incubated samples of αS, βS and αS/βS mixture two distinct populations of the protein were eluted, so it was possible to collect them separately. The flow rate used was 0.5 mL/min.

b. For purification with filters, I used Amicon 0.5 ml filters with two different cutoffs of 50kD and 100kD. To remove oligomers from monomers we applied the monomer/oligomer mixture through the filters. As oligomers exhibit higher molecular weight than monomers, the monomeric sample passed through the filter and the oligomeric fraction remained in the retentate. The sample was spun at least 3 times at 14000 rpm when using either of the filters.

Chapter 3. Comparison of acetylated and non-acetylated βS

The recent article by Bartels *et al.*[27] rediscovered N-terminal acetylation in αS in vivo. Similarly to αS , βS is also acetylated[257], but all biophysical experiments until then had been performed on the non-acetylated form of the protein[258-260]. In the case of αS N-terminal acetylation induced the formation of a transient 9-residue long N-terminal helix. It is possible that the N-terminal helix facilities interactions with the ligands of αS. For example it was shown that the formation of the N-

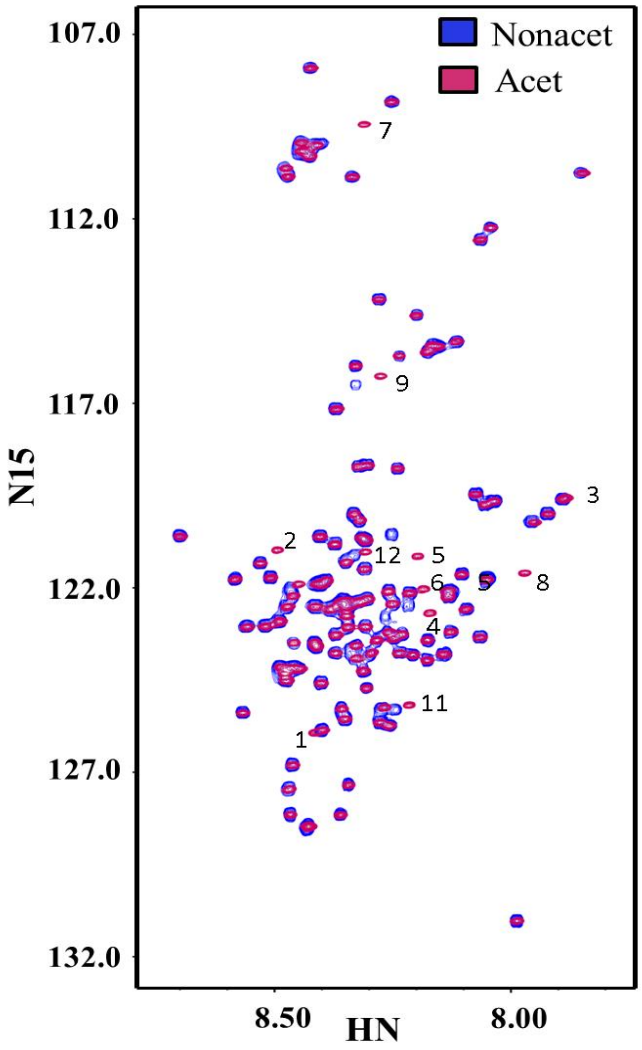

Figure 6. HSQC overlay of non-acetylated (blue) and acetylated (pink) βS. Changes in positions of the peaks are marked on the spectrum with the corresponding residue number.

terminal helix increases aS membrane affinity.[261]

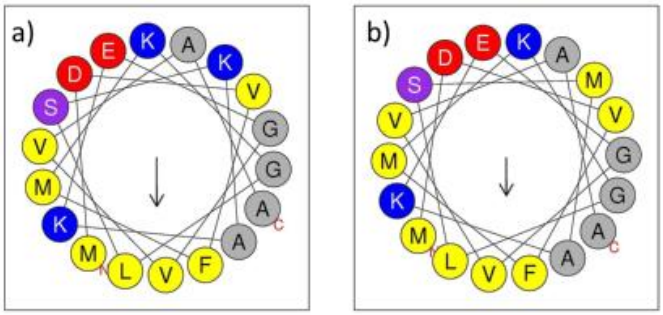

Figure 7. Helical representation of first 18 residues of a) αS b) βS

Since βS is acetylated in vivo similarly to αS, we sought to investigate the effect of the N-terminal acetylation of βS on its ensemble. We performed a characterization of the acetylated form of βS in the solution via NMR and other biophysical methods. NMR characterization of the acetylated βS provided a highly similar HSQC profile to the non-acetylated form of the proteins. HSQC exhibited only local differences between the acetylated and non-acetylated forms of βS, which are located at the N-terminus. (Figure 6) Introduction of N-terminal acetylation induced changes in the first 12 residues according to the HSQC spectra. In the non-acetylated sample the first 2 residues were broadened beyond detection due to their high flexibility, but N-terminal acetylation was able to recover the signal for these two residues. N-terminal acetylation of βS results in changed locations of the peaks of the first twelve N-terminal residues on the HSQC spectra, resulting in better dispersion of the peaks for this fragment.

We compared the effect of N-terminal acetylation for αS and βS, since N-terminal acetylation of both proteins results in the formation of a transient N-terminal helix. αS and βS have very similar sequences in the N-terminal. In the first 25 residues there is only one residue difference between these two proteins: αS has lysine and βS has methionine at position 10. Helical wheel analysis shows that the Met at position 10 expands the hydrophobic surface of βS, suggesting that possibly βS is more prone to formation of an amphipathic helix. (Figure 7) Our data show indeed that due to N-

terminal acetylation the N-terminal helix encompasses the first 12 residues of βS and only 9 of αS according to the HSQC perturbations. It is possible that by exhibiting slightly higher helical propensities in the beginning of the N-terminus bS is could be more likely to bind with membranes than αS.

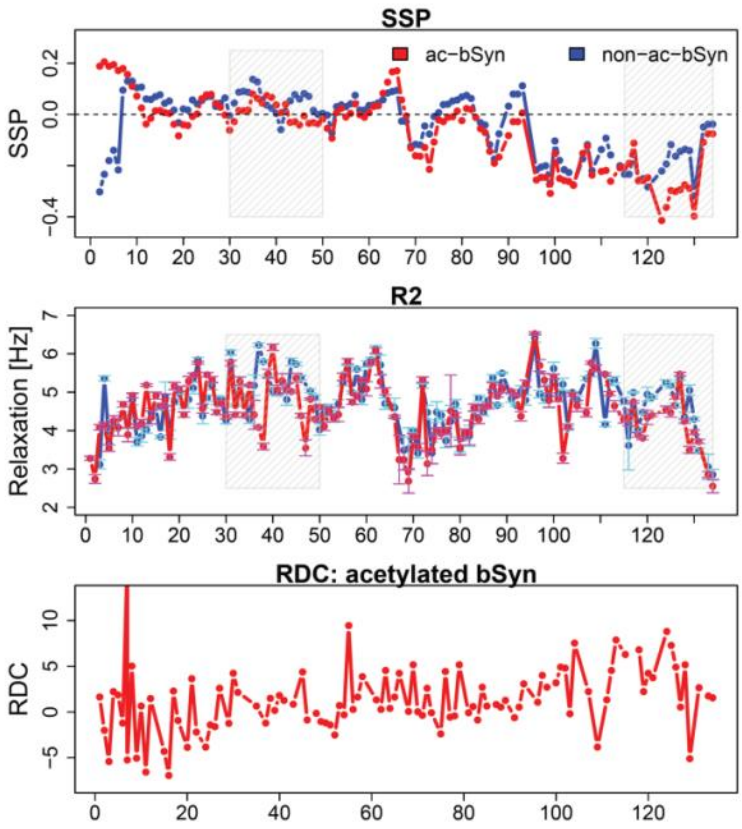

Figure 8. Characterization of acetylated βS (red) and comparison with the non-acetylated form of the protein (blue). (A) SSP of acetylated and non-acetylated forms of the protein. (B) R2 relaxation rates. (C) RDC profile of acetylated βS.

We extended our analysis of the effect of N-terminal acetylation of βS by checking secondary structure propensity changes in the acetylated and non-acetylated forms of the proteins. Secondary structure propensities of acetylated βS suggest the presence of a helix in first 11 residues on average 20% of the time. (Figure 8, A) In general acetylated βS has on average no pronounced secondary structure in the N-terminal and NAC regions, but surprisingly it affects β-sheet propensities in the C-terminal. Overall, acetylation induces only slight changes in the secondary structure propensities (fig.

8A). The acetylated βS, except for the initiating helix and residues 38-42, 63-68 and 115-117, exhibits higher β-sheet propensities than its non-acetylated counterpart. The N-terminal and NAC regions have positive and negative values of SSP without any pronounced trend. As for the C-terminal changes, it appear that there are three distinct regions in the C-terminus where the secondary structure is affected: residues 95-101, 102-116 and 116-126. The long range effect on the secondary structure could be a reason for the decrease in the Cα chemical shifts in in fragment C-terminal at residues 123-130.

Both the acetylated and non-acetylated forms of βS have an NAC domain that is more dynamic than the N and C terminal domains based on the NMR relaxation experiments (fig. 8B). This is consistent with previous data. Overall, the acetylated and non-acetylated forms of βS exhibit highly similar dynamics with a few minor differences. Acetylated βS is more flexible in residues 44-47, 117-125 and 128-130. Stretches 44-49, 117-125 and 128-130 correspond to the regions with less β-sheet propensities in the non-acetylated sample.(Figure 8, B) Surprisingly, acetylation has no effect on the dynamics of the N-terminal domain (as is the case with αS) despite the significant secondary structure changes in that region introduced by acetylation .

To detect if there are any changes that N-terminal acetylation could induce in the general conformation of the proteins, I performed RDC experiments on the acetylated βS. Acetylation induced broadening of first 10 residues in the aligning media, so I was not able to obtain signal from this region of the protein. The general conformation of the protein is not affected by the introduction of N-terminal acetylation as the observed RDC pattern is highly similar to that reported in literature.[194] The N-terminal and NAC domains have RDC values close to 0, while three regions in the C-terminal domain display increased RDC amplitudes. These are residues 92-107, 111-119, and 120-126.(Figure 8, C) The increase in the RDC values is thought to be related to the existence of secondary structure in that region and indeed SSP profiles point to the existence of polyproline II

secondary structure in this region, which is reflected in the increased RDC values that mirror the chemical shifts.

In summary, N-terminal acetylation induces formation of a transient N-terminal initiating helix in the βS ensemble, but it does not significantly affect other properties of the protein. However, this does not mean that N-terminal acetylation is not important for the function of the protein, as it is likely to affect membrane binding of βS.

Chapter 4. Toxic βS mutant characterization: P123H and V70M.

In this chapter I will describe my work on two mutants of βS, V70M and P123H, that are implicated in the respectively sporadic and familiar cases of diffuse Lewy body disease. Disease-related mutations render βS toxic and affect the lysosomal pathway of the cell. However neither of these mutations induces formation of the Lewy Body like inclusions. Possibly the mutations affect βS's oligomerization and aggregation propensities and possibly other cellular pathways. The work presented here on P123H and V70M mutants also provides insights into the non-toxicity of native βS.

4.1. P123H mutant

Data from this paper was submitted to Protein Science. Currently paper is under revision.

β-synuclein mutant P123H associated with Dementia with Lewy Body disease has a similar C-terminal conformation to α-synuclein and accelerates its fibril formation upon co-incubation

Maria K. Janowska[1]and Jean Baum[1]*

Abstract

β-synuclein (βS) is a homologue of α-synuclein (αS), the major protein component of Lewy bodies in patients with Parkinson's disease. In contrast to αS, βS does not form fibrils, mitigates αS toxicity in vivo and inhibits αS fibril formation in vitro. Recently a missense mutation of βS, P123H, was identified in patients with Dementia with Lewy Body disease. The single P123H mutation at the C-terminus of βS is able to convert βS from a non-toxic to a toxic protein that is also able to accelerate inclusions formation when it is in the presence of αS in vivo. To elucidate the molecular mechanisms of these processes, we compare the conformational properties of the monomer forms of αS, βS and P123H-βS, and the effects on fibril formation of co-incubation of αS with βS, and with

P123H-βS. NMR residual dipolar couplings and secondary structure propensities show that the P123H mutation of βS renders it more flexible C-terminal to the mutation site and more αS-like. In vitro Thioflavin T fluorescence experiments show that P123H-βS accelerates αS fibril formation upon co-incubation, as opposed to wild type βS that acts as an inhibitor of αS aggregation. When P123H-βS becomes more αS-like it is unable to perform the protective function of βS, which suggests that the extended polyproline II motif of βS in the C-terminus is critical to its non-toxic nature and to inhibition of αS upon co-incubation. These studies may provide a basis for understanding which regions to target for therapeutic intervention in Parkinson's disease.

Introduction

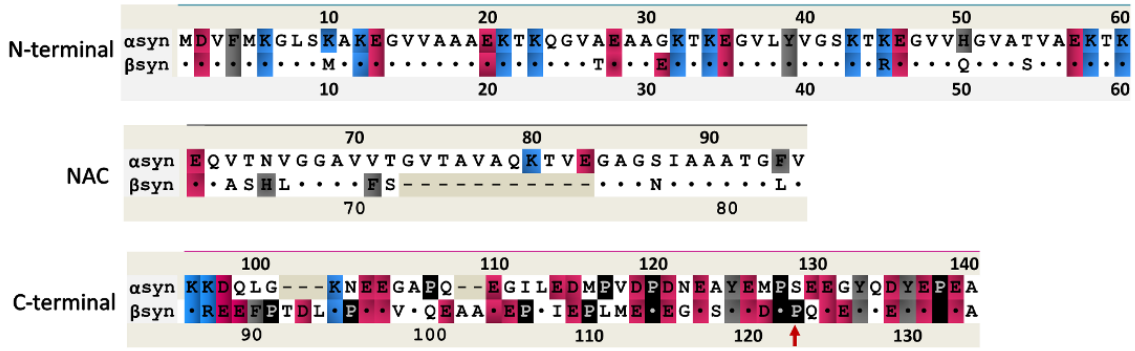

Figure 9 Aligned sequences of αS and βS for three regions of synucleins: N-terminal, NAC, C-terminal. Identical residues are shown by dots in ßS sequence and deletions are shown by dashes. The mutation site is indicated by the arrow below the sequence. Residues are color-coded according to the scheme: blue - positive charges, red - negative charges, black - prolines, grey-aromatic residues.

Alpha-synuclein (αS) is widely known for its involvement in Parkinson's disease, as Lewy Body inclusions that contain αS are found in post-mortem diseased brains.[262,263] αS belongs to the synuclein family of proteins, which in addition to αS contains two homologs: beta and gamma synuclein.[166] All of the members of the family are small neuronal lipoproteins, but only αS and beta-synuclein (βS) co-localize pre-synaptically in the brain.[14,21,264] αS and βS have high sequence similarity (78%) but they differ at the point of their self-association properties. αS self -aggregates to pathological oligomers or

fibrils, whereas βS forms oligomers more slowly and does not form fibrils on its own.[167,193,199,200] Interestingly, there is evidence showing that βS can inhibit αS aggregation in a dose dependent manner, and can mitigate the effects of αS toxicity in vivo.[167,172,174,175,177,265-267]

Although wild type βS does not appear in pathological Lewy Body plaques or fibrils *in vivo*,[7] two βS mutations, V70M and P123H, were recently identified and found in sporadic and familial dementia with Lewy Bodies (DLB), respectively.[190] Studies on cell line models revealed the involvement of P123H and V70M in lysosomal pathology, and studies on mouse models for the P123H-βS mutant proved it to be toxic. P123H-βS exarcerbates αS pathology as the number of lysosomal inclusions increased upon co-expression of βS mutants with αS.[191,192] Furthermore, transgenic mice models of P123H-βS exhibit extensive neuritic pathology (swelling of striatum and globus pallidus, due to formation of small spheroids), but do not result in formation of Lewy Body inclusions.[192] The neuropathy of P123H-βS is not abolished in αS knock-out mice, but is enhanced in the P123H-βS/αS doubly transgenic mice.[192] These facts demonstrate that just a single mutation in βS sequence is able to overcome the non-aggregating and inhibitory nature of wild type βS and that P123H-βS is toxic by itself.[190-192]

αS and βS are intrinsically disordered proteins described by three regions: the N-terminus that contains KTKXGV repeats and forms helices at membranes, the non-amyloid-β component (NAC) region, and the highly acidic and solubilizing C-terminus (fig. 9).[166] The N-terminus of αS and βS are highly similar as there are only six residue differences between αS and βS, and the C-terminus is the least conserved region with more prolines and more negatively charged residues. βS has an 11 residue deletion in the NAC region, which is in the core of the αS fibril. This suggests that the non-fibrillar nature of βS may come from this deletion; however insertion of this region back into βS does not recover the full fibrillation potential of βS.[193,199,200]

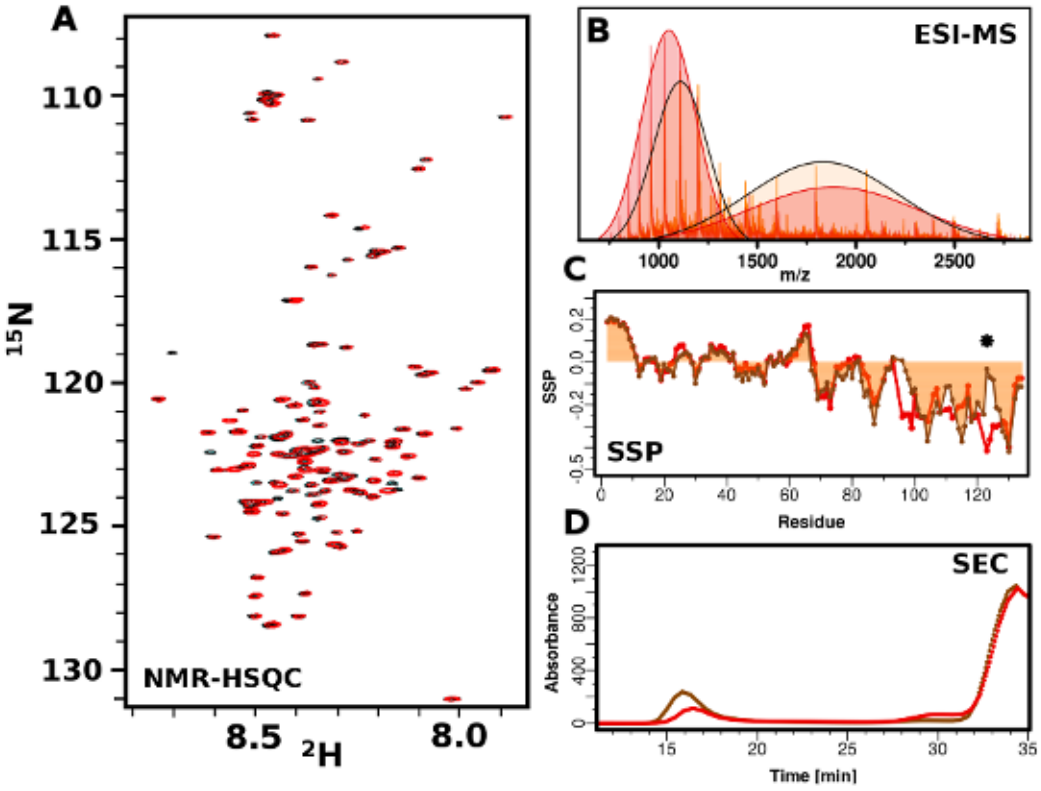

Figure 10 Biophysical characterization of βS and P123H-βS mutant. (A) ^{1}H-^{15}N-HSQC spectra of βS (red) and P123H-βS mutant (black) in 10mM MES, pH6, 100mM NaCl. (B) ESI-MS of βS (red) and P123H-βS (orange) in 10mM ammonium acetate buffer, pH 6. Extended and compact conformations are indicated by fitting two Gaussians. βS populates 46% compact and 54% extended conformations while P123H-βS populates 51% compact and 49% extended conformations. (C) Comparison of secondary structure propensities (SSP) of βS (red) and P123H-βS (orange) in 10mM MES, pH6, 100mM NaCl. Positive values indicate α-helical secondary structure propensity, while negative values correspond to β-Sheet or PPII propensity. The star indicates the position of the mutation. (D) Size exclusion profile using the Superose 6 column, which has a separation range of 5000 to 5000000 Da for βS (red) and P123H-βS (orange) after 5 h of incubation at 37°C with agitation in PBS, pH 7.4. βS and P123H-βS have similar monomer elution profiles and P123H-βS generates oligomers that are eluted in the void volume

From the biophysical point of view the N, NAC and C-terminal regions of αS display different properties. The N-terminus has a small net charge and is best described as a polyampholite chain with more globular-like characteristics, while the C-terminus is highly negatively charged, has 5 proline residues and is best described as a polyelectrolye chain with more chain stiffness.[63,268] Both the N-terminus and NAC region bind membranes and fold to a helix upon binding. The C-terminus

of αS and βS does not bind directly to the membranes and is suggested to have chaperone activity.[91,269,270] Thus in general synucleins have an N-terminal and NAC membrane interactive region, and a C-terminal regulatory domain that may interact with other proteins and other factors. In the case of αS all the disease causing mutations are located in the N-terminus, while in βS the toxic mutations are found in the NAC and C-terminus.

In this paper we compare the monomer conformations of αS, βS and P123H-βS and the ability of αS, βS and P123H-βS to accelerate or inhibit αS fibril formation upon co-incubation. Our results indicate that P123H-βS behaves more like αS both in terms of its conformation C-terminal to the mutation site and in terms of its effect on αS fibril formation upon co-incubation. Both P123H-βS and αS have a less ordered C-terminus, and co-incubation of P123H-βS with αS or simply doubling the concentration of αS result in identical fibril formation kinetics. Our results suggest that the single P123H mutation in the C-terminal region of βS, which removes the double proline motif from the sequence, causes the conformational properties of the C-terminus to be altered and to resemble the C-terminus of αS. This renders P123H-βS unable to perform the protective functions of the wild type βS protein and suggests that the extended PPII motif of βS in the C-terminus is critical to inhibition and to its non-toxic nature.

Results

Comparison of P123H-βS and βS indicates that P123H-βS populates a higher percentage of compact conformational ensembles due to a more compact C-terminus.

To understand the basis for the different toxicity of βS and P123H-βS we performed their characterization via biophysical methods. αS and βS are acetylated in vivo; therefore our studies are performed on the acetylated forms of all proteins. Acetylated P123H-βS, similarly to wild type βS, is mostly unfolded and monomeric as shown through narrow HSQC profiles (fig.10A). HSQC differences between these two proteins are very small and mostly located close to the mutation site.

Electrospray ionization mass spectroscopy (ESI-MS) experiments indicate that both proteins are able to probe compact and extended conformations; however the population distributions are altered for

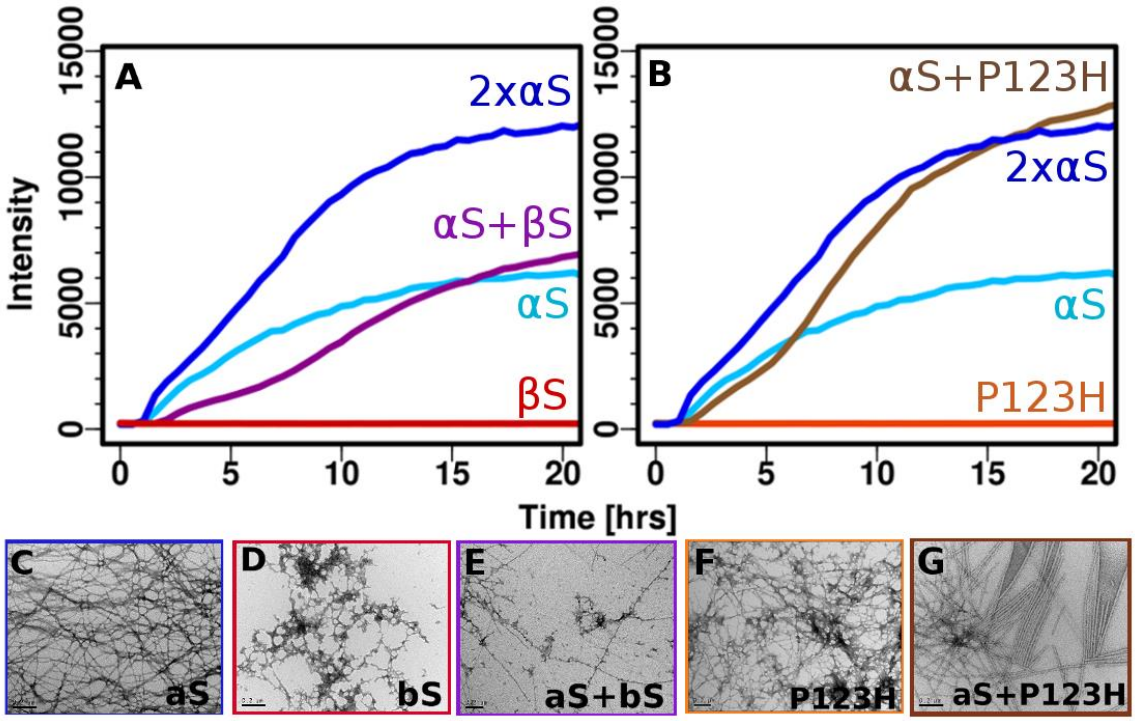

Figure 11 Aggregation inhibiton of αS by βS and aggregation enhancement of αS by P123H-βS (A & B). ThT fluorescence (37°C with shaking and teflon beads, PBS) of αS coincubated with (A) βS and (B) P123H-βS. Negatively stained electron micrographs (scale 200 nm) (C-G) of (C) αS fibrils, (D) βS amorphous aggregates, (E) co-incubated αS with βS, (F) P123H-βS amorphous aggregates, and (G) co-incubated αS with P123H-βS.

P123H-βS with a higher percentage of compact conformation relative to wild type βS (fig.10B). Secondary structure propensities reveal that the N-terminus and NAC region are essentially identical while the C-terminus displays differences particularly near the mutation site (Fig.10C). The βS C-

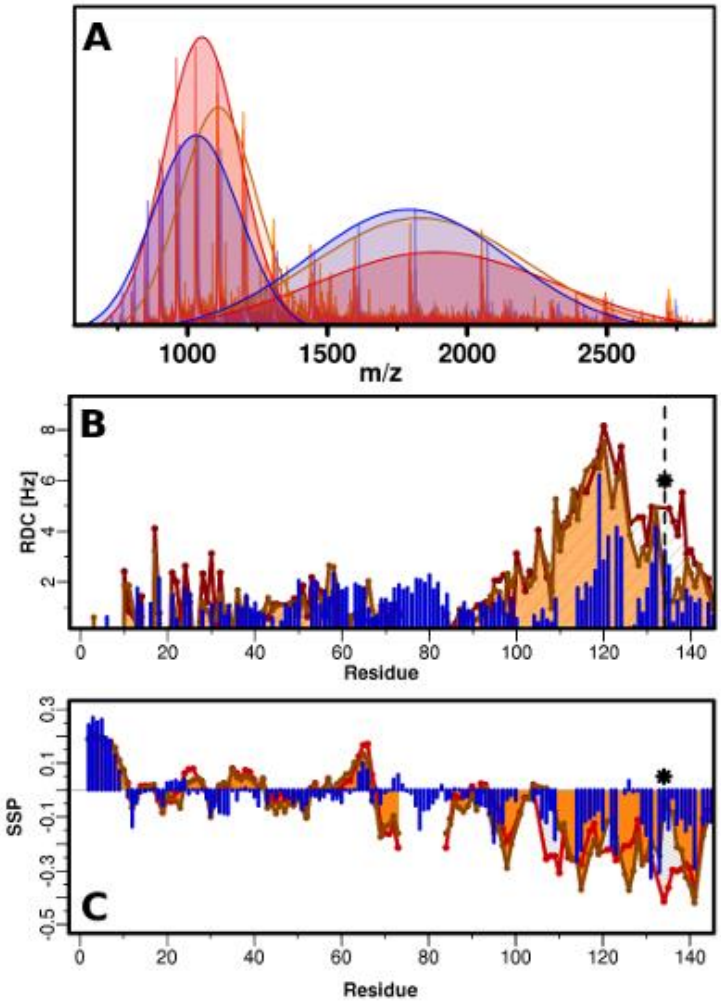

Figure 12 Three way comparison of αS (blue), βS (red) and P123H-βS (orange). (A) ESI-MS in 10mM ammonium acetate buffer, pH 6. Extended and compact conformations are indicated by fitting two Gaussians. αS: compact, 49%, extended 51%; βS: compact 46%, 54%; P123H-βS: compact, 51%, extended 49% (B) RDC profiles of αS (blue), βS (red) and P123H-βS (orange) in 10mM MES, pH 6, 100 mM NaCl, 250μM protein, measured in C8E5-octanol bicelle aligning media. The star and dashed line indicate the position of the mutation. (C) SSP measured in 10mM MES, pH 6, 100 mM NaCl, 350μM proteins for αS (blue), βS (red) and P123H-βS (orange).

terminus is extended and has uniformly negative values, which is suggestive of polyproline II (PPII) secondary structure.[260] The mutation at position P123H causes a discontinuity or break in the negative secondary structure propensities (SSP)[237] values suggesting that the conformation at the C-terminus is not uniformly extended and that the region around the mutation site is more random coil-like. The SSP data in conjunction with the ESI data suggest that the sampling of a higher

population of compact conformations may be due to the more compact nature of the C-terminus. Size exclusion chromatography was used to evaluate the existence of higher order species after five hours of incubation. Most of the protein eluted at 34 min, which is consistent with the monomer, but P123H-βS generated more oligomers that were eluted in the void volume, suggesting that the mutant is more prone to aggregation (fig.10D).

Co-incubation of P123H-βS mutant with aS accelerates aS fibril formation.

Co-incubation of αS with βS or with P123H-βS results in significantly different fibril formation profiles. It has been shown previously with non-acetylated protein that there is a dose dependent concentration dependence of fibril formation of αS co-incubated with βS, and that αS fibril formation is delayed in the presence of βS. We have shown similar dose dependent concentration results upon co-incubation of acetylated αS with acetylated βS (manuscript, submitted). While co-incubation with βS alone results in delayed fibril formation (fig.11A), co-incubation of αS with P123H-βS results in increased fibril formation rates relative to αS alone (fig.11B). More specifically, the kinetics of fibril formation resulting from doubling the original concentration of αS are almost identical to those of the co-incubated αS/P123H-βS. This supports the view that fibril formation is enhanced by P123H-βS and that αS interacts directly with P123H-βS. Co-incubation with P123H-βS and with 2 times αS shows a faster elongation phase as well as a doubling of Thioflavin T (ThT) intensity, suggesting that P123H-βS behaves very similarly to αS in terms of its ability to the form fibrils (fig.11B). P123H-βS when incubated alone is not able to form fibrils (fig.11B) and only forms amorphous aggregates as detected by transmission electron microscopy (TEM) (fig.11F). The differences in fibril formation are mirrored in the TEM data where αS alone forms fibrils (fig. 11C), βS forms amorphous aggregates (fig.11D), fibrils created upon αS co-incubation with βS are thinner and more branched (fig.11E) and where the fibrils formed upon coincubation of αS with P123H-βS are highly ordered (Fig.11G). These data are striking as they show that a single mutation in the C-terminus of βS can completely reverse the inhibition properties of βS on αS and that the mutant

protein behaves, in terms of fibril formation, in the same way as simply increasing the concentration of αS.

P123H-βS exhibits conformational characteristics of aS C-terminal to the mutation site.

A three way comparison of αS, βS and P123H-βS is provided in order to understand, at the molecular level, why a single mutation in βS would alter its inhibitory characteristics towards αS and result in accelerated αS fibril formation kinetics. ESI-MS experiments, SSP, and residual dipolar couplings (RDC) show clearly that there are conformational similarities between αS and P123H-βS relative to βS. ESI-MS experiments show that the population distribution of P123H-βS and αS are more similar with a higher population of compact conformation relative to extended (fig.12A). RDC profiles for all three proteins indicate that they are very similar in the N-terminus and that major differences in conformation arise in the C-terminus (fig.12B). βS has the highest and most uniform RDC values suggesting that the C-terminus from residues 95 to 134 is extended and rigid. αS shows increased RDC values in two distinct C-terminal hydrophobic patches, in agreement with previous literature, signifying increased order in these two fragments.[52,53,55,260] The P123H mutation of βS exhibits characteristics of both αS and βS (fig.12B): the RDCs are essentially identical to βS from residues 95 to 119 and are very similar to αS for residues 126 to 140. The lower RDC values of P123H-βS from residues 126-140 suggests a more flexible and less ordered C-terminus than that associated with βS, for which the RDC values remain very high. SSP comparison of these three proteins additionally highlights the fact that the single mutation in the double proline motif of P123H-βS breaks the uniformity of the beta-like secondary structure observed for βS (fig.12C). SSP shows two distinct C-terminal propensities for structure for P123H-βS with a break that is in the same position as the break in αS.

C-terminal flexibility results from loss of double proline motif.

The role of the double prolines at positions 122 and 123 appears to be very important in defining

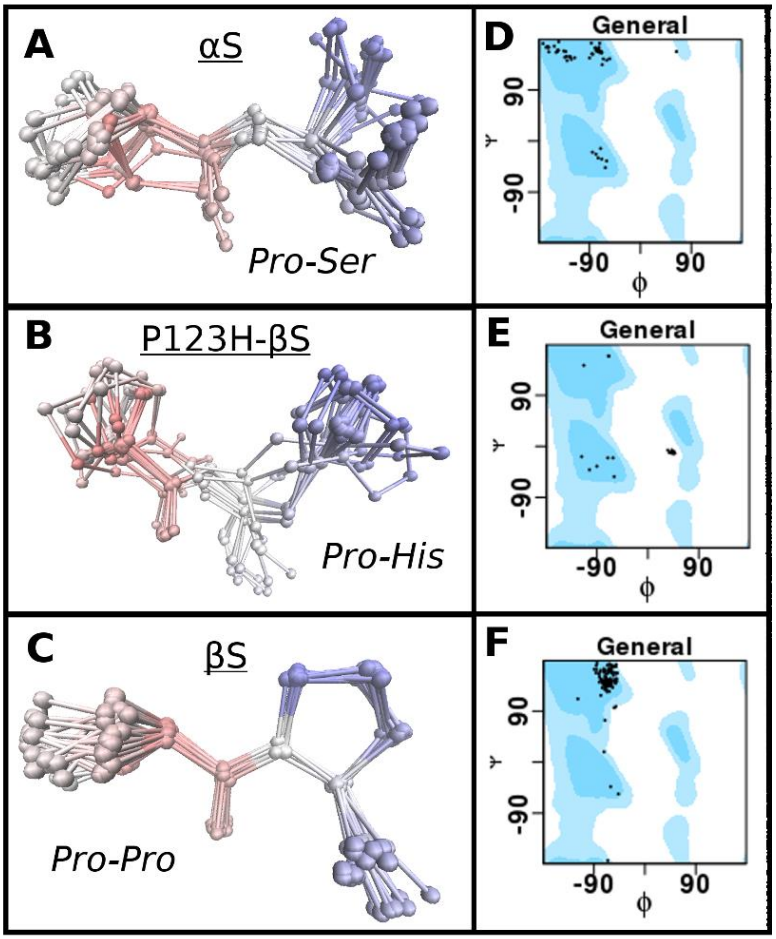

Figure 13 Comparison of possible conformational propensities of C-terminal motifs of αS (PS), P123H-βS (PH) and βS (PP) as described by Ramachandran plots. PDB database search was performed using the Psi-Blast algorithm to obtain fragments which contain motifs PS (αS), PH (P123H-βS) and PP (βS), but also shared similarity to the C-terminal sequences. (A-C) RMSD calculation and structure overlays of the hits were performed for : (A) αS (PS), (B) P123H-βS (PH) and (C) βS (PP). (D-E) Phi, Psi population distribution of the different hits for the respective motifs displayed as Ramachandran plots. General shows all of the allowed areas for proteins in blue and dots represent the positions of the Phi, Psi angles for the hits. Position of the Ramachandran plot shows ability of motifs to exist in certain secondary structures. Position of the secondary structures on the Ramachandran plot (Phi, Psi): helix: (-63, -43), beta-sheet (-135, 135), PPII (-75, 150), L-alpha helix (57, 47). (D) αS (PS), (E) P123H-βS (PH) and (F) βS (PP)

the conformation of the C-terminus as mutation of the ^{122}P^{123}P of βS into ^{122}P^{123}H of P123H-βS results in more flexible conformations C-terminal to the mutation as determined by RDC and SSP

data. To further investigate whether the double proline motif is crucial to maintaining the extended PPII sequence we performed a Psi-blast search to obtain the typical conformations of these motifs in the PDB. The search was performed across a 10 residue window that contained the PP motif of βS and its flanking sequences, the PS motif of αS and the PH motif of P123H-βS. Our results show that the double proline, PP, motif of βS is the most common of the three motifs in the PDB with 117 hits, while the PS motif of αS has 49 hits, and the PH motif of P123H-βS has only 23 hits. RMSD calculation and structure overlays of the hits were performed (fig.13A, 13B, 13C), and interestingly the most common motif is the least diverse (RMSD for the PP residues is the lowest with 0.35Å), while the RMSD for P123H-βS and αS motifs are almost twice as high with 0.77 and 0.70 Å, respectively. Ramachandran plots for these motifs indicate that PP is located primarily in the Phi, Psi region correpsonding to PPII (fig. 13F) whereas the PS motif of αS populates the PPII conformation only approximately 1/3 of the time (fig.13D) and the PH motif in P123H-βS does not populate the PPII conformation at all (fig.13E). The PH motif has a tendency to be located in the forbidden region of the Ramachandran plot just outside the region of the left handed alpha helix (fig.13E). The most varied secondary structure tendencies are sampled by the PS motif of αS with beta sheet, PPII, and the right handed alpha helix region as possibilities (but not in the left handed alpha helix region) (fig.13D). The loss of the double proline motif clearly alters the conformational propensity around this region and explains why P123H-βS and αS may have similar conformational propensities in the full length protein C-terminal to the mutation site.

Discussion

A pathological mutant of βS found in DLB, P123H-βS, shows that just a single mutation renders the normally non-toxic wild type βS into a toxic species, and that it is able to induce aggregation, overcome the inhibitory properties of βS and exarcerbate αS pathology. NMR studies reported here compare the conformational propensities of αS, βS and P123H-βS and indicate that the N-terminal and NAC regions of the three proteins are very similar while the C-terminal regions of these proteins

are more variable. βS exhibits the most rigid and extended structure in the C-terminus, while αS and P123H-βS are more similar to one another at the C-terminus, in particular in the C-terminal region from residues 95 to 119. The mutation at P123H in βS induces a break in the extended PPII secondary structure, suggesting that the double proline motif in the βS sequence is important for the extended conformation of the C-terminus. The mutation at P123H results in a more flexible C-terminus from residues 120-134 and allows a wider range of conformational ensembles to be sampled, thereby making P123H-βS more αS-like. The fact that all three monomer conformations are similar in the N-terminus and NAC region but that P123H-βS and αS are similar in the C-terminus suggests that this region is critical for the non-toxic to toxic conversion of βS to P123H-βS. The more flexible C-terminus may promote self-aggregation, and the conformational heterogeneity arising from the flexible C-terminus may increase the likelihood of sampling an aggregation prone conformation, or sampling aggregation prone inter-chain interactions.

The role of the C-terminus has been extensively discussed in the αS literature and can be viewed as playing a significant role in directing aggregation versus inhibition. It has been shown that the collapse of the C-terminus due to pH changes,[38,40,68] the addition of polycations and metals,[39,140,271] the substitutions of prolines to alanines mutations,[272] and C-terminal truncations increase the aggregation propensities of αS.[65,273] Mutations of the tyrosines in the C-terminus, [274,275] and addition of small molecules that interact with the C-terminus such as dopamine [209] and ECGC [210] result in aggregation inhibition. βS, whose C-terminus is extended, is self-inhibitory, and P123H-βS, whose C-terminus is more flexible is less inhibitory. This αS literature taken together with our data, suggests that a PPII extended C-terminus, as seen in βS, or a C-terminus that is unavailable due to interactions with small molecules, is important for inhibition and that disruption of the extended conformation makes the protein more prone to aggregation.

Our results show that the changes in the conformation of the C-terminus of βS can alter, not only self-aggregation properties, but also its ability to delay or inhibit αS aggregation during co-

incubation. Just as P123H-βS is toxic in vivo, it also loses the ability to delay aggregation in vivo and fibril formation in vitro upon co-incubation with αS. The striking difference in fibril formation of αS with βS, versus fibril formation of αS with P123H-βS suggests that altering the extended conformational propensities of the monomer at the C-terminus will affect inter-chain interactions at the dimer level and beyond. We show the delicate balance in the transition from protective to pathogenic forms of βS, suggesting that the conformation of the protein at the C-terminus may be linked to toxicity and inhibition events.

Methods

Mutagenesis, expression and purification

P123H-βS was prepared by site-directed mutagenesis using AccuPrime pfx from Invitrogen. N-terminal acetylation of all proteins was performed by co-expression with the NatB plasmid as described previously. Protein purification was performed according to previous protocols.[228]

NMR experiments.

All NMR experiments with the exclusion of the RDC experiments were acquired on a Varian 600 MHz spectrometer at 15 °C in pH 6 and 10mM MES buffer with 100mM salt. RDC experiments were acquired on a Bruker 700 MHz spectrometer.

NMR assignments.

Assignments of P123H-βS were performed using the protocol described elsewhere.[228] NMR assignments of αS [227] and βS have been performed previously (manuscript submitted). Experiments were performed on 350uM ^{15}N and ^{13}C labeled sample with 10%D_2O in 10mM MES buffer pH 6 with 100mM NaCl. Secondary structure propensities for P123H-βS were obtained from the SSP program and SSP for αS and βS were obtained previously.[237]

RDC experiments.

C8E5-octanol bicelle aligning medium in 100mM NaCl, 10mM MES buffer pH 6.[238] Reagents: C8E5 and 1-octanol were purchased from Sigma. The quadrupolar deuterium splitting constants were measured prior to the experiment. The sample was prepared by dissolving lyophilized protein in buffer and passing through 100 kD and 3kD filters. Concentration of the protein was adjusted to 250 μM. Aligning media was added to a final volume of 5%. High resolution HSQC_IPAP spectra in the absence or in the presence of an alignment medium were collected.

Kinetics of fibril formation.

Kinetics of fibril formation of αS, βS and P123H-βS were obtained along with kinetics of fibril formation of co-incubation of αS with βS, αS with P123H-βS and doubling of αS using ThT fluorescence experiments. 5-10 mg of lyophilized acetylated αS, βS, and P123H-βS was dissolved in PBS, centrifuged for 10 min in 14000 rpm to remove big oligomers, and purified using size exclusion chromatography (Superdex 75 GL 10/300, from GE Healthcare Life Sciences). Protein was concentrated using 3kDa centrifugal units (Millipore Inc). Final protein concentration was 70 μM with 20 μM ThT for fluorescence measurements. Measurements were recorded at 37 °C with linear shaking at 600 rpm. ThT fluorescence was recorded at 30 minute intervals using a POLARstar Omega reader from BMG, as described previously.[276] Each condition was repeated 4 times and data is averaged. The experimental set up was used as previously described in the presence of PTFE beads (Taylor Scientific).[228]

Electrospray ionization mass spectroscopy (ESI-MS).

ESI-MS experiments were performed as described previously.[241] Samples were prepared in 10mM Ammonium Acetate, pH 6 in final concentration 50uM, by using 100 kDa and 3kDa filters.

Negative straining transmission electron microscopy (TEM).

Samples were incubated for 14 hours and after this time aliquots were taken for imaging. Fibrils were visualized using a JEM-100CXII manufactured by JEOL. Negative staining TEM was performed using the single droplet procedure [242] at ambient temperature. Micrographs were recorded at a magnification of 100,000. All of the chemicals were purchased from Sigma.

Size exclusion chromatography.

Samples of βS and P123H-βS were prepared by dissolving 12 mg/ml of protein in PBS buffer, spinning down for 1h at 14000rpm and incubating with orbital shaking for 5h at 37°C degrees. After that time samples were spun down for 10 min and injected into a Superpose 6 (GE Healthcare) column with a flow of 0.5 ml/min.

PSI-BLAST analysis.

PSI-BLAST [277] analysis was performed to obtain the typical conformations of PP, PS and PH motifs in the PDB. The search was performed across a 10 residue window that contained the PP motif of βS and its flanking sequences, the PS motif of αS and the PH motif of P123H-βS. Alignment to the average structure, and RMSD was calculated for all structures from the set using VMD visualization program.[278] Phi and psi values for all the residues were calculated using AMBER cpptraj analysis tool [279] and represented in Ramachandran plots.[280]

Acknowledgements

We would like to thank Ron Levy for a productive and interesting collaboration in the early stages of the project. We thank Pawel Janowski for assistance with the bioinformatics analysis, and Dr. Valentin Starovoytov for assistance with the TEM experiments. M.J. was supported by a GAANN fellowship.

4.2. V70M mutant

The V70M mutation of βS was found in sporadic DLB disease.[190] βS V70M is located in the NAC region of the βS. It has been shown to cause formation of lysosomal inclusions when overexpressed in the B103 cell line, similarly to the P123H mutant of βS described in previous section. The number of lysosomal inclusions increases upon co-expression of the βS mutant with αS, but the pathology of this mutant is not as pronounced as the P123H mutant.[191] We sought to find the properties of the

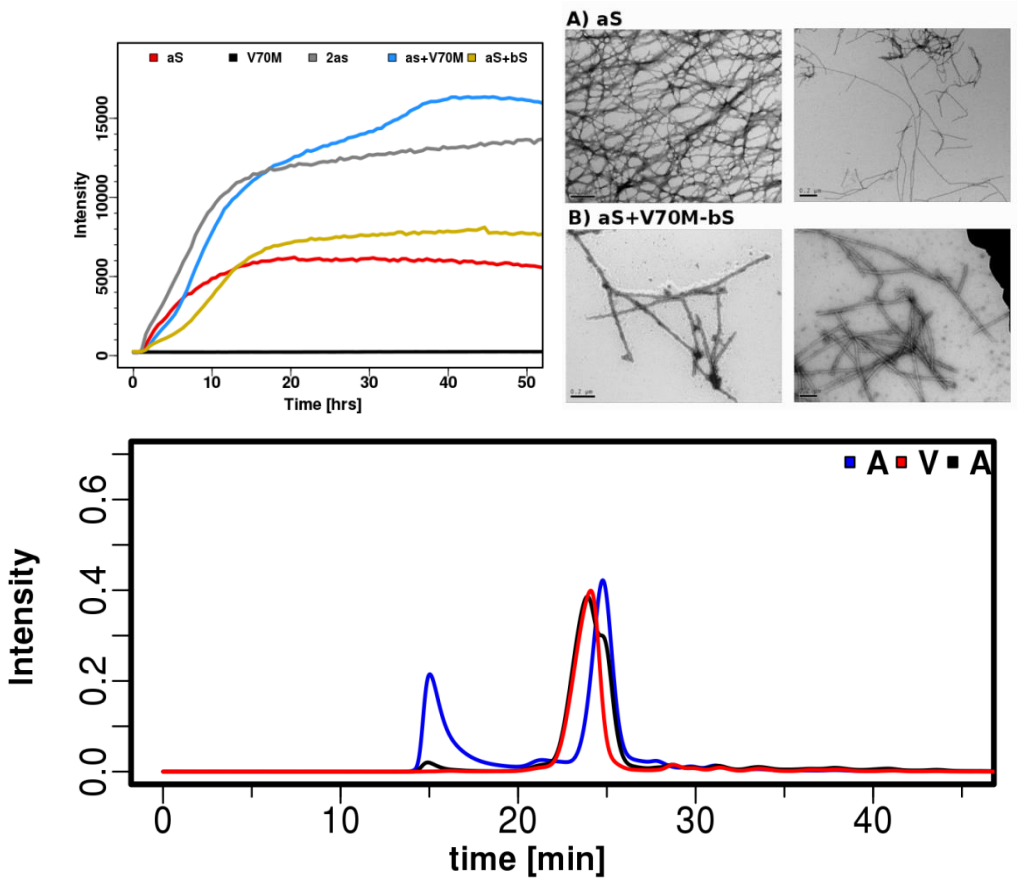

Figure 14. Aggregation inhibiton of αS by βS and aggregation enhancement of αS by V70M-βS (A). ThT fluorescence (37°C with shaking and teflon beads, PBS) of αS coincubated with βS and V70M-βS. (B) Negatively stained electron micrographs (scale 200 nm) αS fibrils and αS fibrils formed in the presence of the V70M mutant (C) Size exclusion profile of αS (blue), V70M (red) and mixture of αS and V70M (black), after 14h incubation.

V70M mutation that affect the βS ensemble and lead to toxicity.

Aggregation and oligomerization of V70M

V70M does not aggregate on its own, but increases aggregation rates of αS in a similar way to the other βS DLB disease-related mutant P123H. Upon addition of V70M-βS mutant to αS, ThT aggregation profiles exhibit aggregation rates twice as high as pure αS , which strongly suggest that both βS mutants either increase αS aggregation rates or are seeded by αS, as αS aggregation could be transferred to βS toxic mutants. βS on its own does not aggregate, inhibits αS aggregation and cannot be seeded by αS aggregation. In fact there is reason to suggest that βS DLB mutants might possibly cross barrier of cross-seeding abilities. Cross-seeding between distinct species is thought to be possible when two proteins share some similarity (possibly conformational)that enables them to form fibrils. Co-incubation of V70M mutant with αS results in slight changes to the morphology of the generated fibrils. Fibrils formed upon co-incubation of V70M with αS are thicker than the fibrils formed by αS alone. Despite the difference in the fibrillation rates induced by coincubation of αS with V70M compared to coincubation with wild type βS, there are no significant changes in the oligomerization rates of V70M compared to wild type βS. Both βS and V70M-βS are not prone to form oligomers, as detected after 14h of incubation, while a similar incubation of αS generates large quantities of oligomers. In addition V70M-βS exhibits decreased oligomer formation upon coincubation with αS, so that even tough fibril formation is increased oligomerization rates are decreased.

NMR characterization of the V70M mutant of βS.

The V70M mutation of βS is located at the beginning of the NAC region of the protein. One of the reasons why βS is thought to be less aggregation prone than αS is the deletion of 11 residues from the NAC region of the protein, since the NAC domain is located in the core of the αS fibril. The NAC deletion in the βS sequence, however, is not the only reason why βS does not aggregate because insertion of the NAC deleted fragement back into βS does not recover full aggregation properties. [193,199,281] The NAC region is important for aggregation, because peptide fragments from

this region can aggregate on their own, but removal of these fragments from αS diminishes aggregation rates.[193,199,281] A recent paper from the Vendruscolo group showed that a switch of 6 residues from αS to βS sequences in the beginning of the NAC region is able to diminish rates of aggregation of αS , suggesting that the entire NAC region of βS is less inhibitory.[200] In the case of V70M, the mutation is located just two residues before the deleted segment, suggesting again that aggregation rates are highly sensitive to even single amino-acid residue changes in the NAC domain.

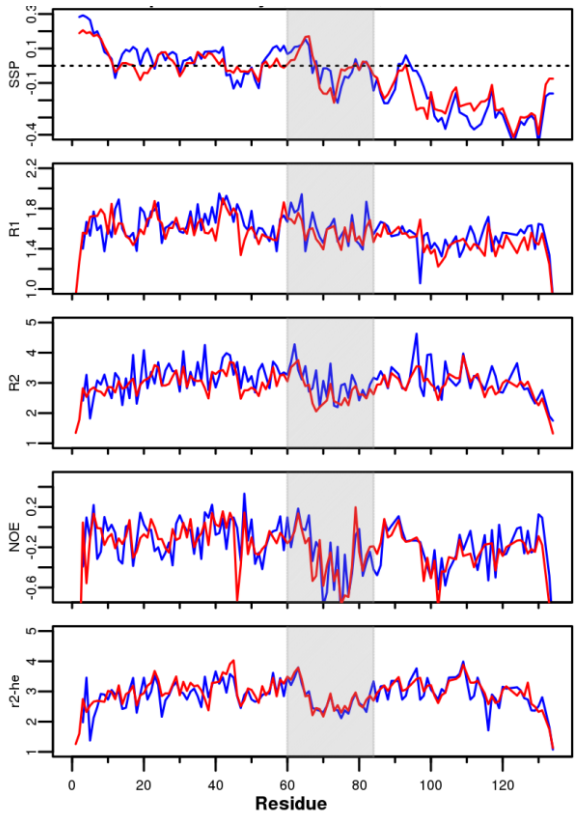

Figure 15. Characterization of βS (red) and comparison with V70M mutant (blue) secondary structure propensities and dynamics. (A) SSP (B) R_1 (C) R_2 (D) NOE (E)$R_2^{Hahn\text{-}echo}$

The V70M mutation of βS induces only small, local changes in the ensemble as compared to wild type βS. There are no changes in the dynamics of the protein as monitored by relaxation experiments while comparison of βS to V70M-βS: R_1, R_2, and NOE. Also there are no significant changes induced in the exchange rates in the $R_2^{Hahn\ echo}$ experiments, which suggests no significant changes in the overall behavior of the protein. However disease-related αS mutants also do not exhibit

significant changes in the protein ensemble dynamics. The conclusion is that the changes invoked by the mutations are mostly local and possibly lead to misfolding of only a small subset of the protein population.

V70M induces local changes in the secondary structure of βS. Helical secondary structure propensity is decreased close to the mutation site, rendering the NAC region more beta-sheet rich. Possibly this induction of beta-sheet secondary structures in βS enables αS to cross-seed it thus allowing fibril formation based on ThT and SSP data.

I also checked the inter-molecular interactions between αS and βS. Interchain PRE profiles of a V70M-βS ^{15}N labeled sample with αS-44-MTSL labeled protein revealed that the interactions between the N and C domains are maintained in the sample. However the magnitude of the interactions appears to be lower than it was before. Therefore it is possible that these interactions are being affected by the mutant through the differences in NAC conformation.

In general the V70M mutant is very similar to βS in its biophysical properties and oligomerization rates, so it is unclear why it is able to seed αS fibrillation. The toxicity of this mutant has been shown to be lower than P123H, and it behaves more like wild type βS, which suggests that the changes and ensemble transitions affected by this mutation are minor.

Chapter 5. Dimers.

Chapter 5 was submitted to Scientific reports and is currently in revision stage..

Unveiling transient protein-protein interactions that modulate inhibition of alpha-synuclein aggregation by beta-synuclein, a pre-synaptic protein that co-localizes with alpha-synuclein.

Maria K. Janowska, Kuen-Phon Wu and Jean S. Baum

Abstract

α-Synuclein (αS) pathology in Parkinson's disease is linked to self-association of αS intrinsically disordered proteins into pathogenic oligomeric species and highly ordered amyloid fibrils. Developing effective therapeutic strategies against this debilitating disease is critical and βS, a pre-synaptic protein that co-localizes with αS, can act as an inhibitor of αS assembly. Despite the potential importance of βS as an inhibitor of αS, the nature, location and specificity of the molecular interactions between these two proteins is unknown. Here we use NMR paramagnetic relaxation enhancement experiments, to demonstrate that βS interacts directly with αS in a transient dimer complex with high specificity and weak affinity. Inhibition by βS arises from transient αS/βS heterodimer species that exist primarily in head- to- tail configurations while αS aggregation arises from a more heterogeneous and weaker range of transient interactions that include both head-to-head and head-to-tail configurations. Our results highlight that intrinsically disordered proteins can interact directly with one another at low affinity and that the transient interactions that drive inhibition versus aggregation are distinct by virtue of their plasticity and specificity.

Protein aggregation is the origin of a wide variety of human neurodegenerative diseases including Parkinson's, Alzheimer's, Huntington's and Creutzfeldt-Jakob disease.[282,283] Parkinson's disease (PD), a highly debilitating illness, is the second most prevalent of the late onset neurodegenerative diseases and affects as many as 6 million people worldwide.[284] As life expectancy continues to increase, neurodegenerative diseases like Parkinson's are becoming increasingly common and a threat to global

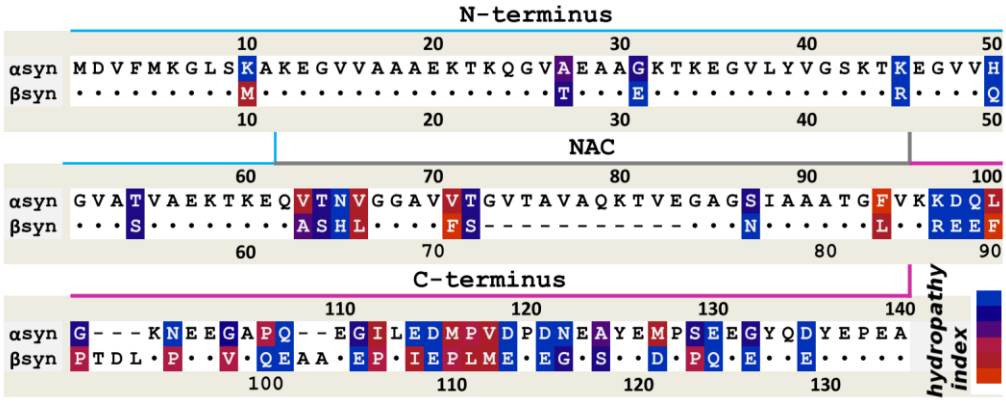

Figure 16 Sequence alignment of αS and βS shows high similarity between proteins. Sequence differences are color-coded according to the hydrophobicity index shown in the bottom right (red-hydrophobic, blue-hydrophilic). Identical residues are shown by dots in βS sequence and deletions are shown by dashes. The line above the sequence shows the N-(blue), NAC (grey) and C-terminal regions (pink).

public health. The diagnostic hallmark of PD is a deposit called a Lewy body that is primarily composed of the pre-synaptic intrinsically disordered protein α-synuclein (αS). Fibril formation of αS is also implicated in other neurodegenerative diseases, including multiple system atrophy and dementia with Lewy bodies, referred to as synucleinopathies. Although the function of αS is not clearly defined it is thought to be involved in promoting SNARE complex assembly,[285-287] in regulation of the synaptic vesicle pool,[288,289] and in remodeling membranes.[290,291] The origin of αS pathology in neurodegenerative disease is clearly linked to the self-association of the intrinsically disordered αS monomers into pathogenic oligomeric species and highly ordered amyloid fibrils.

One approach to developing effective therapeutic strategies against this debilitating disease is to

identify inhibitors of αS aggregation. Small molecule inhibitors of αS have been proposed[206,292-295] along with proteins that interfere with αS assembly such as heat shock proteins (Hsp40, Hsp70, Hsp90, αB-crystallin),[296,297] and the intrinsically disordered β-synuclein (βS), a homologue of αS with which it co-localizes. A number of studies have established a neuroprotective role for βS.[167-169,175,177,184,211,298,299] Masliah and co-workers have shown that βS is expressed at similar levels as, or more abundantly than, αS in the central nervous system, however the ratio of βS to αS at the mRNA level is significantly decreased in diseased brains, suggesting a regulatory role within the synuclein family.[169] *In vivo* it has been shown that over-expression of αS with βS in mouse models significantly decreases the number of plaques formed[172] and that intracerebral injection of the lenti-βS virus reduces the formation of αS inclusions in transgenic mice.[174] *In vitro*, it has been shown that the presence of βS with αS slows its aggregation.[167,172,174,175,177,267] Despite the fact that βS has a very similar sequence to αS, it does not form fibrils on its own,[167,199,200,300] but may form aggregates whose toxicity is debated.[188,189] The *in vivo* data clearly suggest that βS plays an important regulatory role in inhibition of αS pathology but at this stage there is no molecular information about the nature, location and specificity of the protein-protein interactions that initiate the inhibition of αS by βS.

To understand the mechanism by which the intrinsically disordered protein βS interacts with αS, we use NMR to map, at the individual residue level, the monomer-monomer interactions that lead to inhibition (αS/βS) or promotion (αS/αS) of aggregation. Despite the importance of these interactions, the molecular details are extremely difficult to obtain due to their transient nature and low population. Paramagnetic relaxation enhancement experiments (PRE) offer an excellent tool for characterization of weak and transient interactions because they are able to probe states that exist at low populations (even 0.5-5%) and exhibit short life times (250-500 μs).[230,249] Here we use inter-chain NMR PRE experiments to identify weak transient complexes of αS and βS to discriminate between aggregation promoting versus aggregation inhibiting transient interaction.[56] We show that αS homo-dimers sample a heterogeneous range of population distributions, including head- to- head and head-to- tail configurations while αS/βS hetero-dimers exist primarily in head- to- tail configurations.

We have broadened our analysis by applying inter-chain NMR PRE titration experiments previously used on folded proteins[233] to intrinsically disordered proteins. These experiments allow us to obtain residue specific dissociation constants that inform us about the specificity and affinity of dimer interactions in different regions of the transient disordered complexes. These results show that the hetero-dimer transient head- to- tail interactions between αS and βS span a wider range of residues in the C-terminus of βS and are approximately 5 times stronger than the interactions observed in the homo-dimer αS species suggesting a kinetic trap which delays or inhibits the formation of αS fibrils. The novel insight presented in this paper not only defines contact maps between two intrinsically disordered proteins but also links the positions and strengths of the interactions within the homo and hetero-complexes with distinct pathways that lead to aggregation

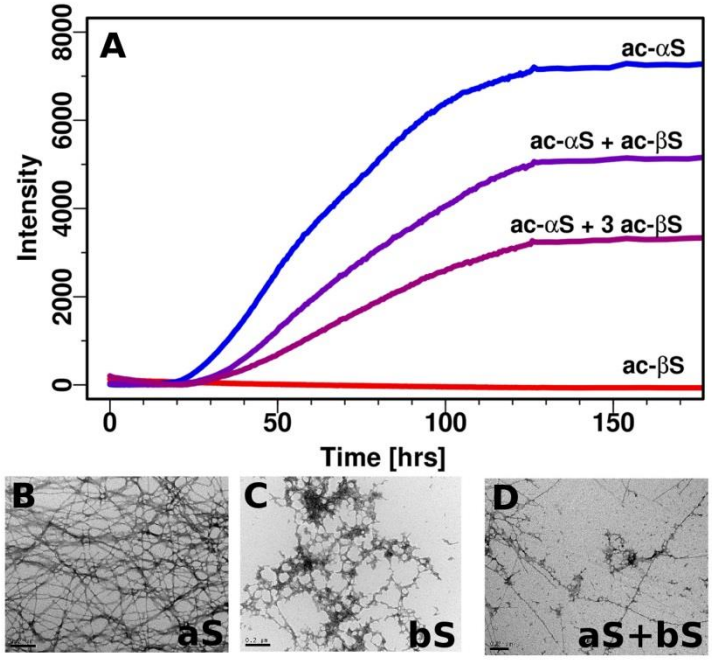

Figure 17 Aggregation inhibiton of αS by βS as monitored by ThT and TEM. (A) βS is able to inhibit fibril formation of αS in a dose dependent manner (measured at 37°C with shaking). Negatively stained electron micrographs (scale 200 nm) (B-D) of (B) αS fibrils (C) βS amorphous aggregates (D) co-incubated αS with βS

versus inhibition.

Results

βS inhibits αS fibril formation in a dose dependent manner. αS and βS are part of the synuclein family that can be described by three regions of the protein: the N-terminus that contains KTKXGV repeats and forms helices at membranes,[49,91,301] the non-amyloid-βS component (NAC) region, and the highly acidic and solubilizing C-terminus (Fig.16). αS and βS have similar sequences, particularly at the N-terminus, but very different fibrillation and oligomerization properties (Fig.16). The N-terminus for all synucleins is highly conserved, with only 6 substitutions between αS and βS sequences. In contrast, the C-terminus is the least conserved region with more prolines and more negatively charged residues with a net charge of -12 in αS and -15 in βS. βS has an 11 residue deletion in the NAC region that was thought to be important in preventing fibril formation but substitution of this region into βS does not recover the fibrillation potential of αS.[199,300]

Similarly to αS it has been established that the physiological form of βS and its pathological mutants *in vivo* are N-terminally acetylated.[151] All experiments in this study are performed on the acetylated forms of the protein that we will refer to as αS and βS. As all previous characterization of βS was performed on non-acetylated protein,[167,175,194,300] we use NMR and other biophysical approaches to determine whether N-terminal acetylation affects the conformation or oligomerization state of the protein. NMR and other biophysical techniques including dynamic light scattering (DLS) and circular dichroism (CD) show that acetylated βS, similarly to acetylated αS, is primarily monomeric and unfolded (Fig. 21). Secondary structure propensities indicate the formation of a transient N-terminal helix relative to the non-acetylated form of βS similarly to αS (Fig.21). In addition, the C-terminus of acetylated βS is more extended that the C-terminus of acetylated αS consistent with previous results on non-acetylated protein.[302] Electrospray ionization mass spectroscopy (ESI-MS) experiments (Fig.21) show that acetylated βS can populate an extended and a compact form with a higher population of extended conformation relative to acetylated αS.

Upon addition of acetylated βS to acetylated αS, fibril formation is inhibited in a dose dependent manner, consistent with previous findings for the non-acetylated forms of the proteins (Fig.17A).[167]

The *in vitro* Thioflavin T (ThT) fibril formation experiments indicate that at least a 1:1 stoichiometry is required for partial inhibition, and *in vivo* studies have shown that βS is expressed at similar level or more abundantly than αS suggesting that the stoichiometry may be consistent with the regulatory role of βS on αS aggregation *in vivo*. Most striking is a significant change in the rate of the elongation phase and in the total ThT intensity as well as a small change in the lag phase. Previous work has shown that ThT can be used as a semiquantitative method to estimate relative amounts of fibril formed, although caution should be applied in interpreting ThT intensities.[303,304] In this case the inhibition of fibril formation is supported by Transmission Electron Microscopy (TEM) data which shows significant changes in fibril morphology of αS/βS relative to fibrils of αS alone (Fig. 17B-D). βS does not form fibrils but does form amorphous aggregates similar to what has been described in the literature for non-acetylated βS, and the αS/βS mixture forms significantly fewer fibrils as seen in TEM.[167]

Mapping of residue specific transient interactions in αS/αS homo- and αS/βS hetero-dimer complexes using NMR inter-chain PRE experiments. ThT fluorescence experiments and TEM data (Fig.17) have established that βS alters the aggregation kinetics of αS however there has been no evidence to date of a direct interaction between these proteins. To determine the existence of, and to characterize transient inter-chain interactions between homo-dimers (αS/αS, βS/βS) and hetero-dimers (αS/βS, βS/αS), inter-chain NMR paramagnetic relaxation enhancement experiments were performed. In this experiment, in which NMR blind ^{14}N-MTSL labeled protein is mixed with NMR visible (^{15}N) unmodified protein, the broadening of the signal is limited only to residues on the NMR visible chain that interact with the MTSL labels on the NMR invisible chain (Fig.22).[56,230,249,305]

NMR PRE experiments were performed on all four combinations of possible homo- and hetero-

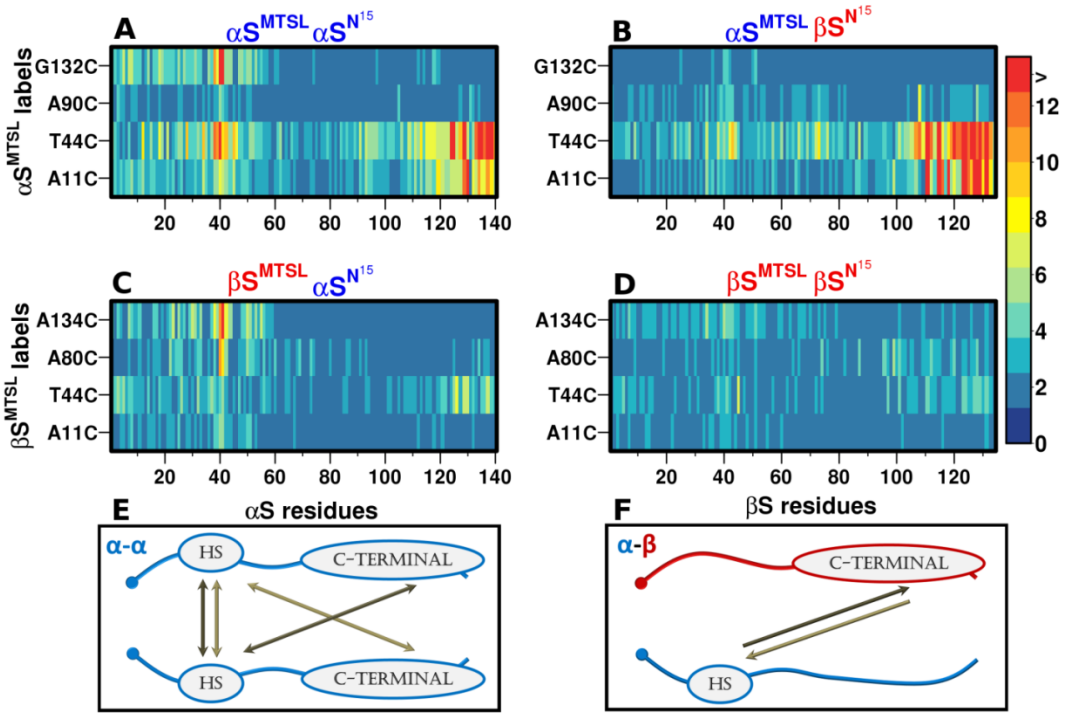

Figure 18 Contact maps of αS/αS homo-dimers and αS/βS hetero-dimers show distinctive interaction profiles. Contact maps of transient dimers, shown as heat maps where each strip represents the color coded value of the residue-specific inter-chain paramagnetic relaxation enhancement rate (PRE rate - HNΓ2) induced by the proximity of the MTSL label to the residues in the indicated protein. Contact maps (A-D): figures A-D show four heat maps for all possible permutations of the spin label and NMR detectable chains of αS and βS: (A) 14N-αS-MTSL/15N-αS, (B) 14N-αS-MTSL/15N-βS, (C) 14N-βS-MTSL/15N-αS, (D) 14N-βS-MTSL/15N-βS. Contact maps show the PRE values colored in accordance with the legend; residues that do not exhibit interactions are colored blue and interactions higher than 12 Hz are colored red. Each strip on the contact maps corresponds to the spin label (y-axis). In one strip there are bins which correspond to the residue number on the NMR visible chain (x-axis). (E-F) Schematic representations of possible interactions of homo αS/ αS and hetero- αS/βS synuclein dimers. (E) αS/αS corresponds to interactions from contact map (A), (F) αS/βS corresponds to contact map (B-C); no homo-dimer for βS is shown as we observe no inter-chain interactions between βS chains. HS in the schematics stands for interactive "Hot Spot".

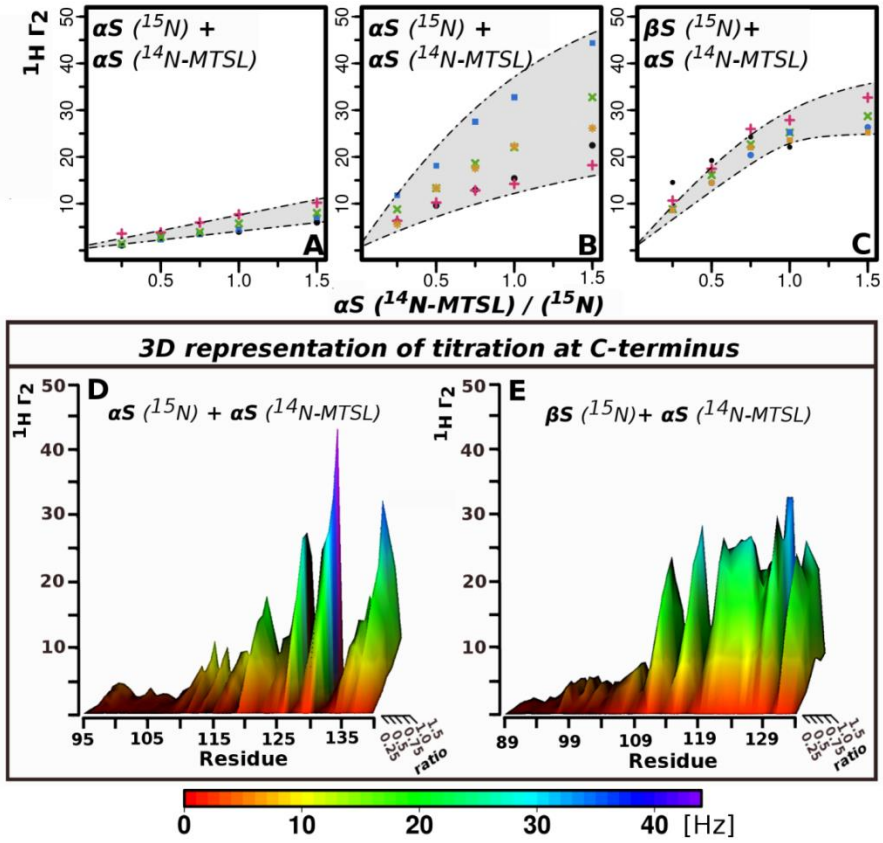

Figure 19 Residue specific binding affinities for transient αS/βS hetero-complexes show higher specificity and affinity than αS/αS homo-complexes. (A-C) Representative examples of titration curves from PRE titration profiles of αS-44-MTSL to ^{15}N-αS and ^{15}N-βS. Illustration of how the K_D is obtained from fitting the PRE titration data as a function of the molar ratio of ^{14}N-αS-T44C-MTSL labeled to ^{15}N-αS (A-B) and to ^{15}N-βS (C).: (A) αS residues 38-41 show a linear dependence between PRE values and concentration indicating non-specific interactions at these site, (Residues colors: 38 - black, 39- blue, 40 - pink, 41 – green), (B) αS residues 125-140 exhibit non-linear titration curves indicating specific interactions. (Residues colors: 125 - orange, 130 - blue, 135 - pink, 137 - green, 139 - black), (C) βS residues 109-134 interact strongly and more uniformly with αS-44-MTSL (Residues colors: 115 – green, 120-orange, 121-blue, 129 – pink, 131 - black). Shaded areas indicate the range of possible K_D values. Titration profiles for αS/βS show a higher degree of saturation consistent with more specificity and higher affinity than those for αS/ αS (D-E) 3D representation of titration curves in the C-terminus (D) ^{15}N-αS C-terminus titrated with T44C-MTSL labeled ^{14}N-αS (E) ^{15}N-βS C-terminus titrated with T44C-MTSL labeled ^{14}N-αS titration. The x-axis shows the C-terminal residues of both αS and βS after sequence alignment, the z- axis depicts the PRE values, the y- axis the ratio of T44C-MTSL labeled ^{14}N-αS to ^{15}N sample concentration. Surface is colored using a rainbow palette, where low $H_N\Gamma_2$ values are red and the highest values are purple (according to legend below the plot).

dimers including $\alpha S^{15N}\alpha S^{MTSL}$, $\alpha S^{15N}\beta S^{MTSL}$, $\beta S^{15N}\alpha S^{MTSL}$, $\beta S^{15N}\beta S^{MTSL}$ to determine first, whether

there is evidence for direct residue specific transient interactions and secondly to establish the location of the interactions. The results of Fig. 18 are striking as they show immediately that the four combinations of possible hetero and homo-dimers have different transient interaction profiles (Fig.18 and Supplementary Fig.23). There is evidence for interactions between the homo-dimer complexes of αS, and the hetero-dimer complexes of αS and βS; interactions between βS are essentially non-existent. We have introduced four spin labels along the sequence at positions 11, 44, 90 and 132 for αS and 11, 44, 80, 134 for βS to probe interactions in the N, NAC and C-terminal regions. Experimental results are presented as heat maps (Fig.18A-D), where each strip shows color-coded values of residue-specific inter-chain paramagnetic relaxation enhancement rates (PRE rate - Γ) induced by the proximity of the MTSL label to another chain. Under the conditions of the experiment, αS and βS do not form fibrils or oligomers; therefore dimer detection arises as a result of low populations of dimers existing in equilibrium with the monomer precursor (for αS lack of higher order species in the sample has been confirmed by ESI-IMS-MS experiments[227] and for hetero-species this has been confirmed with ESI-MS.

αS populates a heterogeneous range of transient complexes while αS/βS hetero-complexes sample primarily head-to–tail non-propagating interactions. The heat map for the αS/αS homo-dimer shows strong interactions between the N-terminal αS-MTSL labeled positions A11 and T44 with the N-terminal region 36 to 44, and the C-terminal region 124 to 140 (Fig. 18A). Earlier studies by our group[56] on αS showed transient inter-chain interactions between the N- and C-termini (N-C), but by increasing the number and positions of the MTSL spin labels we now observe new inter-chain interactions between the N-termini showing that αS can populate multiple dimer configurations. In noticeable contrast, the αS/βS hetero-dimers show strong interactions between the N-terminal αS-MTSL labeled positions A11 and T44 and the C-terminus from residues 105 to 134 and extremely weak N-N terminal interactions between 37 and 41 (Fig. 18B). According to the heat map, the hetero-dimer interactions between the N-terminus of αS and the C-terminus of βS appear to be more extensive and stronger (residues 105-134 compared to residues 124-140 in αS/αS homo-

dimers) (Fig. 18A-C) than those in αS. βS shows extremely minimal interactions with itself supporting the view that βS does not form fibrils (Fig. 18D).

A schematic representation of the dominant homo and hetero-dimer interactions shows that both N-N and N-C configurations are sampled by the αS homo-dimers while only N-C terminal interactions are sampled in the αS/βS hetero-dimers (Fig. 18E, 18F). The favorable interactions of the N-terminal hydrophobic region 36 to 44 of αS with itself (N-N), and with the C-terminus of αS and βS suggests that it acts as a 'hot spot' for aggregation initiation. In the αS homo-complexes, the interactions detected by N- and C-terminal probes show symmetry, implying that the interactions we observe are not experimental artifacts. The NMR PRE data show that αS homo-dimers can sample a heterogeneous range of populations, including head- to- head and head- to- tail configurations while αS/βS hetero-dimers sample only head- to- tail dimers suggesting that the hetero-dimers have a more limited range of possible conformational preferences for the dimer species.

Aggregation versus inhibition of αS by βS is due to a balance between specificity and affinity of transient interactions. The inter-chain NMR PRE experiments described above are powerful as they provide us with direct evidence for the existence of transient interactions and allow us to pinpoint the specific residues involved in these encounter complexes, however the specificity and affinity of the interactions remains unknown. We extend an approach proposed before[233,234] to study transient encounter complexes of folded proteins to obtain residue-specific equilibrium dissociation constants (K_D) for transient encounter complexes of IDPs. Experiments are performed by titration of ^{15}N labeled αS with MTSL-labeled ^{14}N-αS, and K_Ds are obtained by fitting the intermolecular transverse ^{1}H relaxation rates to a titration curve (see methods) (Fig.19).

NMR PRE titration experiments and data analysis is complex as K_Ds are anticipated to be weak due to the disordered nature of the monomers. The titration curves are grouped according to their profiles and three different types of patterns emerged (Fig. 19.A-C). Representative examples of

titration curves arising from interactions between αS-44-MTSL and residues 38-41 of the N-terminus (Fig. 19A), and residues 125-140 of the C-terminus (Fig.19B), show that they are distinct from one another. The titration curves for the N-N interactions show a linear dependence between PRE values and concentration indicating non-specific interactions at this site, while interactions with the C-terminal 125-140 exhibit non-linear titration curves suggesting specific interactions. The range of K_D values in this group is between $K_D \sim 500$ μM (range 90-1200 μM) using the data analysis described in methods. While we observe both non-specific (N-N) (Fig.19A) and specific interactions (N-C) (Fig.19B) in homo-αS complexes, the hetero-complexes Ac-αS/βS (Fig.4C) have only specific N-C interactions. The titration profiles of αS-44-MTSL with βS in the region 115-134 have a narrower range of K_D values ($K_D \sim 100$ μM, range 40-350 μM) than those associated with the K_D values of αS-44-MTSL αS with its own C-terminus ($K_D \sim 500$ μM- range 90-1200 μM) suggesting more uniform behavior across this region and higher specificity and affinity by approximately 5 fold (Tables 2&3). The differences between the strengths of the interactions and the range of residues over which the interactions are occurring is seen clearly in the 3D plots where the interaction regions in αS are more rugged while the interactions between αS and βS are smoother, more uniform and extend over a wider range of residues (Fig. 19D-E).

Discussion

βS plays a role in the inhibition of αS aggregation but the mechanism by which this occurs and the stage in the aggregation pathway at which βS first interacts with αS has been unknown. We demonstrate that the monomer species of αS and βS interact directly with one another at specific sites suggesting that inhibition may begin at the very earliest stages of the fibril formation process. The molecular interactions and affinities obtained in the NMR PRE experiments described here support the view that early stages of aggregation versus inhibition may be due to a balance between conformational heterogeneity, specificity and affinity. Early stages of aggregation in αS may be promoted by sampling or searching co-existing conformational structures with weak transient

affinities, including both non-specific head- to- head and weak specific head- to- tail dimers (Fig.20A). In contrast early stages of inhibition may be favored by sampling only head- to- tail interactions with higher affinity and specificity within the αS/βS hetero-complex (Fig.20B) while dis-favoring head- to –head αS/βS hetero-dimer interactions.

Head- to- tail interactions exist in both the homo- and hetero-dimer complexes, which is strongly suggestive that they may play a regulatory role on αS folding or misfolding. In light of the fact that the fibril state of αS assembles into in-register parallel cross-β-structure[306,307] and that hetero-αS/βS fibrils do not exist[167] , the NMR data suggests that head-to-tail αS/βS dimers would have to undergo conformational rearrangement to reach the final fibril form thereby delaying or inhibiting the kinetics of fibril formation. We propose that the αS homo-complex is more aggregation prone than the αS/βS complex for two reasons: first, αS can sample head- to- head interactions that are potentially aggregating promoting while the αS/βS complex does not sample these; second, the head- to- tail αS complex has weaker, lower affinity interactions relative to the αS/βS complex suggesting that the conformational rearrangement towards a more aggregation prone species is more easily accessible to the αS/αS homo-complex.

Despite the fact that both the αS/αS homo-dimer and αS/βS hetero-dimer sample head- to –tail interactions, there are notable differences in terms of the strength of the interactions and the range over which the interactions extend. For both homo- and hetero-dimers the interaction of the αS "hot spot" with the C-terminus of either αS or βS extends over ~20-30 residues, suggesting that the dimers are flexible and are able to probe a big surface area, possibly adopting multiple dimer conformations. In addition, the αS and βS C-termini are highly negatively charged and contain aromatic and hydrophobic residues suggesting that initial interactions are mediated by electrostatics, which are anchored and stabilized through the hydrophobic and aromatic interactions.

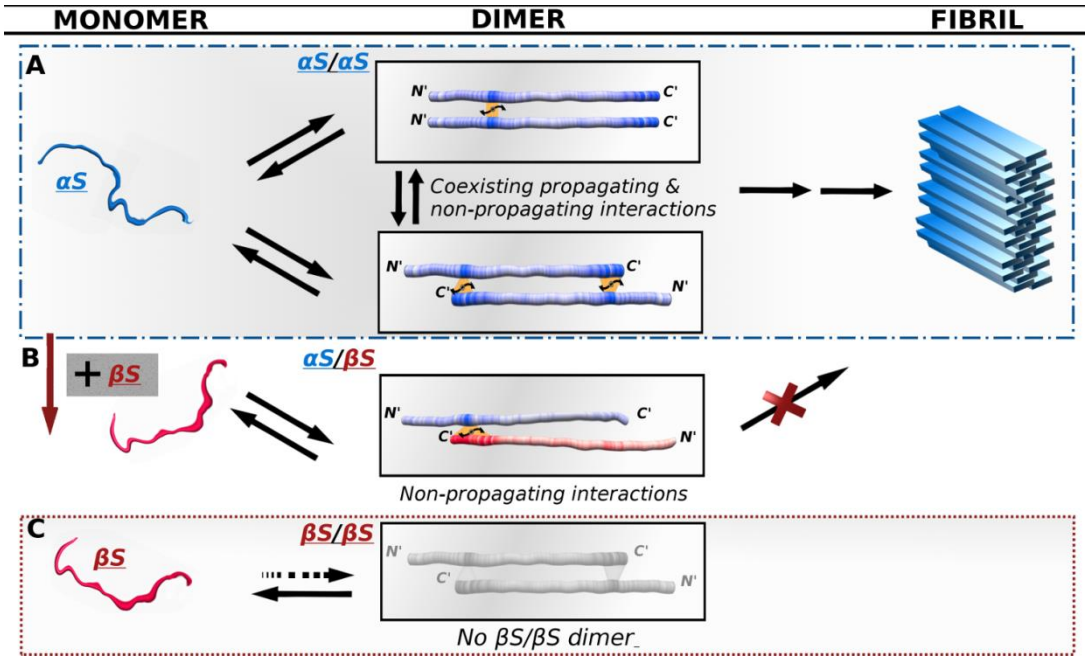

Figure 20 Schematic model of αS/αS and αS/βS transient interactions suggest a new molecular view of inhibition routes to αS aggregation. (A) αS/αS homo-dimer interactions: head-to-head aggregation prone interactions at residues 36-44 co-exist with head-to-tail inhibitory interactions at residues 125-140. (B) αS/ βS hetero-dimer interactions: head- to- tail inhibitory interactions span a broader range of C-terminal residues 115-134 with higher affinity. (C) No interactions are observed between monomer chains of βS. Protein chains are color-coded according to the interactivity of the regions as shown in Supplementary Fig.3. The NMR data show that αS homo-dimers can sample a heterogeneous range of poulations including N-to-N and N- to C-terminal configurations while αS/βS hetero-dimers sample only N- to C- terminal configurations with higher affinity and specificity. In light of the fact that the fibril form of αS forms β-strands that assemble into in register parallel β-sheets this would suggest that the N-C terminal dimers would have to undergo conformational rearrangement to reach the final fibril form, thereby delaying or inhibiting the kinetics of fibril formation

Using NMR PRE titration experiments we demonstrate that interactions between the C-terminus of βS with the N-terminus of αS are approximately 5 times stronger and more extensive than the interactions of the C-terminus of αS with its own N-terminus. This increased specificity and affinity may be attributed to a higher content of negative C-terminal charges thereby enhancing electrostatic interactions, and a higher proportion of proline residues thereby altering the conformational ensembles sampled by the C-terminus. NMR and ESI data indicate that the C-terminal of βS has a

higher population of more extended species (Fig.21) and may therefore provide a more accessible surface area for interactions with the N-terminus "hot spot' of αS. These differences suggest that small changes in the binding surface, even in these highly dynamic IDP complexes, can lead to substantial changes in interactivity that can modulate the pathway of protein aggregation versus inhibition.

In conclusion, our studies highlight that transient and weak interactions are important for protein recognition pathways of IDPs that lead to diseases such as amyloidosis where the proteins self-associate and propagate to highly ordered fibrils. Work by Radford *et. al.*[308] have shown that weak interactions are also important for folded proteins in directing aggregation versus inhibition. By performing NMR inter-chain PRE titration experiments we have identified and characterized the strength and affinity of transient interactions between αS and βS, both IDPs. As IDPs are highly flexible, obtaining this information at the residue specific level is critical as the binding affinities are likely to behave in a non-cooperative manner across the protein.[309] Our data support this view and highlight the variable nature of the binding affinities, within and between αS and βS, that result in aggregation promoting versus aggregation inhibiting configurations.

Knowledge about the distinct dissociation constants of different interaction regions provides a new framework for thinking about therapeutic intervention by providing direct information about which regions to target for small molecule intervention and about the conformational features that may be most effective at intervention. There have been some small molecule inhibitors that have targeted the N-terminus of αS but now we based on our detailed molecular understanding of αS/βS interactions we can optimize the surface interactions to design novel more powerful inhibitors.[205,207,292-294,310,311] In addition, the powerful methods used here to identify the early stages of interaction of αS by βS can be extended to design inhibitors by biologics and can be applied even more widely to study other cross amyloid interactions, such as those between αS and amyloid- β-

protein, or αS and tau, that have been shown to play a critical role in cross-seeding in neurodegenerative disease.[222,308,312-314]

Methods:

1. Mutagenesis, expression and purification

Cysteine mutants of αS (A11C, T44C) and βS (A11C, T44C, A80C, A134C), were prepared by site-directed mutagenesis using AccuPrime pfx from Invitrogen. To obtain N-terminal acetylated forms of αS and βS proteins, co-expression with the NatB plasmid cloning N-Acetyltransferase B were performed, as described previously.[227] Protein purification was performed according to previous protocols.[228] Similarly, MTSL spin label conjugation to cysteine mutants was performed using previously established protocols.[56]

2. PRE experiments/controls

All NMR PRE experiments were performed in 10mM MES, pH 6, without addition of salt and with 10% D_2O required for NMR experiments. NMR inter-chain PRE experiments were performed by mixing NMR blind ^{14}N-MTSL labeled protein with NMR visible ^{15}N unmodified protein.[56] Samples were prepared as follows: lyophilized samples of ^{14}N-MTSL-cysteine mutants or ^{15}N non-modified proteins (αS or βS) were separately dissolved. Samples were passed through a 100kDa filter to remove higher order oligomers, and then concentrated using 3kDa filters to be able to dilute the sample to a final concentration of 250uM. Low sample concentration was chosen to minimize non-specific interactions. The total sample concentration was 500uM, with 250uM non-modified ^{15}N protein and 250 μM ^{14}N-MTSL labeled protein. All combinations of proteins were mixed in order to see all possible interactions. Diamagnetic samples were prepared by reducing samples with 10x excess of Ascorbic Acid and 5x buffer exchange using 3kDa cutoff filters from Millipore Inc. All the

controls have similar patterns and are in the range of experimental error. Additionally, the pattern for the reduced diamagnetic control is consistent with the pattern for the mixture of ^{14}N and ^{15}N non-modified samples. The ^{1}H-^{15}N HSQC of the cysteine mutants with the reduced spin label did not disrupt the HSQC pattern of αS and βS.

All ^{1}H-R_2 measurements of paramagnetic and diamagnetic (reduced) samples were acquired on a 600 MHz Varian at 15 °C using previously published pulse sequence and protocols.[56,229,230] The inter-chain paramagnetic relaxation enhancement rate (PRE rate – Γ_2) is the residue specific difference of the ^{1}H-R_2 values of the paramagnetic and diamagnetic samples. Increased ^{1}H-R_2 relaxation rates on the ^{15}N visible chain indicates that the NMR blind ^{14}N -MTSL labeled protein is in the proximity of specific residues in the NMR ^{15}N labeled visible chain. Para- and diamagnetic ^{1}H-R_2 were analyzed and processed using nmrpipe[231] and sparky.[232] For all experiments 10 relaxation delays were used: 12, 32, 104, 12, 124, 64, 48, 94, 64, 20 ms. Two data points (12 ms, 64 ms) were repeated in the experiment for obtaining good statistics for the error analysis. Errors of Γ_2 were calculated using error propagation, and errors were below 2 Hz. All of the interactions that were considered significant were at least 2 times higher than the mean value, and all of them were higher than the 3rd quantile and 8Hz.

3. NMR PRE titration experiments.

For NMR PRE titration experiments we used protocols described before.[233,234] Spin label sample concentrations were reduced to low volume > 32 uL and were added to 350uL of 250uM ^{15}N sample of either αS or βS; the changes in the sample volume were less than 10% of the overall sample volume. For αS titrations we used the following ratio of ^{14}N- αS-44-MTSL labeled samples to ^{15}N NMR visible samples: 0, 0.25, 0.5, 0.75, 1, 1.5, and in the case of βS we went up to ratio of 2. αS in this ratio exhibited shifts in the HSQC spectra, thus we removed this point from the analysis. We ran 6 data points ranging from 12-125 ms with the first point repeated twice for statistics. The PRE

profiles during the titration did not show significant contributions from the non-interactive regions. The relaxation rates for the non-interactive NAC region for the titration ratio $^{15}N/^{14}N$ equal to 1.5 are well below 8 Hz.

4. NMR PRE titration fitting and analysis.

Titration curves of ^{14}N-MTSL labeled protein with ^{15}N protein were fit using equation (1):

$$^{1}H_{N}\Gamma_{2}^{app} = \frac{1}{1 + xK_{d}^{-1}}\Gamma_{2}^{free} + \frac{xK_{d}^{-1}}{1 + xK_{d}^{-1}}\Gamma_{2}^{bound} \quad , (1)$$

where x is the concentration of ^{14}N-αS (T44C-MTSL) in solution, Γ_2^{free} – represents paramagnetic relaxation enhancement for free protein, and Γ_2^{bound} represents the maximum observed saturation value. The fitting scheme was based on the papers by Bax[234] and Clore.[233] We used a nonlinear regression model with three fitting parameters $\Gamma_{2,free}$, Γ_2^{bound} and K_d. The χ-squared statistic that measures the difference between the observed and predicted increase in $^{1}H_N\Gamma_2^{app}$ was optimized using the R statistics package minpack.lm, via the Levenberg-Marquardt algorithm.[235] The resulting fit was robust to small changes in Γ_2^{free}, K_D, and Γ_2^{bound} and provided us with residue specific K_D values between ^{14}N-αS-44-MTSL and ^{15}N-αS or ^{15}N-βS. The K_d calculations were performed for residues whose 5th titration point had PRE values higher that 15 Hz (tables 2&3). Results are summarized in the tables 2&3.

7. Other NMR experiments. Assignments on βS and αS were performed using the protocol described elsewhere.[228] Backbone atom assignments were established in acetylated βS for all residues except for the prolines. Acetylation of the protein facilitated assignment of the first few residues, which are highly flexible in the non-acetylated form of the protein. Experiments were performed on 350uM ^{15}N and ^{13}C labeled sample with 10%D_2O in 10mM MES buffer pH 6 with 100mM NaCl. Secondary structure propensities were extracted using the SSP program by Julie Forman-Kay.[237] If

the values are positive then this region has helical propensities, if the values are negative then the beta-sheet propensities are more pronounced.

8. Thioflavin T (ThT) aggregation assays.

ThT assay is an assay to monitor formation of cross-beta structure, which is the secondary structure found in fibrils. Experimental set up for measuring time dependent aggregation with ThT has been previously described.[228] 5-10 mg of lyophilized αS and βS was dissolved in Phosphate Buffer Saline, centrifuged for 10 min. at 14000 rpm to remove big oligomers, and purified using size exclusion chromatography (Superdex 75 GL 10/300, from GE Healthcare Life Sciences). Protein was subsequently concentrated using 3kDa centrifugal units (Millipore Inc). Final concentration of αS and/or βS was 70 μM. Addition of βS to αS were performed in multiples of 70 μM. Concentrations of the proteins were chosen based on findings by Uversky *et al.*[167] on non-acetylated protein. Concentrations were αS and βS alone, and αS +1xβS, and Ac-αS+3xβS. Each sample was repeated at least4 times to ensure suitable statistics, and data on the plot is average of 4 or 5 repeats.

9.Electrospray ionization mass spectroscopy (ESI-MS). ESI-MS experiments were performed in order to determine the population distributions of the monomeric ensembles of αS and βS using methods described previously.[241] Samples were prepared in 10mM Ammonium Acetate, pH 6 in final concentration 50uM, by using 100 kDa and 3kDa filters.

10.Dynamic light scattering (DLS). DLS measurements were carried out using a Zetasizer Nano ZS (Malvern Instruments, UK). Data was collected using a 3 mW He-Ne laser light at a 633 nm wavelength back scattered light at an angle of 173°. Autocorrelation functions were determined from 6 correlation functions, with an acquisition time of 10 s for one correlation function. The sample concentration was 200uM.

11.Negative straining TEM. Fibrils were visualized using a JEM-100CXII manufactured by JEOL. Negative staining TEM was performed using a single droplet procedure[242] at ambient temperature. Micrographs were recorded at a magnification of 100,000. All of the chemicals are purchased from Sigma.

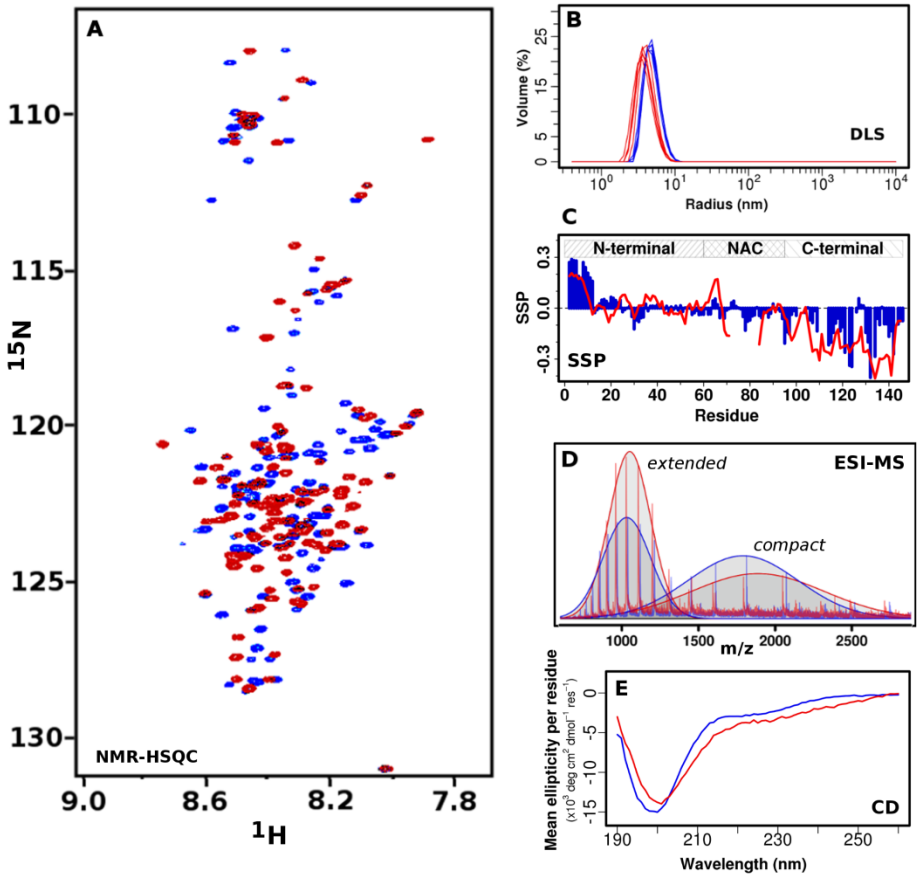

Figure 21 Comparison of monomer conformational features of acetylated αS and acetylated βS**.** (A) ^{1}H-^{15}N-HSQC spectra of αS and βS at 15°C and pH 6. (B) DLS spectra showing that αS and βS both have hydrodynamic radii in the range of 5-6 nm. No oligomers were detetected and proteins are monomeric (>99%). (C) SSP indicates that N-terminal acetylation induces transient N-terminal helix formation in βS that is similar to acetylated αS; the transient helix in βS spans residues 1 to 12. (D) ESI-MS shows that both αS and βS are 100% acetylated and that both proteins can exist in compact and extended conformations (indicated by fitting two Gaussians). αS has a 59% compact/ 41% extended ratio while βS has a 46% compact/ 54% extended ratio. (E) Circular Dichroism spectra indicate that both αS and βS have very similar profiles consistent with unfolded nature of the protein.

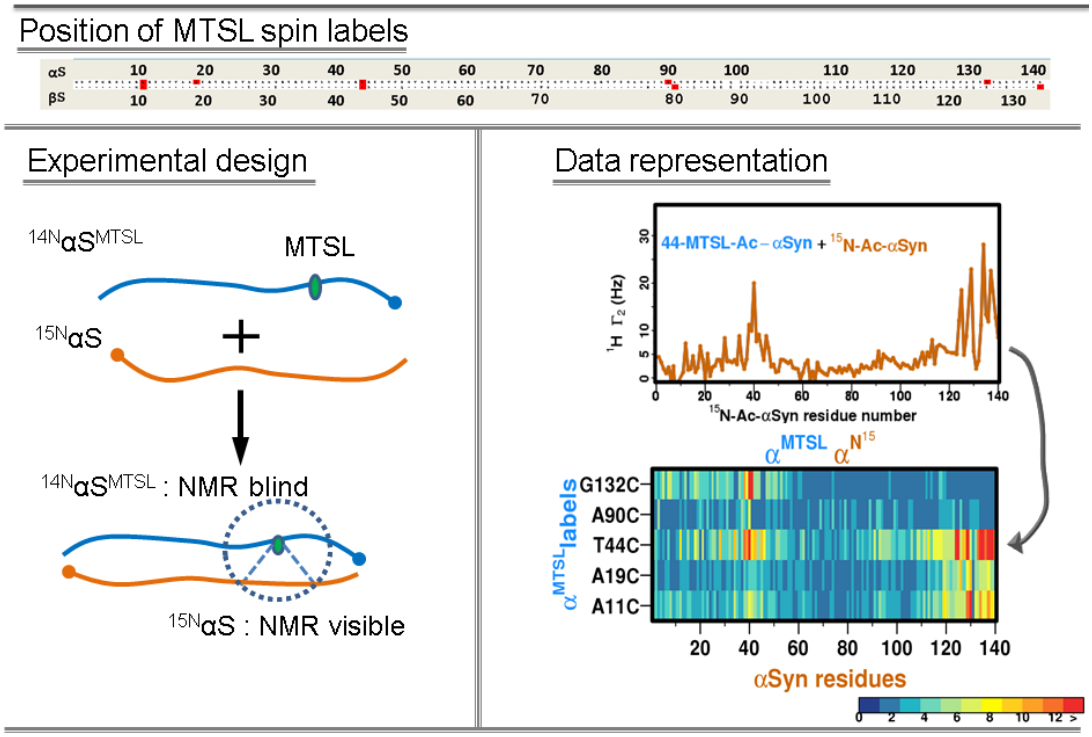

Figure 22 Schematic of experimental design for NMR PRE experiments. (A) 4 spin labels were introduced on each of the chains of the proteins, indicated by red box in the sequence of the protein. A->C and T->C mutants were selected in order to minimize effects of mutations. (B) Two different species are mixed in a 1:1 ratio: the NMR visible (^{15}N protein) and the NMR invisible MTSL spin labeled ^{14}N -protein. If the spin label is in the proximity to the ^{15}N labeled chain, the relaxation rates are increased (C) Example of the data representation. The top plot shows the relaxation enhancement rates (PRE rate - Γ) detected on the NMR visible chain (^{15}N). The lower plot shows the interactions in a pseudo contact map representation with the four spin labeled positions mapped against the 15N residues in the protein. The contact map is represented as a heat map with the color index shown in the inset.

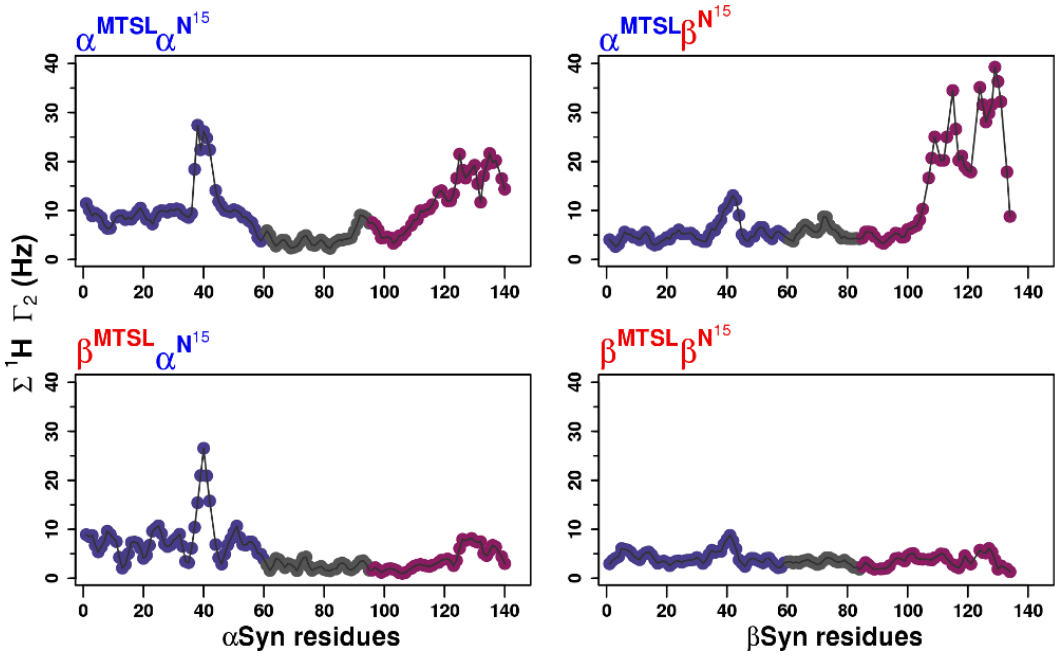

Figure 23 Interactive regions of dimeric complexes. Summation of the PRE rates as a function of residue indicates that (A) in αS homo-dimeric complexes interactions occur at the N and C-termini. (B) In βS/αS hetero-dimer complexes, interactions with αS are mediated primarily through the C-terminus. (C) In the αS/βS hetero-dimer interactions are mediated by the αS N-terminus. (D) in βS homo-dimer there are essentially no interactions. In all plots N-terminus is plotted violet, NAC is grey and C-terminus is pink.

Table 2 K_D values for αS/αS homodimer as fitted χ-squared statistic using equation (1).

α/α homo-dimer			
residue number	**K_D [μM]**	**Γ_2^{bound} [Hz]**	**Γ_2^{free} [Hz]**
119	151.5 ± 22.6	24.8±1.4	0.1±0.4
124	269.7± 115.3	26.6± 5.5	-0.1±0.9
125	397.8±143.7	56± 11.5	-0.6±1.1
126	87.1 ± 59.4	33.9± 6.9	-0.4±3.5
129	157.4±53.2	41.2± 5.4	-0.2±1.7
130	719.7±216.1	128.1±26.1	0.4±1.1

135	241.2± 45.4	29.2±2.5	0.1±0.5
137	1219.8+-/858.6	133.9±72.7	0.9±1.2
139	934.3±532.1	75.5±31.2	0.6±0.8

Table 3 K_D values for αS/βS hetero-dimer as fitted using χ-squared statistic.

α/β hetero-dimer			
residue number	**K_D [μM]**	**Γ_2^{bound} [Hz]**	**Γ_2^{free} [Hz]**
111	36.8±34.2	22.5±3.5	-0.2±3.6
112	107.8±39.4	22.6±2.4	-0.3±1.4
115	348.8±111.1	60.7±9.1	0±1.7
116	84.8±29.4	19.2±1.7	-0.2±1.2
118	141.3±34	23.4±1.8	-0.3±0.9
119	140.5±88.4	35.3±7.3	-0.9±3.5
120	338.3±166.7	55.3±12.7	0.1±2.4
121	187±56	40.1±4.4	-0.5±1.6

124	54.7±31.5	29.3±3.6	-0.2±3.1
125	98.3±31.9	28±2.5	-0.3±1.6
126	105.3±21.2	29.9±1.7	-0.2±1
127	36.8±34.2	22.5±3.5	-0.2±3.6
128	90.7±56.2	38.2±6.3	0±4.2
129	133.5±63.6	40.7±6.2	-0.7±3.1
131	80.7±21.8	32.3±2.2	0.1±1.6
133	142.6±20.1	31.2±1.4	-0.2±0.7

Chapter 6. Oligomers on aggregation pathway and influence of βS on αS oligomers formation.

Oligomers of αS are implicated to be the primary toxic species in Parkinson's disease. [98-103,105,110,315,316] They are suspected as the main means of spreading disease through the propagation of misfolded proteins from cells to cells, and they are implicated to be the intermediates to forming Lewy Body inclusions which are found in brains of patients with Parkinson's disease.[98-103,105,110,315,316] The toxicity of oligomers may possibly be related to the oligomers themselves, as they could block some essential pathways of cell function and organization or they may affect degradation pathways and induce formation of pores in the membranes.[317] One of the main objectives in Parkinson's disease research is to generate oligomers whose toxicity is diminished. Characterization of the oligomers is extremely challenging as they are highly heterogeneous and non-uniform. [95,99,109,110,112,113,115,117-119,121,124,316,318-325] Understanding the basis of the oligomer toxicity-structure relationship is of the highest importance if we would like to develop strategies to prevent αS from accumulation. As αS coexists with βS in presynaptic brain regions we believe that βS could also regulate to some extent the formation of oligomers of αS, and possibly the co-presence of αS with βS could lead to changes in oligomer structures. Here, in this chapter I will describe oligomeric species of αS, βS and how co-incubation of αS with βS affects oligomer formation. I will also describe attempts to prepare oligomers at different time points of aggregation: how they differ in terms of their general characteristics, toxicity and aggregation rates.

6.1. Characterization of αS oligomers.

6.1.1. αS oligomers preparation.

We prepared different types of oligomers by generating and isolating them in different stages of aggregation. There are three main stages of aggregation: lag phase, elongation phase and mature amyloid phase (see section 1.2.6.). Here in this chapter we describe separation of (A) non-incubated oligomers, present at the beginning of the incubation (type 0) (B) early oligomers (type 1) and (C) late oligomers (type 2). Description of the oligomers is shown in table 4, and is shown on figure 24.

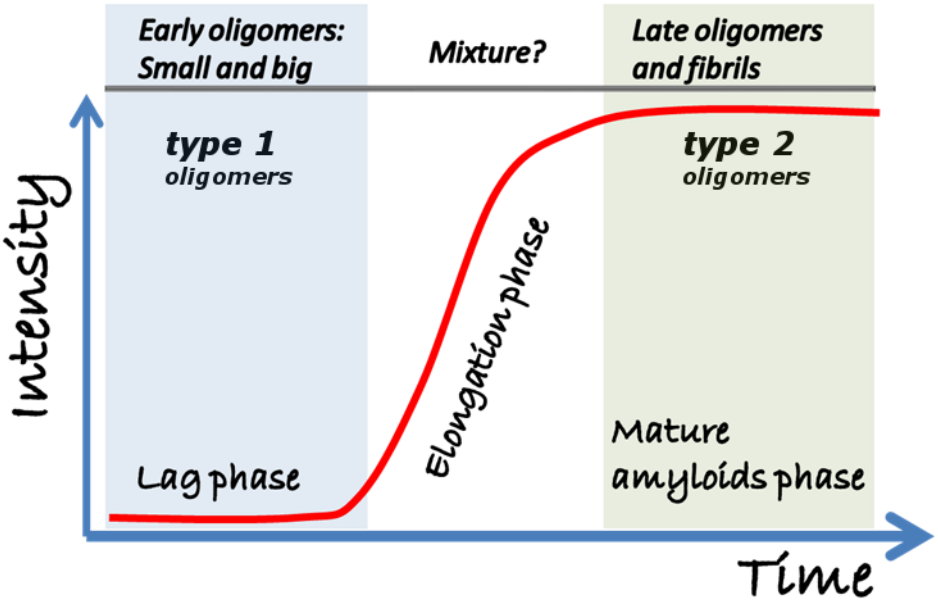

Figure 24 Schematic of the aggregation pathway for αS. Three different stages of aggregation are shown: lag phase, elongation phase and mature amyloids phase. Presence of the higher order species is marked above the axis. Oligomers purified in the lag phase will be called early oligomers or type 1 oligomers, while oligomers purified at the mature amyloid phase will be referred to as late oligomers or type 2 oligomers.

Type 1 oligomers (early oligomers) are formed in the lag phase of aggregation. A second type of oligomer that we purified (type 2) is obtained in the later stages of aggregation and co-exists with fibrils, and we will call them late oligomers. To obtain type 1 oligomers we purified oligomers before the fibrils are formed at 5h of incubation. Late oligomers were purified after the turbidity of the sample increased, which is indicative for fibril formation.

Oligomers were prepared using a modified protocol of Lorentzen *et al.* [326] In short, 12 mg/ml of αS was dissolved in PBS, sample was incubated in 37°C for about an hour or until dissolved. Later sample was centrifuged in 14000rpm for 30 min to remove un-dissolved protein and big oligomers. Mostly monomeric sample was incubated for 5h to create early oligomers, which we will call type 1 oligomers, and for at least 24 hours to prepare late oligomers which we will call type 2 oligomers. Time resolved analysis of incubation pointed out that the sample at 24h already has fibrils present in solution. Fibrillation starts to be pronounced at 12 h of incubation. Samples were prepared with linear shaking 700 rpm in 96 well plates and the volume of each sample ranged from 100-150 uL.

6.1.2. Oligomer purification

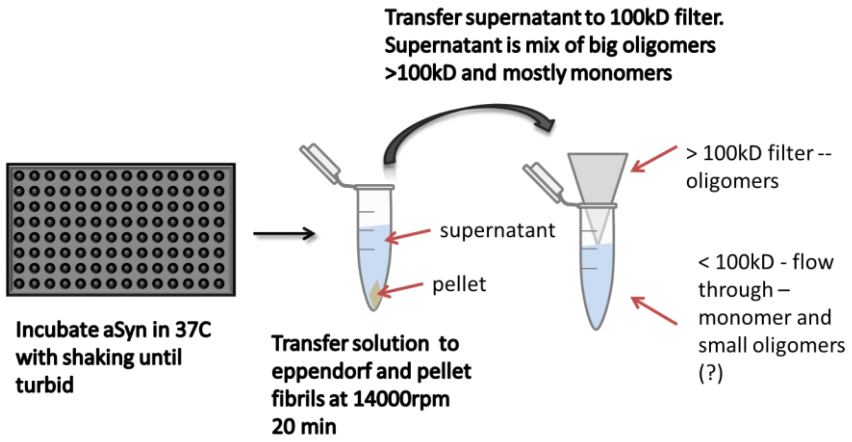

Figure 25 Schematic description of the preparation of the oligomers. Oligomer preparation consists of shaking the protein at 37°C for desired amount of time to prepare mixture of monomers, oligomers and eventually fibrils. To isolate monomers, soluble oligomers, insoluble oligomers and fibrils, first we remove higher order species: insoluble oligomers and fibrils by centrifugation. In the next step we purify oligomers from the monomers using either size exclusion column of filters. Here, on the figure we show preparation with filters, where monomer, oligomer mixture is applied to the filter, and taking advantage of the filter cut off which enabled us to purify oligomers from monomers based on molecular weight.

For example αS protein solution which was incubated to obtain the type 2 (late) oligomers contained three main species of synuclein: monomers, oligomers and fibrils. Therefore to be able to

isolate all types of oligomers (types 0,1&2) from the sample, we assumed that we need to purify oligomers from monomers and fibrils. Fibrils in general are insoluble as they are high molecular weight species, which enabled us to remove oligomers from the solution by centrifuging them out. To remove fibrils we spun down incubated sample for 1h at 14000rpm. In the next step supernatant was carefully collected, to prevent disturbance of fibrillar pellet. Supernatant contains both monomers and oligomers, so further purification was necessary. Oligomers were separated from monomers based on the differences in their molecular weights, using two general approaches: (A) size exclusion column purification (B) Filter usage. Purification of the oligomers using size exclusion column was generally used on type 1 oligomers for few reasons: a) the amount of the early oligomers was higher than the late oligomers, so it was possible to purify oligomers using this approach b) early oligomers of αS can be divided into two subtypes, based on their mass, so they are further purified. c) size exclusion column approach ensures that the sample we purify is solely oligomeric and that monomer can be removed. We also attempted to purify oligomers using filters with 50kD and 100kD cut offs. We used filters as follow: samples were applied to the filter top and spun down for 3 min, at speed 8000 rpm or 14000 rpm. Next, concentrate which contained oligomers was washed with buffer 5x at 14000 or 8000 rpm. Size of the samples was checked using DLS. Size exclusion column approach seems to work better for the early oligomers, and filter purification approach is better for the late oligomers as they are less concentrated.

Table 4 Description of all the oligomeric species prepared for αS.

αS oligomers type:	Incubation time	Purification description
Oligomers type 0	No incubation	Oligomers present in monomeric sample due to lyophilization
Oligomers type 1b	5h	Purification with SEC column, bigger size fraction
Oligomers type 1a	5h	Purification with SEC column, smaller size fraction

Oligomers type 2	24h	Oligomers co-present with fibrils, purified using filter

6.1.3. αS oligomers characterization – time dependent oligomer formation

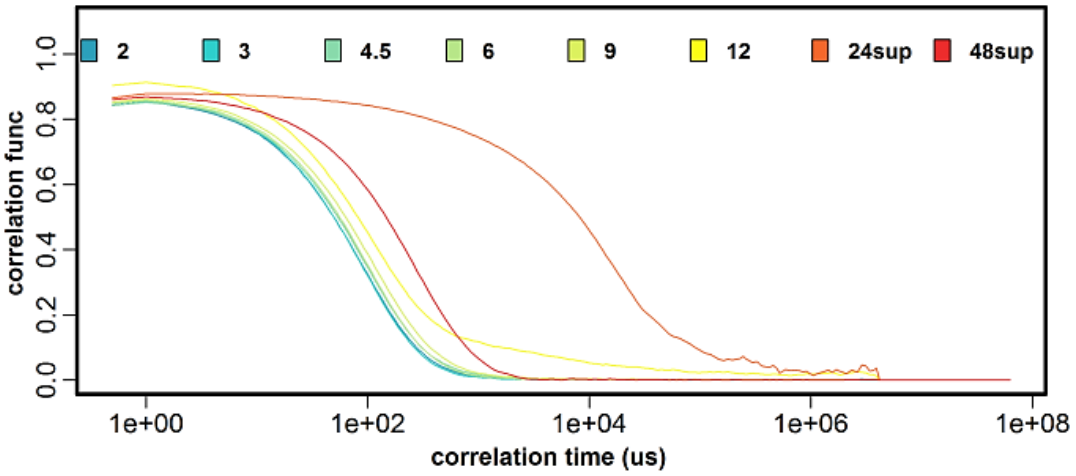

Figure 26 Size of oligomers at different incubation times. 12 mg/ml of αS were incubated at 37˚C with shaking. 5uL aliquots of the samples at the different time points were taken and diluted to ~50uM sample, which is an appropriate concentration for the DLS measurements. For each sample 3 measurements were taken with 10s averaging each. Here we present data as the correlation function at the different times of incubation, which is colored according to the legend on the top. Sup label for the 24 and 48 hours of incubation means that fibrils were removed from the sample by centrifugation, so sample used for DLS was just supernatant.

To determine how the sizes of αS oligomers change during the aggreation pathway we dissolved 12 mg/ml of αS and incubated at 37˚C with shaking and took aliquotes of the samples at the different timepoints of incubation. We diluted aliquotes that we took from the stock to ~50uM sample, which is an appropriate concentration for the DLS measurments. As we show in fig. 25 the correlation function for the first 9 hours of incubation is almost unaffected suggesting no changes in the size of the oligomers or their heterogeneity. At 12 h of incubation samples increase in size and

polydispersity, but there is still no fibril, as monitored by the turbidity changes. At 24 and 48 hours, the sample is turbid signifiying that the fibril is present. Thus to obtain reasonable DLS readings we pelleted the fibril for 10 min in 14000 rpm and performed experiments on the supernatant. Oligomers that are present in the sample at 24h are highly heterogenious and contain species with high molecular weight sizes. At 48h of incubation, the size of the oligomers decreases, compared with the sample at 24h hours of incubation, but the protein mixture is still bigger than it was in first hours of incubation. Additionally, we tested if the sample gave a ThT signal which would signify that

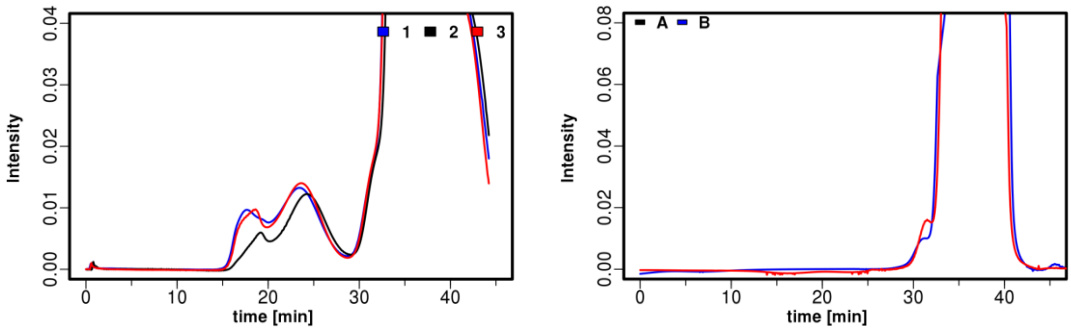

Figure 27 Size exclusion column profiles for αS sample incubated for (A) 5h (type 1 oligomers), (B) recovered sample from the monomer incubated for 5h. Triplicates of the samples incubated for 5h exhibit nice separation of monomers from oligomers, for the recovered sample there is no oligomers formed, only monomers were present in the sample.

fibrils are present in the mixture, only samples at 24 and 48 hours of incubation show increased fluorescence intensity. Results presented here show that there is a transition from early to late oligomers upon aggregation. These data are consistent with results by the Dobson laboratory,[316] who suggested that there are two types of oligomers that are able to transition from one type to another. Oligomer sizes upon αS incubation increase slightly along with polydispersity, and at a certain point there is a big transition to fibril-like oligomers.

6.1.4. Comparison of early and late oligomers of αS formation and secondary structure.

Time incubation of αS enabled us to distinguish two types of oligomers: type 1 (early) and type 2 (late). Oligomers formed at the early stages of oligomerization can be separated based on the molecular weight as monitored by SEC. Two types of early oligomers can be separated using SEC; we will call these oligomers small and big or respectively type 1a and type 1b. Triplicates of the sample was made to check if the oligomeric pattern is changed, and we saw that oligomers show similar pattern for all three samples (fig 27).

Early oligomers are not the same as late oligomers; early oligomers are not present at the late stages of aggregation, possibly because they are being incorporated into fibrils or because they transition to late oligomers. However, it seems that early oligomers are on the pathway to fibril formation because their removal from the sample retards not only fibril formation, but also oligomerization. Removal of early oligomers (type 1) from the sample, and re-incubation of monomeric sample did not result in fibril or even oligomer formation even when incubated for 14h (fig.27b). These facts suggests that the early and late oligomers (type 1 and 2 oligomers) are distinctly different from each other. It is however possible that early oligomers are being incorporated into the fibril or later being transformed into the late stage oligomers. Additionally, we purified αS monomers from oligomers after 5h of incubation and then attempted to generate oligomers from these recovered monomeric samples. However, even after 5h of incubation recovered monomeric samples show no indication of oligomers suggesting that the oligomers that are present in the initial stages might be crucial for fibril formation.

We characterized the secondary structure of the oligomers formed at the early and late stages of aggregation using CD. Type 1a and 1b (early small and big) oligomers exhibit similar secondary structure, meaning that despite their different sizes their secondary structure and conformational organization might be similar (fig. 28A, lines blue and black). Late oligomers however exhibited highly beta-sheet like secondary structure (fig. 28A, red line). Literature concerning oligomers is highly complicated, but there are two general trends in the characterization of αS oligomers. It is

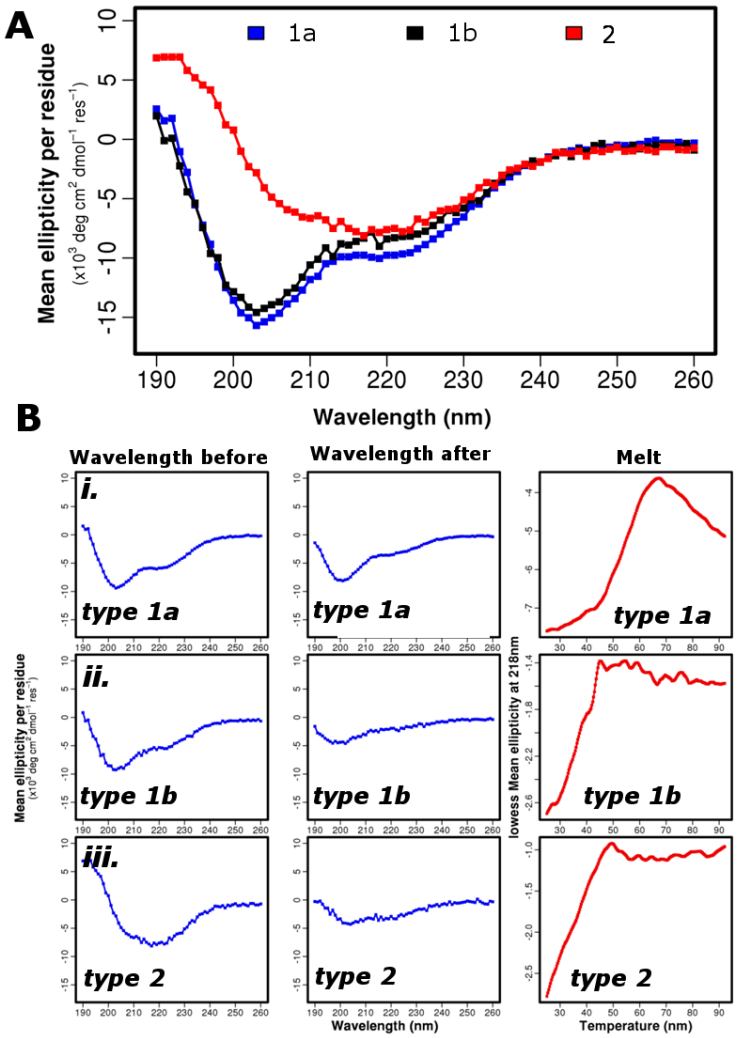

Figure 28 Secondary structure of αS oligomers purified at the different aggregation time points.(A) type 1a and type 1b (early small and big) oligomers have similar secondary structure, while type 2 (late) oligomers are more beta-sheet like. (B) Melts of the oligomers prepared at different time points. First column shows the wavelength scan before the melt, second column secondary structure after the melt, thirdcolumn represents melts of the oligomers. The melt was performed for temperatures from 25˚C to 90˚C, detection was centered at 218 nm wavelength, which is the wavelength typical for the beta-sheet. Wavelength scans before, after and melt for i) type 1a oligomersii) type 1b oligomers, iii) type 2 oligomers.

believed that αS can form two types of oligomers: (1) oligomers that exhibit mixed helical and unfolded secondary structure and (2) oligomers with highly beta-sheet like structure.[95,99,109,110,112,113,115,117-119,121,124,316,318-325] Moreover, data suggests that toxicity of oligomers is rather linked with beta-sheet structure of oligomers. As the fibrils are beta sheet like it seems

plausible that beta-sheet like oligomers will be on the pathway to fibril formation and may be intermediates for aggregation.

6.1.5. Stability of early and late oligomers of αS (type 1 and 2 oligomers).

We attempted to check the stability of the oligomers by doing CD melts of different αS oligomeric species (see figure 28B). We performed wavelength scans before the melt and after the melt. As described in the previous section and shown on figure 28A, αS type 1 and type 2 oligomers have different secondary structure. Secondary structure propenisties for type 1a and 1b oligomers are similar (fig 28A), but as we can see from stability analysis done with CD melts, they have distinctly different melting temperatures (fig. 28B.i and 28B.ii). Type 1a (small,early) oligomers have higher melting temperature than type 1b (big, early) oligomers, respectively ~55°C vs. ~40°C. Type 2 oligomers which exhibit significantly different secondary structure (beta-sheet) from type 1 oligomers (mixed unfolded with helix), have melting temperature around ~40°C, which is similar to the melting temperature of type 1b oligomers (fig. 28B.ii and 28B.iii). These data suggest that the stability of the oligomers is not directly linked to the secondary structure that they exhibit, but rather suggests that the conformation in which oligomers might exist could be important.

Type 1 and 2 oligomers of αS are heterogeneous species, theirs polydispersity value (DLS) is high (data not shown). Wavelength scans recorded after the melt showed that melting of the type 1b oligomers, and type 2 significantly lowered the CD signal suggesting that with high likelihood temperature change caused denaturation or are unfolding of oligomers. (fig. 28B.ii and 28B.iii). Only in case of the type 1a oligomers signal after the melting could signify that the proteins is unfolded by the temperature, as the spectrum looks more unfolded. αS oligomers: types 1a, 1b and 2 melt in different ways. Melt induced changes in the secondary structure of the oligomers, and decreased its polydisperity as checked with DLS data, but did not affect avarage size of the oligomers, suggesting that in this heterogeneous oligomeric sample there are more stable (which act as core) and less stable oligomers (data not shown).

6.1.6. Toxicity of αS oligomers.

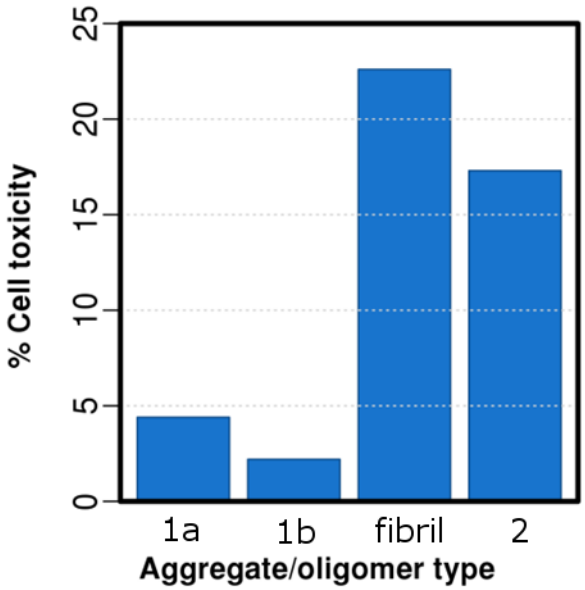

Figure 29 LDH toxicity assay for oligomers. 3 different types of the oligomers were coincubated with SH-SY5Y cells for 24h: type 1a, 1b and type 2 oligomers as well as fibril was coincubated with the cells.

Another question we wanted to answer concerned the toxicity of different types of oligomers to the SH-SY5Y cells (fig. 29). We incubated the cells for 24h at a 5uM concentration for type 1a and type 2 oligomers and 1.5uM for type 1b oligomers. Only type 2 oligomers show cell toxicity after 24h of incubation. It is possible that the type 1 oligomers would exhibit toxicity after incubation for a longer time. These results suggest again that type 1 and type 2 oligomers are different, since they have different aggregation propensities.

6.1.7. Thioflavin T seeding experiments: evaluating ability of type 2 oligomers to seed αS aggregation.

Controls for seeding experiments.

After we detemined which oligomeric species are able to induce toxicity in cell lines, we planned to investigete the ability of these species to seed aggregation and to form oligomeric species in the cell lines. As a control to characterize fibrillar and propagating properties of type 2 (late) oligomers

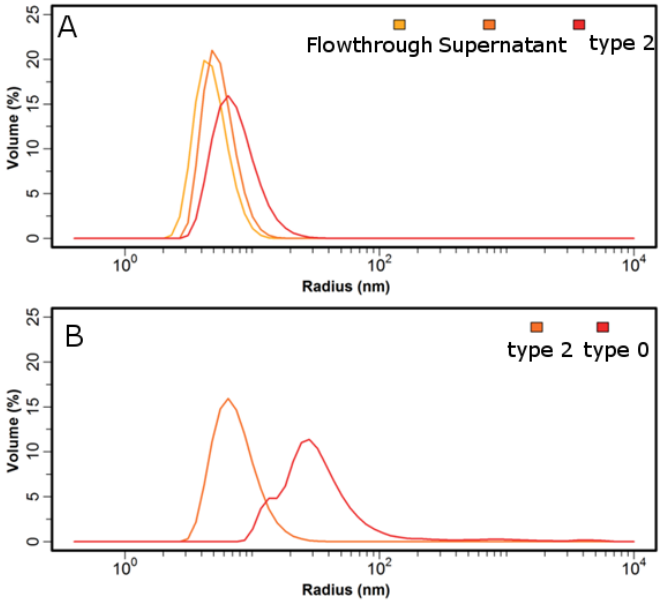

Figure 30 DLS profiles for αS oligomers: (A) oligomer purification using filter: supernatant (mixture of flow through and oligomeric sample), flow through and type 2 oligomers , (B) Comparison of the sizes of type 0 and type 2 oligomers).

we used type 0 oligomers, that is oligomers which are present at the time 0 of incubation of αS, formed due to lyophilization and sample flash freezing in liquid nitrogen (see table 4). Type 0 oligomers provide good control to test fibrillization properties of type 2 oligomers of αS, as they are formed not on the aggregation pathway but rather spontanously through lyophilization, suggesting that theirs conformation is not related to the conformation of on-pathway, toxic oligomers.

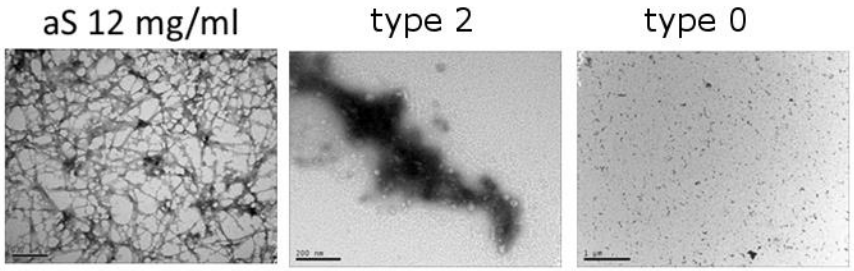

Figure 31 TEM profiles for αS sample and purified oligomers. (A) fibrils in the sample after 24h of incubation (B) type 2 oligomers(C) type 0 oligomers

Comparison of the type 0 and type 2 oligomers pointed out to the changes in their size and secondary structure. DLS analysis showed that using filter purification approach (see section 2.4)we

were able to separate some oligomeric species from the supernatant. DLS profiles for type 2 oligomers, points shows higher molecular weight than size of supernatant and flow through. As we compared two different species of the oligomers, we showed that there are significantly different in size as shown on DLS (fig. 30). Type 2 oligomers (late oligomers) are much smaller that type 0 (oligomers present in the lyophilized sample), meaning these two samples of the oligomers showed evidently different initial architecture. However differences between these two different types of oligomers can be also seen in the general secondary structure of the oligomers: type 2 oligomers seem to be more unfolded and type 0 seem to exhibit highly ordered secondary structure. Also CD profiles point out the differences in the secondary structure of the type 2 and the supernatant and the flowthrough, which are both unfolded and bear signature of the monomeric unfolded αS, while

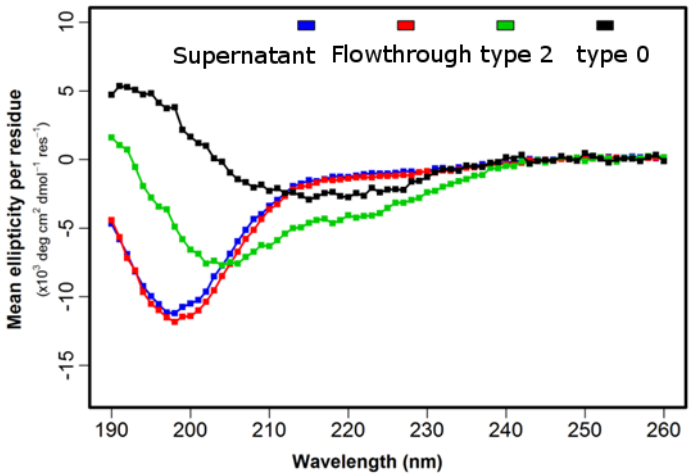

Figure 32. CD spectrum of oligomers prepared for seeding experiments: type 0 (oligomers present at the initial time points of the incubation), type 2 (oligomers present in the sample after 24h of incubation), supernatant (type 2 with monomers), and flowthrough (monomers). Type 0 oligomers were purified using size exlusion column and concentrated using 3kDa filter. Type 2 oligomers, coexist with fibrils, and incubated with shaking for 24 h, and purified first by removing fibrils and later by using 100kD filter. Mixture of the oligomers and monomers we will call supernatant, and flowthrough, should contain mostly monomers.

oligomers distinctly exhibit more ordered secondary structure. (fig. 32) TEM analysis of the oligomeric samples of these species showed that the only initial fibrilar sample was visible using TEM, and both oligomers type 0, and type 2 are too small to be visualized using TEM. Initial sample from which type 2 oligomers are obtained is also shown as control, to prove that fibrils were abundantly present in the mix before type 2 oligomers purification (fig. 31).

Seeding αS monomers with oligomers.

Samples used for seeding

To test the seeding properties of the oligomeric species on monomeric samples we performed

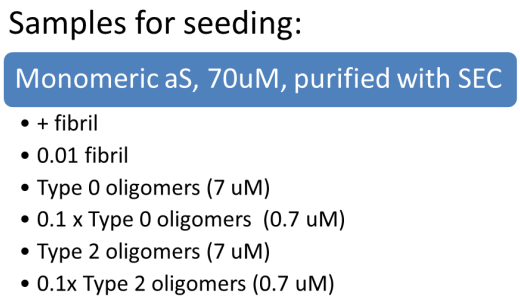

Figure 33 Samples prepared for the seeding experiments for ThT assay. Concentration of the samples was measured using BCA assay.

ThT seeding assay where we compared how different oligomers or fibrils are affecting monomeric sample aggregation and fibril morphology (See fig. 33). Main goal was to see how toxic type 2 oligomers are affecting aggregation kinetic and how its kinetics compare to seeding with positive (fibril) and negative (type 0 oligomers) controls.To do so, we prepared pure αS protein with size exclusion column at a concentration of 70uM, and we treated that monomeric sample as a control. We coincubated this monomeric αS sample with different oligomeric species (type 0 and type 2) and a fibrilar mixture. Concentration of the oligomers that was used was 10x and 100x lower than concentration of the monomer (7uM, or 0.7uM). For monomeric αS at a concentration lower that

30uM it is very hard to form fibrils that are detectable using ThT assays, so using a low concentration of αS oligomers was to ensure non-aggregating initial concentrations. As a positive control we seeded αS with fibrillar samples, which seeds formation of the fibrils of the αS .

ThT seeding experiments

The effect of seeding of αS was monitored by ThT assay for 4 repeats of each sample: monomers and monomers seeded with type 0, type 2 and fibrils. There are two main effects that we can observe by seeding with different samples: changes in the ThioT intensities and changes in the aggregation kinetics upon seeding. Addition of fibrils and type 2 oligomers changed the level of ThT binding suggesting that there are either more fibrils formed or that the fibril architecture is more compatibile with the binding mode of ThT. Type 0 oligomers decrease ThT binding. Seeding with 0.1x type 0 oligomers and low concentration of the fibril keeps the level of ThT binding the same as the control sample (fig. 34A).

Changes in the kinetic of the aggregation can be seen on the normalized data for the aggregation.

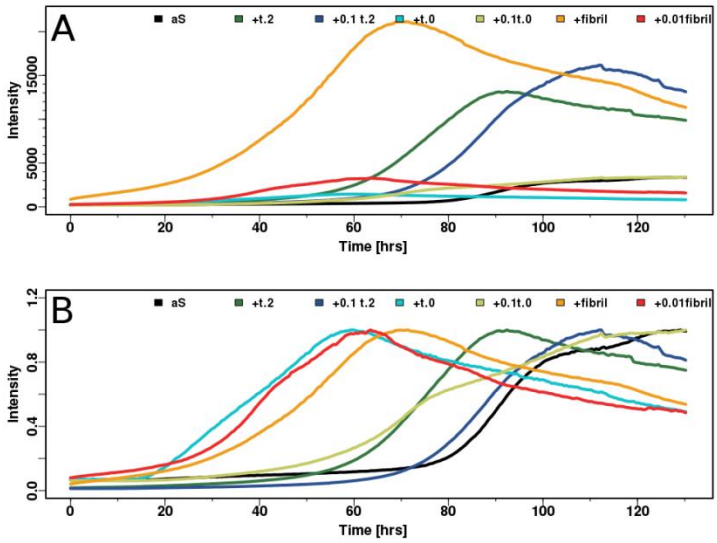

Figure 34. Aggregation assay of αS seeded with different oligomers: type 0 (oligomers present at the initial stages of aggregation) and type 2 (oligomers present at 24h of incubation) and fibrils. ThT assay of 70uM monomer with different oligomers in concentration of 7uM or 0.7uM was conducted. (A) Averaged ThT assay of 4 sample repeats was performed, curves not normalized. (B) Averaged and normalized curves of ThT seeding with oligomers and fibrils.

There are two main parameters that are considered while describing aggregation kinetics: changes in the lag phase and slope of aggregation. First parameter tells us how prone is sample to aggregate, while second how fast aggregation occurs. Seeding with Type 0, 0.1x type 0, type 2 and fibrilar samples decreases the lag phase, meaning that the all of these samples are more prone to aggregate, but the slope of the aggregation is very similar to the control monomeric sample. The only sample that showed different behavior was the 0.1x type 2 oligomer sample, which has aggregation rates very similar to the control samples in both lag phase and slope of aggregation. (fig.34, B-D) In general it seems that addition of all, but one the species is enhancing aggregation rates.

Characterization of the fibril morphology formed in seeding experiments

Characterization of end products of all of the seeding events by TEM provides an excellent contemplement for the ThT assays. We compared morphologies of the fibrils formed during seeding experiments with monomeric control and fibrilar sample which we used for seeding, and from which we purified type 2 oligomers. The fibrils formed by the high concentration sample are different from

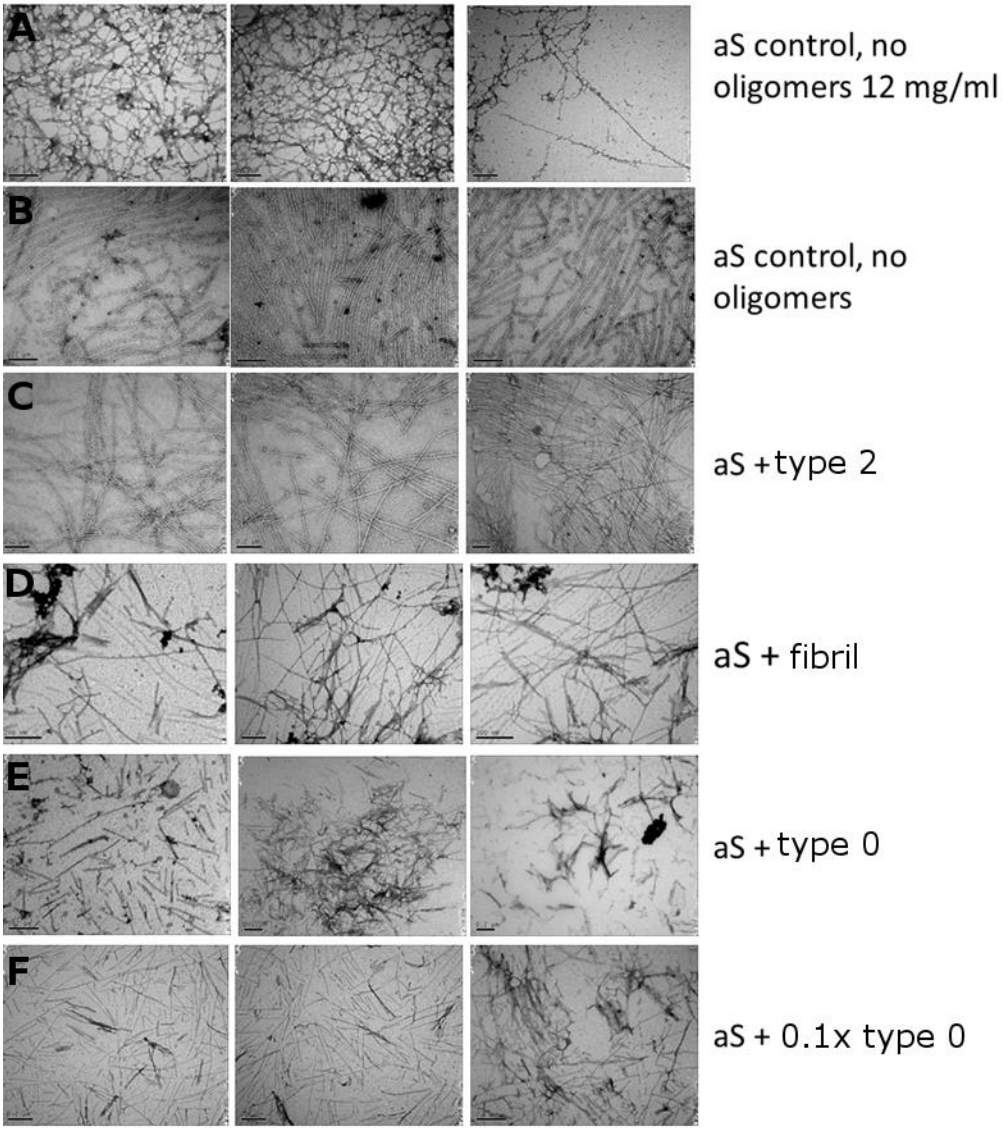

Figure 35 TEM profiles for the samples after seeding. Oligomers of the different type are able to induce different type of fibrils. (A) Initial sample from which type 2 oligomers were purified. (B) Monomeric αS sample alone (C) αS oligomers seeded with type 2 oligomers (D) αS seeded with fibrillary sample from the αS 12 mg/ml sample (E) as seeded with type 0 oligomers (F) αS seeded with 0.1 type 0 oligomers (0.7um)

fibrils formed from monomeric αS sample, as a control we show sample from which type 2 oligomers were purified and which we used as positive fibrilar control. The fibrillar sample used for seeding. It exhibited fibrillar but branched morphology, and lack of symmetric organization. Fibrils formed by the pure monomeric αS (control) are highly organized and thick (fig.35B). Highly similar to them are fibrils which were formed by addition of type 2 purified oligomers to monomeric sample. Oligomers formed by addition of fibril mix are less organized and thin (more similar to the sample from which they were taken 35A&D). These two facts suggest that the oligomers which are prepared from the fibrillar mix result in less organized and uniform fibril structure; fibrils are formed faster but their final organization is heterogenious. Possibly the oligomers that were purified at the late stages of aggregation are not only increasing aggregation rates but also promote formation of the uniform, possibly highly ordered fibrils.

Type 0 oligomers have distinctly different effect on αS fibril formation from type 2 oligomers.

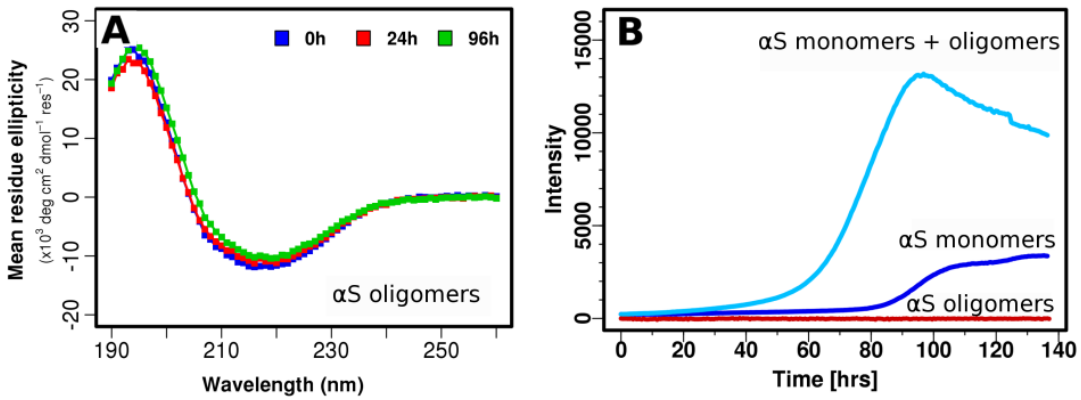

Figure 36 Oligomers are stable with time in vitro A.) CD measurement of type 2 oligomers incubated at room temperature immediately after isolation (blue), after 24 hours (red) and 96 hours (green). CD shows oligomers are stable and maintain essentially the same secondary structure in vitro for at least 4 days. B.) ThT fluorescence measurement of αS oligomers alone (red), αS monomers (blue) and αS oligomers co-incubated with αS monomer (cyan). ThT measurements show that oligomers alone do not form fibrils in vitro for at least 5 days. Co-incubation of αS monomer with αS oligomer significantly accelerates fibril formation relative to αS monomer alone. Samples were incubated at 37°C with agitation.

Type 0 oligomers decreases ThT binding, and leads to formation of shorter fibrils. Decreasing concentration of the type 0 oligomers leads to fibrils lengthening, as fibrils formed in presence of 0.1 type 0 are longer than type 0. It would seem that whatever oligomers are formed by addtion of this type of oligomers is done faster but with decreased efficiency.

In summary it is clearly seen from this data that the type of the oligomers that is introduced to the sample can affect greatly aggregation rates of αS . However it is still unknown what would be the most toxic form of the oligomers. It would seem from the data that the most toxic would be type 2

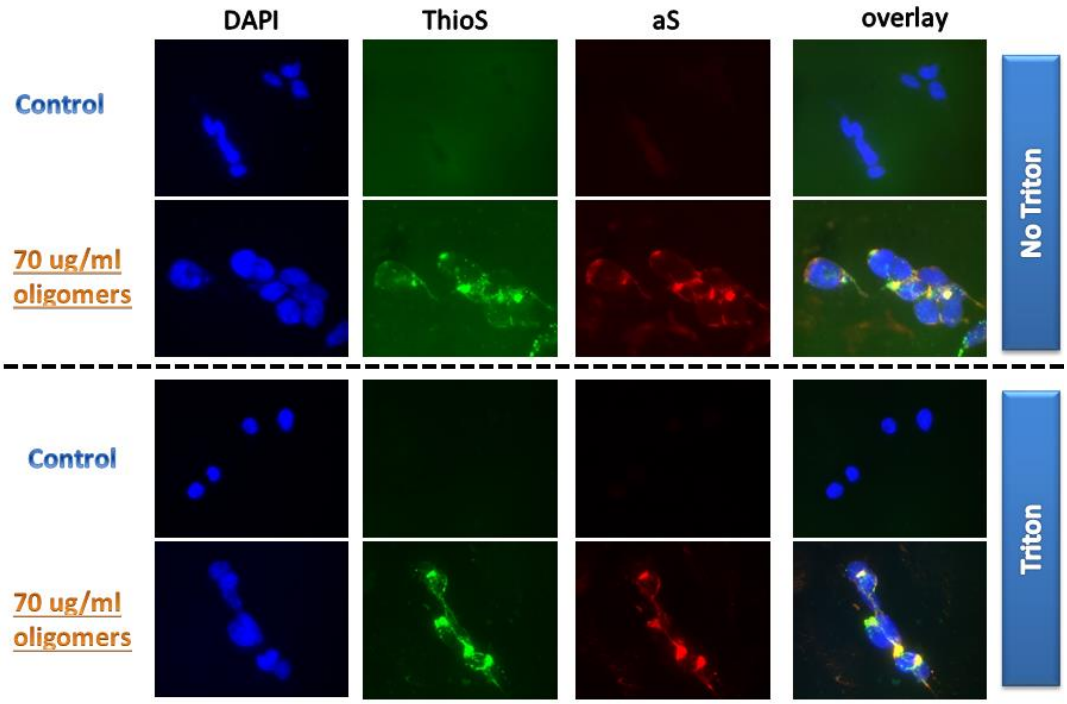

Figure 37 Oligomers undergo a transition to fibrillar inclusions in SH-SY5H cells. Immunofluorescence experiments on αS were performed in human neuroblastoma SH-SY5Y cell lines: A) Untreated cells (Control cells with no added oligomers) show no fibrillar αS inclusions; B) Cells treated with type 2 oligomers (5μm) show formation of αS fibrillar inclusions after incubation for 5 days before fixing with 4% paraformaldehyde and 1%TritonX100. Inclusions were immobile as they were not removed through Triton x100 extraction. First column: immuno-staining with αS antibody (red), second column: staining against fibril with ThioS (green), third column: staining with DAPI against nucleus (blue), fourth column: overlay of all the channels (αS, ThioS and DAPI) demonstrates co-localization of αS inclusions and ThioS signal.

oligomers. Type 2 seem to be able to accelerate formation of the highly ordered species, which suggests that they are important for fibril formation, as it might be possible that these less ordered species might be cleared from brains much faster, or be non-toxic.

6.1.8. Oligomers are stable with time in vitro.

We have performed experiments to assess the time dependent stability of the late type 2 oligomers which were shown to be toxic to cells (fig. 29). First, we show that the secondary structure of the oligomers as detected by CD remains essentially the same over 96 hours, at ambient temperatures (fig. 36A). Second, the oligomers do not transition to fibrils over the period of 5 days as measured by ThT fluorescence assays (fig. 36B). This is very important data as it demonstrates that the oligomers alone are stable with time and that the proposed structural experiments are measuring properties of stable species. In contrast, co-incubation of oligomers with αS monomers shows a dramatic increase in fibril formation relative to αS monomers alone suggesting that oligomers may be 'recruiting' monomer for rapid fibril formation

6.1.9. Oligomers undergo a transition to fibrillar inclusions in SH-SY5H cells.

Immunofluorescence imaging experiments in cells show that soluble αS oligomers (type 2 oligomers) undergo a transition from toxic soluble oligomers to fibrillar inclusions in SH-SY5Y cells (fig. 36B). We prepared type 2 oligomers in concentration 5uM/ml and we incubated them for 5 days with cells, in DMEM media with addition of 2% FBS. Samples were prepared with and without triton extraction. Control samples did not show any inclusion formation; cells shown in control samples were healthy, and did not show penetration with ThioS, which is fibril staining dye. There was only faint signal from αS antibody was observed in the cytosol. Samples co-incubated with fibrils exhibited significant amount of fibrillar inclusions, which co-stained with αS antibody. Inclusions were not removed in the extracted sample, which again suggests that the αS, fibrillary inclusions were immobile. Results presented here are in sharp contrast to *in vitro* studies in which oligomers alone do

not form fibrils (fig. 36B). One hypothesis for this difference, supported by our *in vitro* co-incubation

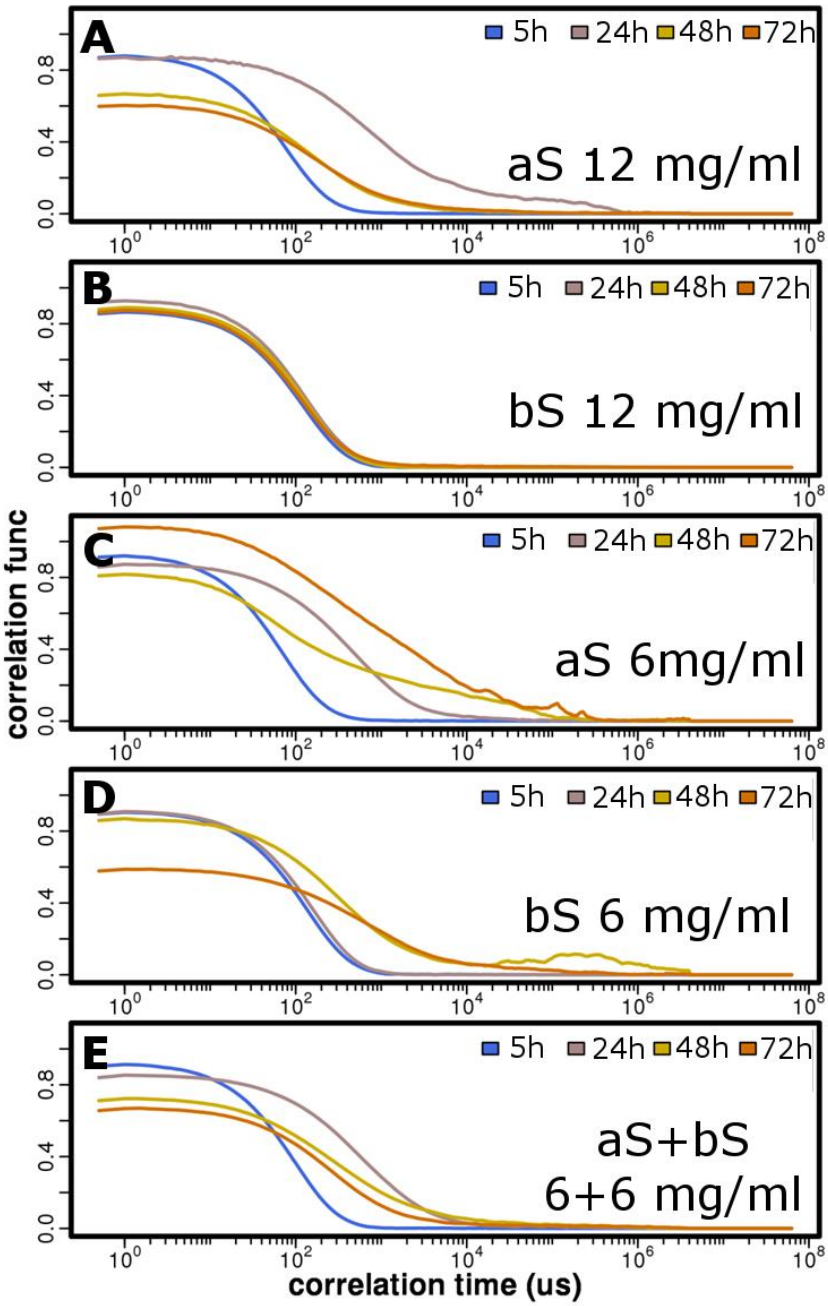

Figure 38 Size changes of oligomers at the different time points of the incubation measured using DLS. Samples were incubated for 5h (blue), 24h (dirty-pink), 48h (yellow) and 72h (orange). (A) αS 12 mg/ml oligomers (B) βS 12 mg/ml (C) 6 mg/ml αS (D) 6mg/ml βS (E) 6mg/ml αS + 6mg/ml βS

studies of αS monomer with αS stable oligomers (fig 36B), is that cells treated with oligomers

undergo a transition to fibrillar inclusions by recruitment of intra-cellular αS monomers. These data strongly argue that the oligomers that we isolate are 'on pathway' to fibril formation, and are therefore of extreme physiological relevance.

6.2. αS oligomers in presence of βS.

As αS co-localizes with βS in the brain it is possible that presence of βS may have an effect on oligomer formation of αS; this could affect the amount of oligomers formed, the secondary structure and toxicity. In this section we will describe effect of βS co-incubation with αS on oligomerization of αS.

6.2.1. Time incubation

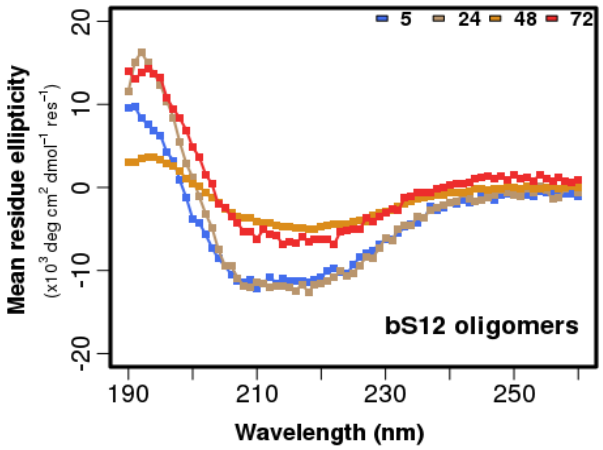

Figure 39 Comparison of the secondary structure of βS samples across the time series. βS oligomers were only oligomers for which we were able to analyze the secondary structure changes for 72h. Time incubation of βS 12mg/ml sample.

To assess the effect of time incubation and how the initial protein concentration affects the formation of the oligomers we performed time incubation of αS , βS and αS /βS oligomers (αS 12mg/ml, αS 6mg/ml, and βS 12 mg/ml, βS 6 mg/ml, and αS /βS 6+6 mg/ml). We observed that the samples which contained αS at 24 hours of incubation underwent a transition to form higher

order species. The samples were turbid at these times and we believe that the oligomers were present in the samples (fig.38.A.). After the fibrils are formed the amount of oligomer in the sample is significantly decreased, suggesting that the oligomers which are present in the sample at the initial stages are tranformed into fibrils. In case of βS incubation does not change the sizes of the samples significantly for time incubation for 12 mg/ml sample of βS, but for the 6mg/ml sample we observe that there is not enough of the oligomers at the later stages of the incubation (fig.38 and 39.). These fact show that in accordance with previous literature βS is slow to both oligomerize and fibrillize which is in stark contrast with αS behavior. [167,193,199,200]

βS oligomers maintain their secondary structure across the entire incubation, but αS oligomers change. At early incubation times oligomers of αS are more helical, then they undergo a transition to a beta-sheet structure (see section 6.1). The amount of late oligomers (type 2) of αS in presence of βS is significantly diminished as there is less of the late oligomers detected (fig. 38, 39, 40). We also show that αS coincubation with βS decreases the polydispersity of the oligomers formed by αS samples. Coincubation of αS with βS for 24h decreased size of species present in the sample, compared to αS

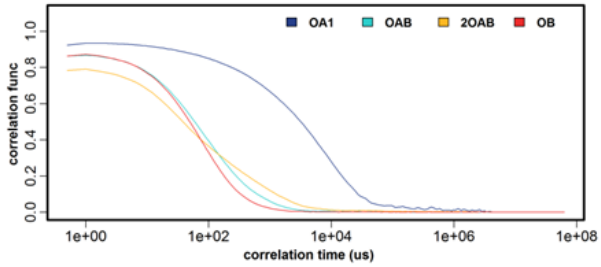

	PIdp	Intercept	Z-ave [nm]	Pk 1 [nm]
A	1	0.95	2133	5 or 23
AB	0.95	0.93	60	10.5
2AB	0.77	0.9	77	10.1
B	0.6	0.93	55	8.6

Figure 40 Sizes of the oligomers of αS and βS upon 24h co-incubation measured by DLS: αS 12mg/ml (dark blue), αS+βS 6mg/ml +6mg/ml (teal), αS+βS 12mg/ml+12mg/ml (orange), βS 12mg/ml.

samples alone.

Despite the high heterogenity of the oligomers, one thing is clear: coincubation of αS with βS decreases the amount of oligomers formed and renders the size of the species present in the samplesmaller, and decreases the polydispersity of the sample. As αS alone forms highly heterogenious samples while incubated alone (12 mg/ml), coincubation of βS with either 12mg/ml or 24 mg/ml decreases the polydispersity of the samples. βS alone had the smallest polydisperisity (0.6) (fig.40). Does it mean that the βS is affecting the aggregation pathway,by affecting the extent of oligomer formation is unclear, but the data presented here points out the importance of βS presence for αS oligomers formation, as it affects fibrillization and oligomerization process.

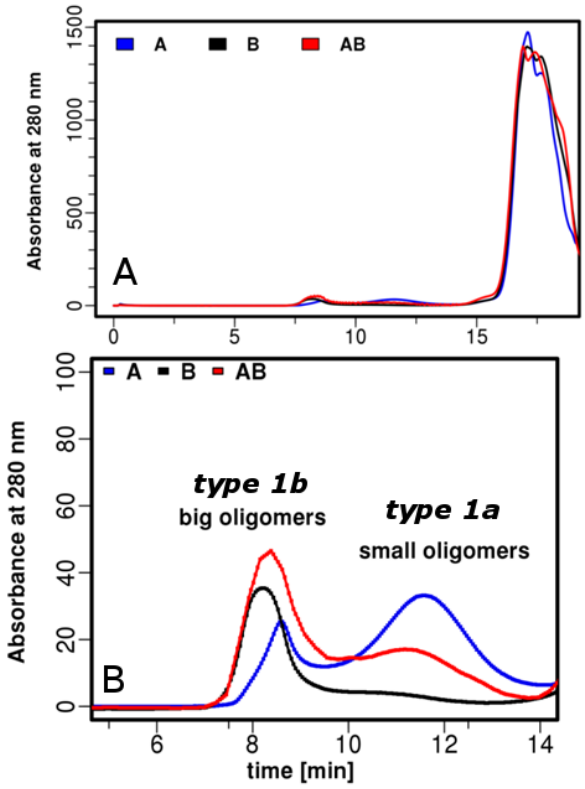

Figure 41 Size exclusion column profiles (superose 6) for samples incubated for 5h with shaking 12 mg/ml for αS and βS mixture (A) comparison of the αS (blue), βS (black) and αS/βS mixture elution profiles. (B) close up of the oligomeric region of the elution. The close up shows two distinct sizes of type 1 oligomers that can be formed: small and big, respectively type 1a and type 1b.

6.2.2. Type 1 (early) αS/βS oligomer characterization

We described how the oligomers of αS are being affected by βS on the different aggregation time points, now we will focus on the changes which βS induce on type 1 (early) oligomers. To do so, we first we assessed the effect of co-incubation of αS with βS on the formation of type 1 oligomers. We incubated αS, βS and a mixture of αS/βS sample for 5h and purified all oligomers using superose 6. In all cases the main fraction of the protein was monomeric, with just a small amount of oligomers. αS forms two types of type 1 (early oligomers): type 1a and 1b, while βS forms only one type of type 1 oligomers: type 1b (big, early oligomers). Co-incubation of αS with βS reduced the amount of the type 1a oligomers and increased the amount of the big oligomers formed. However, it is unclear if these changes are important for inhibition of αS aggregation. In summary, oligomerization properties of αS and βS differ; αS can form two types of oligomers while βS can form only one type of oligomer. Co-incubation of αS with βS seems to affect the fractions of oligomers formed: more type 1b oligomers are formed in αS/βS sample comparing to samples of αS or βS incubated alone.

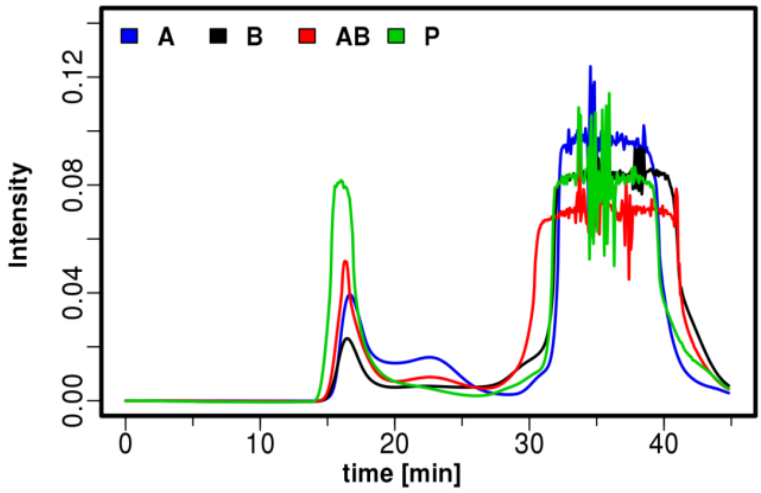

Figure 42 Comparison of amount of oligomers formed by different species of αS and βS. αS (blue), βS (black), αS/βS (red) and P123H-βS (green). αS forms two types of the oligomers 1a and 1b,while βS forms only type 1b oligomers. Toxic mutant of βS P123H also forms only type 1b oligomers, but amount of the oligomers formed is significantly increased compared to its non-toxic counter-part.

We also characterized oligomers formed by the toxic mutant of the βS – P123H (fig.42). As αS forms two different types of the oligomers, it would be plausible that the toxic mutation of βS, could

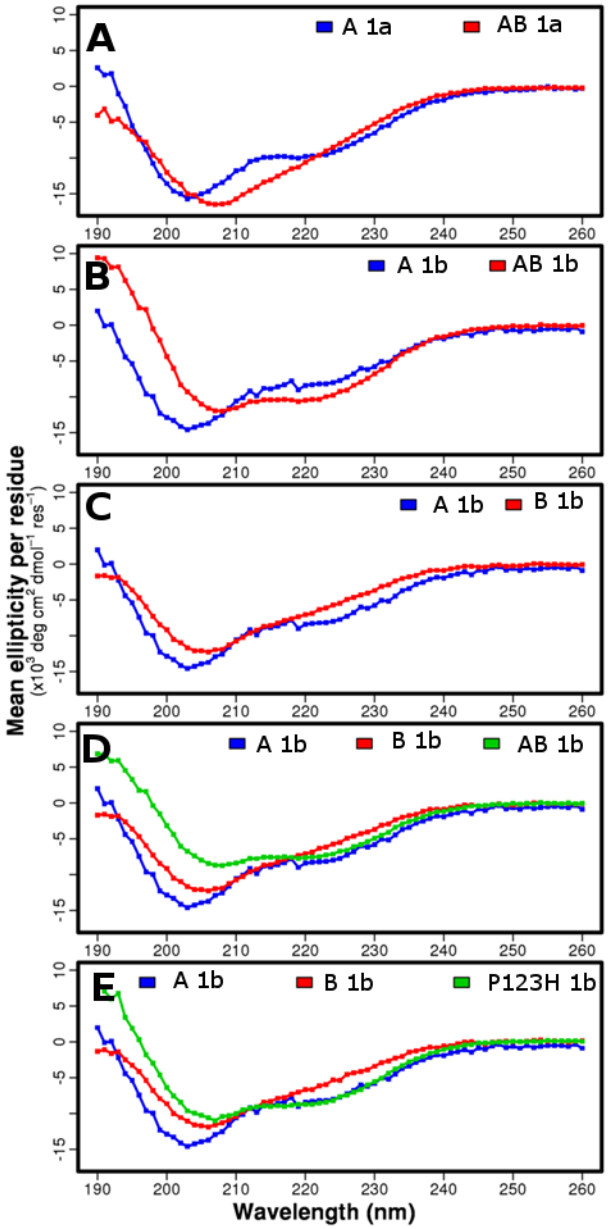

Figure 43. Secondary structure characterization of the oligomers purified using size exclusion column using CD at 5h of incubation, type 1 oligomers. Different types of the oligomers of αS, βS, αS/βS mixture, and P123H oligomers. Comparison of the type 1a and 1b oligomers for αS and αS/βS mixture is presented. For βS species (βS and P123H-βS) only type 1b are showed. A in the legend stands for αS, B stands for βS and AB stands for mixture of αS and βS.

also allow formation of type 1a oligomer. We prepared oligomers for αS , βS, αS/βS mixture, and P123H, and we show that P123H mutation did not result in formation of oligomers which are in similar sizes to αS, but rather it increases the amount of type 1b oligomers formed. These results suggest that the mutation in the C-terminus relates to forming more oligomers by mutant of βS, suggesting that the conformation of the C-terminus is important for the oligomerization properties. Moreover, increase in the formation of type 1b oligomers in the case of the P123H mutant might be at the basis for its toxicity, which might suggest that not the size of the oligomers, but some other characteristic might be responsible for toxicity of P123H-βS mutant.

To check if the secondary structure is maintained across the species within the same oligomeric type, we analyzed the secondary structure propensities of the different oligomeric species using CD. We checked the following types of oligomers: αS type 1a, αS type 1b, αS/βS type 1a, αS/βS type 1b, βS type 1b and P123H type 1b. Comparison betweeen these species provides us with information about the changes in secondary structures. αS type 1a and type 1b oligomers secondary structure is similar to each othe. Addition of βS to the αS sample is affects secondary structure of oligomers formed: (fig.43) Secondary structyre for αS/βS type 1a oligomers (early, small) seems to have more unfolded and beta-sheet secondary secondary structure tendencies, while comparing to αS type 1a oligomers alone. Comparison of αS and αS/βS type 1b oligomers show that αS/βS oligomers exhibit more helical secondary structure than the oligomers of αS alone. βS type 1b oligomers seem to have unfolded secondary structure with some beta-sheet structure present, so mixture of the oligomers of αS/βS type 1b obtain secondary structure more similar to the oligomers of βS which seems to be non- or less toxic. These changes might be important for the toxic function of the oligomers, but further analysis is required to be able to determine if that is the case.

6.2.3. Late oligomers

One of the mechanisms of αS aggregation inhibition through βS may be the inhibition of αS oligomer formation or redirection to different off-pathway oligomeric species. To check this

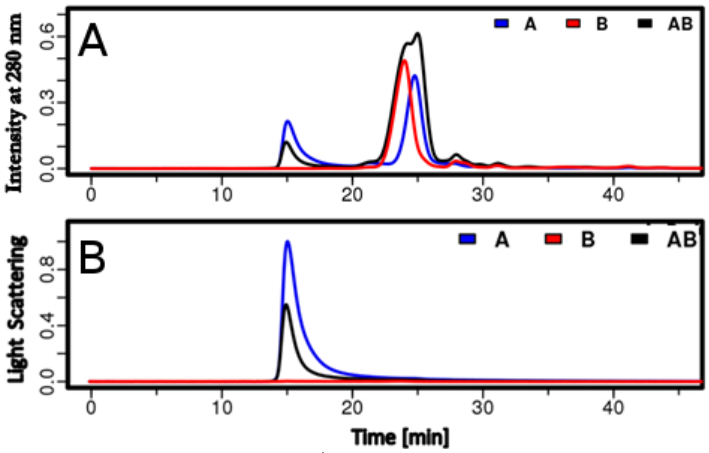

Figure 44 Type 2 oligomers formation of αS, βS and αS/βS samples. αS sample (blue), βS (red), αS/βS mix (black) (A) size exclusion profile (B) Raleigh ratio.

possibility we examined the effect of co-incubation of αS with βS on oligomer formation of αS at the late aggregation stages (type 2). Purification of these oligomers was performed using 100kD filters, where the pellet part of the sample was removed by centrifugation, and monomers and oligomers were separated using the filters. Using this procedure we obtained samples which we will call: supernatant (mixture of the oligomers and monomers), type 2 oligomers, and flowthrough which will consists mostly of monomers.

Initial analysis of the supernatant showed that there are oligomers and monomers in the sample. Monomers were highly populated in contrast to the oligomers. The quantitative analysis of the amount of oligomers with SEC-MALS showed that if αS is co-present in the sample with βS there is less oligomer formed in the samples (fig.44). That could suggest that the amount of oligomers in the samples upon incubation is highly sensitive to conditions and proteins co-present in the solution.

Purification of the different species of synuclein revealed that the αS mixture of oligomers and monomers (supernatant) differs significantly for αS, βS and αS/βS mixture. βS supernatant, has highly unfolded and similar to monomeric spectrum, the mixture of αS and βS samples lead to a profile slightly more folded than βS, which suggests that βS retards oligomerization of αS. For αS supernatant has a highly folded profile (fig. 45).

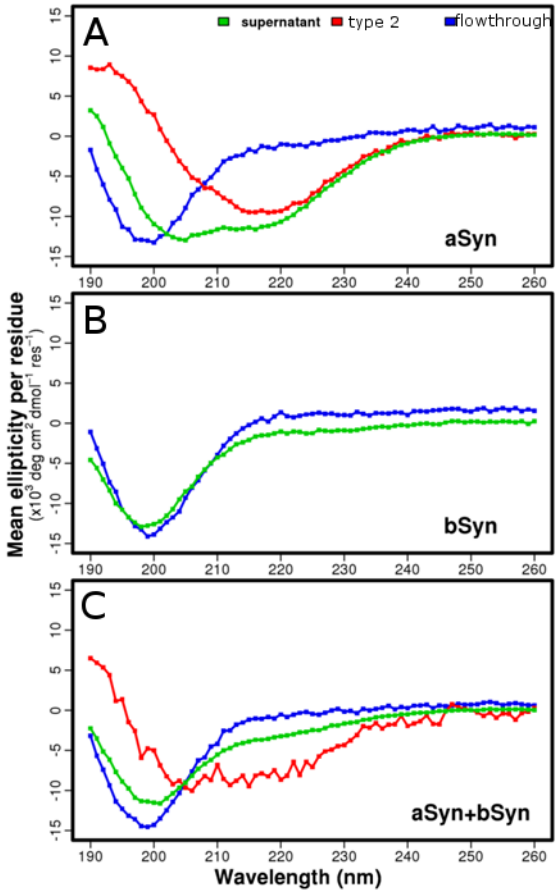

Figure 45 Secondary structure propensities of the type 2 oligomers of αS, βS and αS/bS mixture. Oligomers and monomers mixture – supernatant (green), αS monomers, flowthrough (blue), and type 2 oligomers) (A) αS samples (B) βS sample (C) αS+βS sample.

Our results show clearly that the inhibition of αS aggregation by βS can be acheived at multiple stages of aggregation. To check if the average secondary structure of oligomers differs we checked their secondary structure using CD. CD profiles for type 2 αS oligomers are beta sheet rich

(indicated by the minimum at 218 nm), while coincubation of the αS with βS keeps αS unfolded. Addionally there is less oligomer formed upon co-incubation of αS with βS. αS/βS oligomers seem to have more helical structure than the oligomers for αS alone. βS is not forming enough oligomers to be able to separate them, which is consistent with readings from SEC-MALS.

In summary we see that the oligomers of αS are affected by co-incubation with βS at all stages of aggregation. Late oligomer formation of αS in the presence of βS leads to the formation of oligomers that are different from the oligomers of αS formed alone. However, the significance of these changes at this stage is unknown. At this stage we were able to characterize some species on the aggregation pathway, that might be responsible for the inhibition of αS aggregation by βS. We were able to detect αS/βS heterodimers, as well as perform initial characterization of oligomer formation at the different stages aggregation (early and late). We showed differences on the aggregation rates at the different time points. The work presented here provides a good initial platform for future research in oligomer formation.

6.3. Challenges and future directions.

Characterization of oligomers at the different stages of aggregation is highly challanging, as there is significant variation in the oligomer formation between the runs, which suggests that the approach presented here requires refinement, and possibly some more uniform sample preparation.

Another big pitfall of the in vitro oligomer preparation is the fact that the oligomers formed in vitro, might not be representative of the oligomers formed in vivo or on the aggregation pathway. Intensive cross-checking with cell toxicity assays need to be performed to ensure the relevance of the research on the oligomers formed during in-vitro incubation.

Oligomers are highly variable suggesting also that there is high dependence on the conditions in which oligomers are formed, and preparation of oligomers under "more physiological conditions"

might be a key to ensure both uniform behavior of oligomer formation, but also might help oligomers to resemble more oligomers formed in cells. One of the possibilities here would be to use molecular crowding agents, what are mimicking cellular enviroment.

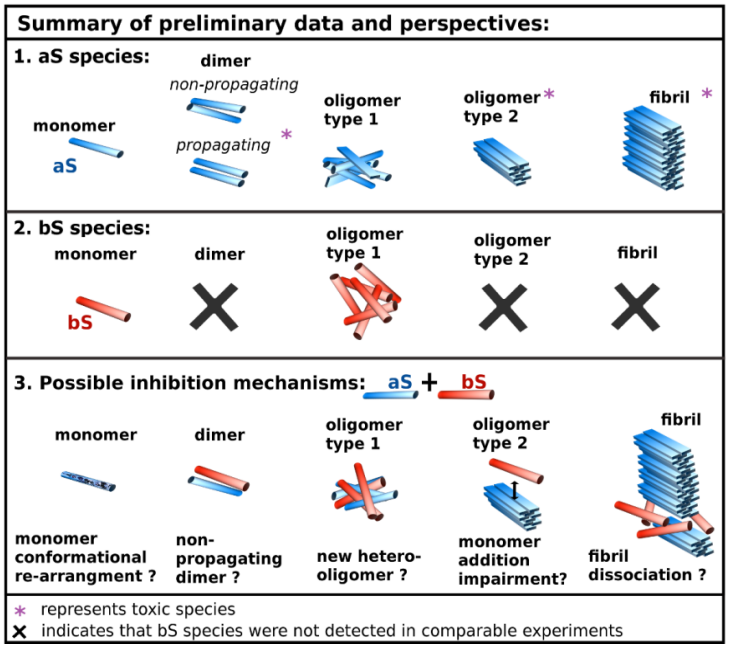

Figure 46 Schematic representation of the preliminary data and possible mechanisms of αS inhibition by βS.

In this chapter we were able to show that oligomers of αS are being affected by addition of βS to the mix. We see with our studies that βS can change the secondary structure of the αS oligomers, as well as the amount of oligomers formed. These facts make us hopeful that the approach presented here might be successful in uncovering the basis for the toxicity of αS oligomers, and may also provide us with some ideas for further drug development for Parkinsons's disease.

List of papers

Maria K. Janowska & Jean Baum, *"*β-synuclein mutant P123H associated with Dementia with Lewy Body disease has a similar C-terminal conformation to α-synuclein and accelerates its fibril formation upon co-incubation*"*. (in revision)

Maria K. Janowska, Kuen-Phon Wu, Jean Baum, *"Unveiling transient protein-protein interactions that modulate inhibition of alpha-synuclein aggregation by beta synuclein, a pre-synaptic protein that co-localizes with alpha synuclein"*. (in revision)

Maria K. Janowska & Jean Baum, *"Intermolecular PRE studies of protein aggregation",* Methods in Molecular Biology (accepted)

Lijuan Kang, **Maria K. Janowska**, Gina M. Moriarty, Jean Baum, *"Mechanistic insight into the relationship between N-terminal acetylation of alpha-synuclein and fibril formation rates by NMR and fluorescence"*. PLOS One, 10.1371/journal.pone.0075018 (2013).

Gina M. Moriarty, **Maria K. Janowska**, Lijuan Kang, Jean Baum, *"Exploring the accessible conformations of N-terminal acetylated alpha-synuclein,"* FEBS Lett. 587, 1128-38 (2013).

Maria K. Janowska, Ruben Zubac, Bojan Zagrovic. *Computational analysis of binding of GBD domain of WASP to difference binding partners.* Croat Chem Acta, 84:211–220 (2011).

Appendix

Dimer paper additional information

Salt dependence

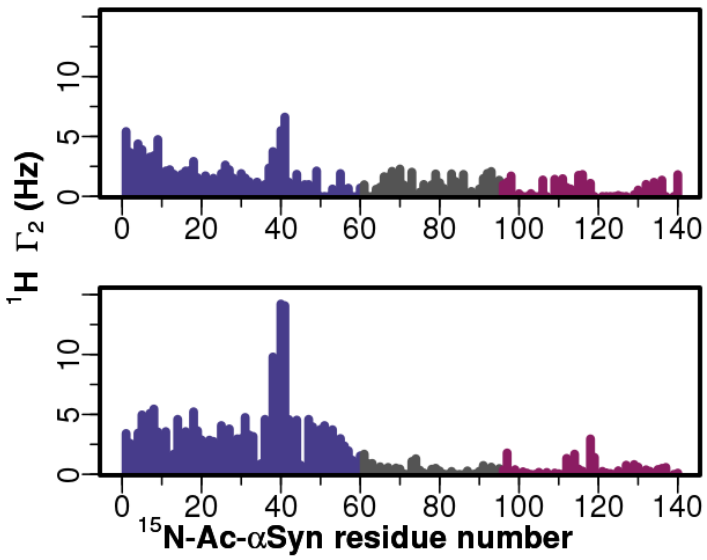

Figure 47 Correlation of salt concentration with PRE values of 15N aSyn with aSyn-G132C-MTSL (A) 100mM salt, (B) 0 mM salt

PRE are highly sensitive to the electrostatics. Both αS and βS have highly negatively charged C-terminus, and both positively and negatively charged N-terminus, thus it is highly susceptible to variation in the charges. Plot shown below shows high correlation of salt concentration with PRE values of 15N αS with αS -G132C-MTSL (A) 100mM salt, (B) 0 mm salt.

Pattern of 1H-R2 shares pattern with non-labeled and non-reduced sample.

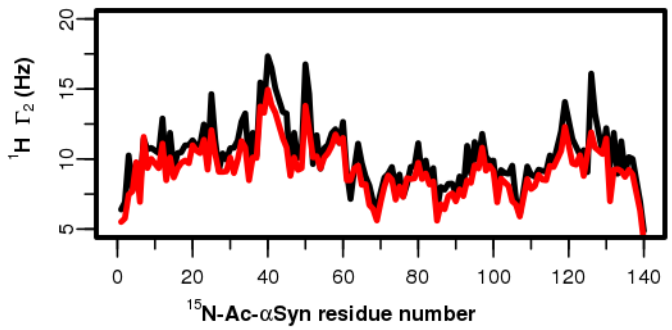

Figure 48 Diamagnetic control looks shares the pattern of the mixed non-MTSL labeled sample. (A) Diamagnetic 15N aSyn+ N14 aSyn-dia-MTSL-a11C (red), vs N15 aSyn + N14 aSyn without any spin label (black).

Diamagnetic control looks shares the pattern of the mixed non-MTSL labeled sample, which confirms: a) full reduction of the spin label, b) no changes in the conformation of the proteins conformation upon the experiment and sample manipulation.

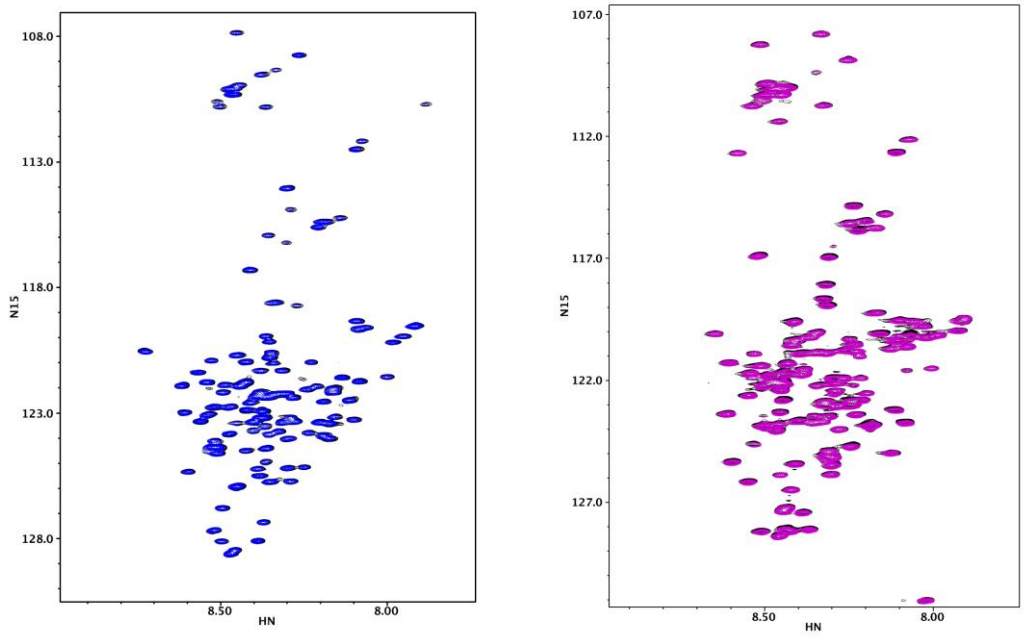

Figure 49 Overlay of HSQCs βS (black)and βS 5x addition of aSyn (blue). Overlay of HSQCs aSyn (black) and aSyn 4x addition of aSyn (pink).

Insensitivity of other experiments to addition of excess of either αS or βS.

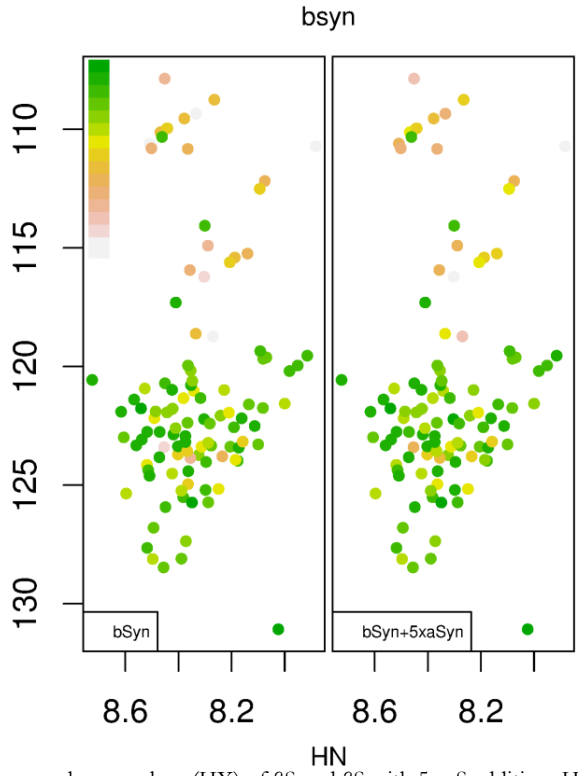

Figure 50 Hydrogen exchange values (HX) of βS and βS with 5x aS addition. HX from R1zz experiments were plotted color coded into the HSQC spectra of βS and βS with 5x excess of aSyn. HX values were color-coded according to the legend on the left and plotted as HSQC.

To evaluate how αS monomeric ensemble is affected by presence of βS, we performed series of experiments to assess changes of monomeric αS or βS. To do so firstly we performed NMR titration of βS to αS and αS to βS. We noticed no changes on the ensemble of αS addition to βS or vice versa, on the HSQC profiles upon addition of the other molecules. We saw no changes on the HSQC spectra (neither profile or peak intensity) even upon addition of 5x excess of the other protein to the sample, which would suggest that there are no interactions, or proteins interact weakly and transiently in low populations. To test if there are any interactions we would detect in αS addition to αS , we also made this control titration, and we detected again no interactions, despite the fact that αS is thought to interact with itself to form oligomers and fibrils.

As it would be possible that interactions of αS with βS may change accessibility of the certain residues, we decided to perform hydrogen exchange experiments, using cleneax and R1zz approaches. As example we are showing here that the hydrogen exchange rates for βS sample did not

changes upon addition of 5x αS . Hydrogen exchange values (HX) were plotted color coded into the HSQC spectra of βS and βS with 5x excess of αS . Generally, HX values of βS are not significantly affected by addition of αS . HX values were color-coded on the HSQC spectra to show that the high values of the HX are clustered. On the HSQC for the unfolded proteins similar residue types (ex. Gly) are not widely spread, they have similar chemical shifts, thus we show that the HX is highly correlated, as it was reported before, with the residue type.

To assess changes of αS on βS population we used ESI-MS for αS , βS and αS +βS samples. All of

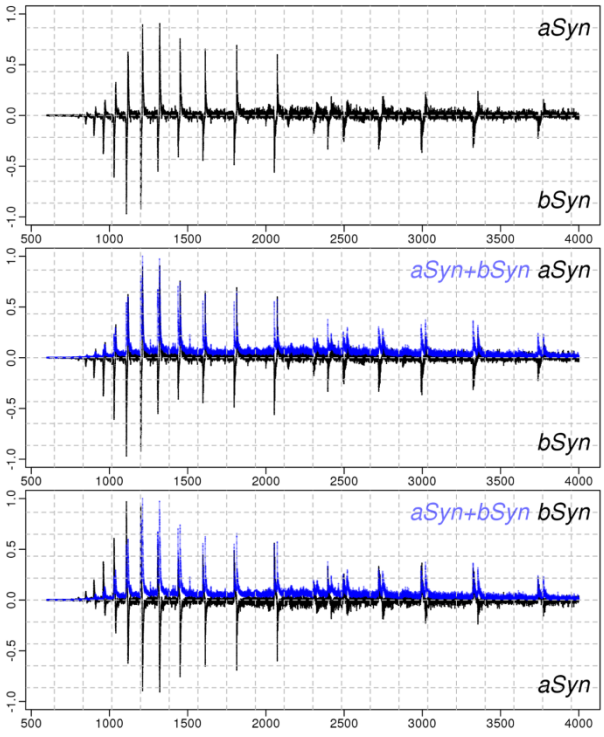

Figure 51 Effect of aS on βS ensemble and vice versa. On first panel plot aS (positive) and βS (negative). On second plot the same scheme of aS and βS with overlaid aS+βS sample (blue). On third panel βS (positive) and aS (negative), with overlaid aS+βS sample (blue).

the ESI-MS spectra exhibited compact and extended conformations. On each plot we plotted two different ESI-MS profiles, where we plotted one sample and we subtracted next sample. This approach for plotting was necessary as mixed αS /βS mixed samples have 2 sets of peaks: one for αS

, second for βS. First panel shows ESI-MS spectra of αS and subtracted from it ESI-MS spectrum of βS (negative values). On second panel has the same scheme as on panel one with additionally overlaid ESI-MS spectrum of mixture of 1:1 mixture of αS and βS. On third panel in black there is reversed plot from the first panel with overlaid mixture sample. As shown population of αS , and βS are not significantly affected by addition of the other protein. While in βS the extended form seems to compact slightly in αS compact population seems to be more affected upon addition of βS.

ThT of αS compared with the most interactive mutant.

Plot below is showing ThT fluorescence assay, monitoring fibril formation of αS and αS MTSL labeled cysteine mutant T44C in paramagnetic and diamagnetic form. Results are average of 5

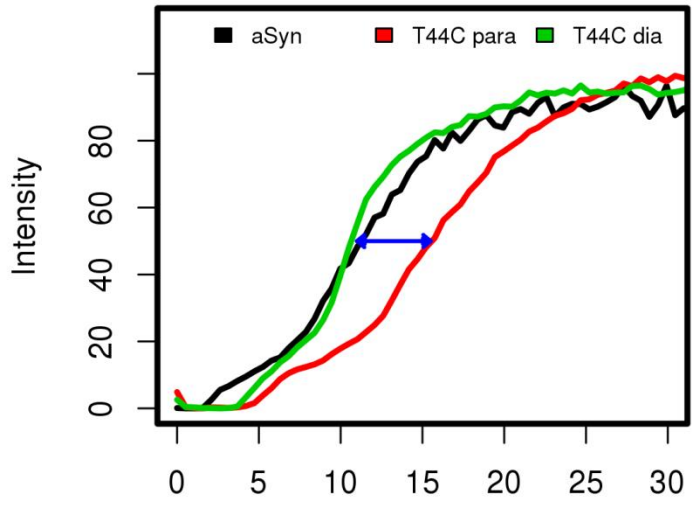

Figure 52 ThT aggregation rates for aS (black), aS-T44C-MTSL labeled mutant with paramagnetic (red) and diamagnetic spin label (green). Experiments performed in 37C with shaking in PBS using Teflon beads.

independent runs for each type of the sample. Results here are showing that αS have similar aggregation rates with diamagnetic form of T44C-MTSL labeled mutant. Paramagnetic form of the same mutant has diminished aggregation rates, which we attribute to the ThT fluorescence quenching by unpaired spin label on MTSL. It might be possible to use MTSL quenching method to measure where, if the ThT binds close to the MTSL, that modes of the binding of ThT to fibrils.

Statistical distribution of PRE values.

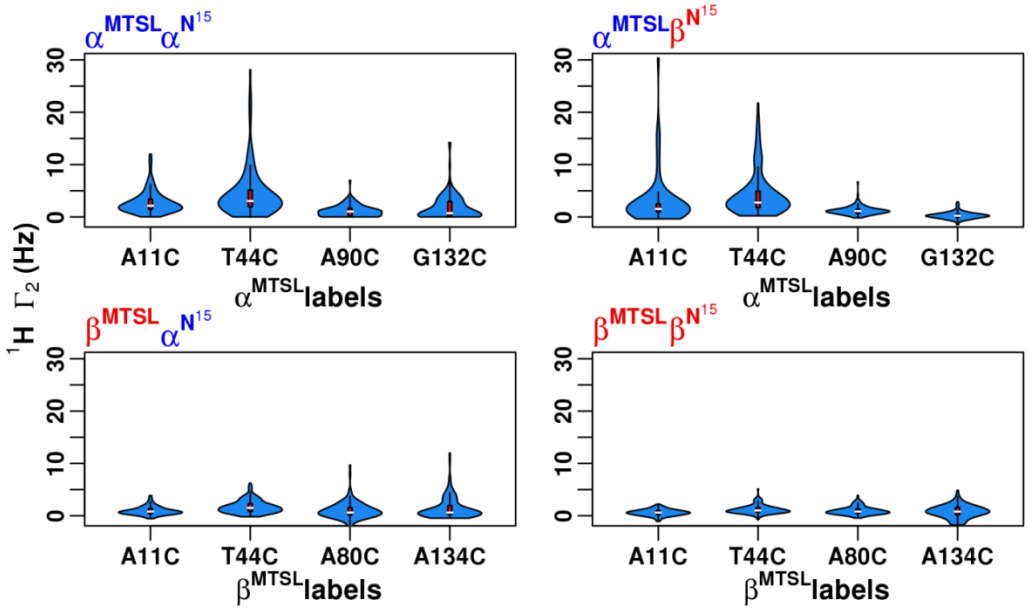

Figure 53 Violin plots for different spin labels for interchain PRE values for aS homodimer, aS/βS heterodimers and βS homodimers. Violin plots are mixture of the boxplots (red, with white line for median), and density distribution plots.

Statistical distributions of the PRE values per each spin label are showed on the violins plots.

Violin plots mixture of the boxplots (red, with white line for median), and density distribution plots. Information presented on violin plots gives us important insight about significance of interactions, and show that results we obtained do not exhibit significant amount of non-specific interactions. If first 2 quartiles boxplots are skewed, it means values with low PRE frequency are more frequently populated. The more elongated and broad top of violin plot is the higher interactions this spin label exhibits. For, symmetric violin plots median (white line) is in the middle of the shape; there is no difference in distribution between values below and above median, which suggest no significant interactions probed by this spin label, and its small magnitude and range, suggests small number of non-specific interactions. Such shape of the violin plot is mostly for βS homo-dimer, or rather lack thereof. In elongated boxplots, we attributed values from up to 3rd quartiles to the background coming from non-specific interactions and experimental error. PRE values that we consider as

significant lay in outlier range or eventually that were higher than 3rd quartile of the boxplot. Thus boxplots help us see that the interactions that we consider significant are mostly in the outliers region, thus the probability of them occurring accidentally is low, since we exclude possibility of error that high. Additionally, violin plots show us that some spin label positions are more likely to interact. For example G132C is interacting significantly only in the homodimer not in the heterodimer.

Stable dimers

Inter-chain NMR PRE experiments presented in previous section and in chapter have provided information about the location, nature and strength of transient interactions that are favored in homo and hetero-dimer complexes. It is reasonable to assume that the dimer interactions seen in the equilibrium form are similar to those that drive the early stages of aggregation. In order to characterize the dimers more fully in terms of their conformation, cell toxicity, and relevance to the kinetics of aggregation and inhibition we have modeled the interactions by designing stable cross-linked homo- and hetero-dimers with the parallel and anti-parallel architectures

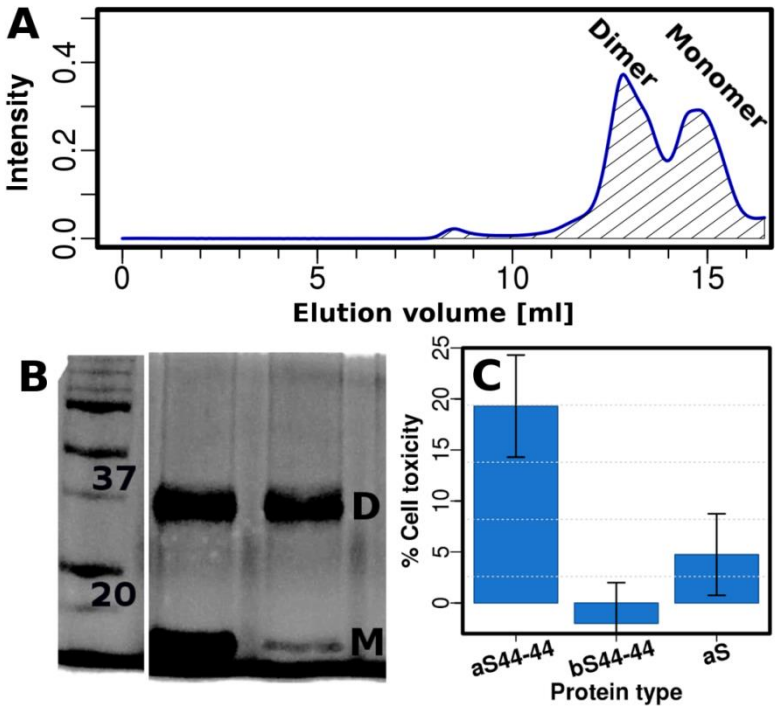

Figure 54 Generation of stable cross-linked homo-dimers and their cytoxicity. (A) Crosslinked dimers were prepared by dissolving lyophilized cysteine mutants in PBS in non-reducing conditions and incubating for at least 3h. (B) Purity of the dimers is >90% by SDS-page gels. (C) LDH cell toxicity measurments of crosslinked dimers. Human dopaminergic neuroblastoma SH-SY5Y cells were coincubated with 12.5 μM crosslinked dimers for 24h in media containing DMEM and 0.5% FBS. Cell toxicity was checked using an assay measuring the release of LDH activity from damaged cells after 24 hours of incubation. We measured the toxicity of the following homodimers: αS44-44 (αS-44-44-αS), βS44-44 (βS-44-44-βS), and monomeric αS (25 μM) as a control.

Isolation and toxicity studies of stable cross-linked homo-dimer species. The goal is to create αS N-N and N-C stable dimers based on the interactive regions observed on the transient dimeric contact maps and contrast these with N-C αS/βS hetero-dimers. Toxicity studies will help establish whether the transient dimer species are physiologically relevant. Stable cross links will be generated using disulfide cross links and the positions of disulfide bonds will be selected based on the interactions observed on transient contact maps. A limitation of this approach is that although the interaction regions are modeled directly, the interaction strengths in the stable dimers are likely to differ from the interaction strengths of the transient dimers. Despite this, we believe that this approach provides us with a tool to model the different dimer architectures and to test the role of these dimer species in toxicity,

aggregation and monomer seeding. Results for αS-44-44-αS homo-dimers, modeling a highly interactive region, show that they can be formed, isolated and separated with high purity. Cell toxicity

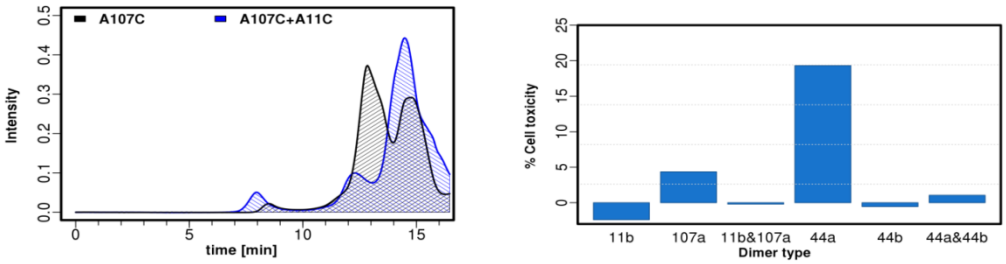

Figure 55 Stable dimers preparation and toxicity. (A) Preparation of homo- and hetero-dimers. (B) LDH toxicity assay on stable dimers. Samples used for cell toxicity βS-11-11-βS, aS-107-107-aS, mixture of βS-11-11-βS, aS-107-107-aS and βS-11-107-aS, aS-44-44-aS, βS-44-44bS, and mixture of aS-44-44-aS, βS-44-44bS and aS-44-44bS.

data show that the αS stable homodimers are toxic while the βS homodimer controls βS-44-44-βS are not. These preliminary data are very exciting as they suggest that toxicity may be present at a very early stage in aggregation, when the regions are interactive and the dimer architecture is similar to that of the fibril. Our prelimary data are consistent with the literature, where overexpression of Y39C αS *in vivo* induced enhanced neuropathology and aggregation properties (cell lines and mouse model), and overexpression of Y39C βS did not have such effect on cell lines.[97,327] The toxicity results also suggest very strongly that the N-terminal differences in sequence between αS and βS are highly relevant to the differences in the propensity to form toxic/non-toxic oligomers and fibrils of αS. In addition to the data on the homo-dimers we additionally attempted to research the effect of the formation of the hetero-dimeric mixtures. Formation of the dimeric species of for the two different position will results in the mixture which is not homogenious, suggesting that the interactions that formation of the heterodimers is much more complex than we were able to do. LDH assay for different homo-dimers and mixed hetero-dimeric mixture, showed that only αS -44-44-αS dimer is toxic, while non other homo or heterodimer mixture was toxic, suggesting again important role of the hydrophobic patch in the N-terminus for the toxicity of αS .

1. Johnson, M., Coulton, A. T., Geeves, M. a. & Mulvihill, D. P. (2010). Targeted amino-terminal acetylation of recombinant proteins in E. coli. *PloS one* **5**, e15801.
2. Moriarty, G. M., Janowska, M. K., Kang, L. J. & Baum, J. (2013). Exploring the accessible conformations of N-terminal acetylated alpha-synuclein. *Febs Letters* **587**, 1128-1138; PMC Journal – In Process.
3. Spillantini, M. G. & Goedert, M. (2000). The alpha-synucleinopathies: Parkinson's disease, dementia with Lewy bodies, and multiple system atrophy. *Ann N Y Acad Sci* **920**, 16-27.
4. Stefanis, L. (2012). alpha-Synuclein in Parkinson's Disease. *Cold Spring Harb Perspect Med* **2**, a009399.
5. Hindle, J. V. (2010). Ageing, neurodegeneration and Parkinson's disease. *Age and ageing* **39**, 156-61.
6. Spillantini, M. G., Crowther, R. A., Jakes, R., Cairns, N. J., Lantos, P. L. & Goedert, M. (1998). Filamentous alpha-synuclein inclusions link multiple system atrophy with Parkinson's disease and dementia with Lewy bodies. *Neurosci Lett* **251**, 205-8.
7. Spillantini, M. G., Crowther, R. A., Jakes, R., Hasegawa, M. & Goedert, M. (1998). alpha-synuclein in filamentous inclusions of Lewy bodies from Parkinson's disease and dementia with Lewy bodies. *Proceedings of the National Academy of Sciences of the United States of America* **95**, 6469-6473.
8. Breydo, L., Wu, J. W. & Uversky, V. N. (2012). A-synuclein misfolding and Parkinson's disease. *Biochimica et biophysica acta* **1822**, 261-85.
9. Fink, A. L. (2006). The aggregation and fibrillation of alpha-synuclein. *Accounts of Chemical Research* **39**, 628-634.
10. Lashuel, H. A., Overk, C. R., Oueslati, A. & Masliah, E. (2013). The many faces of alpha-synuclein: from structure and toxicity to therapeutic target. *Nature Reviews Neuroscience* **14**, 38-48.
11. Maroteaux, L., Campanelli, J. T. & Scheller, R. H. (1988). SYNUCLEIN - A NEURON-SPECIFIC PROTEIN LOCALIZED TO THE NUCLEUS AND PRESYNAPTIC NERVE-TERMINAL. *Journal of Neuroscience* **8**, 2804-2815.
12. Shibayamaimazu, T., Okahashi, I., Omata, K., Nakajo, S., Ochiai, H., Nakai, Y., Hama, T., Nakamura, Y. & Nakaya, K. (1993). Cell and Tissue Distribution and Developmental-Change of Neuron-Specific 14 Kda Protein (Phosphoneuroprotein-14). *Brain Research* **622**, 17-25.
13. Jakes, R., Spillantini, M. G. & Goedert, M. (1994). Identification of 2 Distinct Synucleins from Human Brain. *FEBS letters* **345**, 27-32.
14. Iwai, A., Masliah, E., Yoshimoto, M., Ge, N., Flanagan, L., de Silva, H. A., Kittel, A. & Saitoh, T. (1995). The precursor protein of non-A beta component of Alzheimer's disease amyloid is a presynaptic protein of the central nervous system. *Neuron* **14**, 467-75.
15. Bottner, M., Zorenkov, D., Hellwig, I., Barrenschee, M., Harde, J., Fricke, T., Deuschl, G., Egberts, J. H., Becker, T., Fritscher-Ravens, A., Arlt, A. & Wedel, T. (2012). Expression pattern and localization of alpha-synuclein in the human enteric nervous system. *Neurobiol Dis* **48**, 474-80.
16. Barbour, R., Kling, K., Anderson, J. P., Banducci, K., Cole, T., Diep, L., Fox, M., Goldstein, J. M., Soriano, F., Seubert, P. & Chilcote, T. J. (2008). Red blood cells are the major source of alpha-synuclein in blood. *Neurodegener Dis* **5**, 55-9.
17. Davidson, W. S., Jonas, A., Clayton, D. F. & George, J. M. (1998). Stabilization of alpha-synuclein secondary structure upon binding to synthetic membranes. *Journal of Biological Chemistry* **273**, 9443-9449.

18. Bisaglia, M., Tessari, I., Mammi, S. & Bubacco, L. (2009). Interaction Between alpha-Synuclein and Metal Ions, Still Looking for a Role in the Pathogenesis of Parkinson's Disease. *Neuromolecular Medicine* **11**, 239-251.
19. Chandra, S., Gallardo, G., Fernandez-Chacon, R., Schluter, O. M. & Sudhof, T. C. (2005). Alpha-synuclein cooperates with CSPalpha in preventing neurodegeneration. *Cell* **123**, 383-96.
20. da Costa, C. A., Ancolio, K. & Checler, F. (2000). Wild-type but not Parkinson's disease-related ala-53 --> Thr mutant alpha -synuclein protects neuronal cells from apoptotic stimuli. *J Biol Chem* **275**, 24065-9.
21. Murphy, D. D., Rueter, S. M., Trojanowski, J. Q. & Lee, V. M. Y. (2000). Synucleins are developmentally expressed, and alpha-synuclein regulates the size of the presynaptic vesicular pool in primary hippocampal neurons. *Journal of Neuroscience* **20**, 3214-3220.
22. Dev, K. K., Hofele, K., Barbieri, S., Buchman, V. L. & van der Putten, H. (2003). Part II: alpha-synuclein and its molecular pathophysiological role in neurodegenerative disease. *Neuropharmacology* **45**, 14-44.
23. Maries, E., Dass, B., Collier, T. J., Kordower, J. H. & Steece-Collier, K. (2003). The role of alpha-synuclein in Parkinson's disease: Insights from animal models. *Nature Reviews Neuroscience* **4**, 727-738.
24. Jin, H., Kanthasamy, A., Ghosh, A., Yang, Y., Anantharam, V. & Kanthasamy, A. G. (2011). alpha-Synuclein negatively regulates protein kinase Cdelta expression to suppress apoptosis in dopaminergic neurons by reducing p300 histone acetyltransferase activity. *J Neurosci* **31**, 2035-51.
25. Uversky, V. N. (2003). A protein-chameleon: Conformational plasticity of alpha-synuclein, a disordered protein involved in neurodegenerative disorders. *Journal of Biomolecular Structure & Dynamics* **21**, 211-234.
26. Uversky, V. N. & Fink, A. L. (2004). Conformational constraints for amyloid fibrillation: the importance of being unfolded. *Biochimica Et Biophysica Acta-Proteins and Proteomics* **1698**, 131-153.
27. Bartels, T., Choi, J. G. & Selkoe, D. J. (2011). α-Synuclein occurs physiologically as a helically folded tetramer that resists aggregation. *Nature* **477**, 107-110.
28. Wang, W., Perovic, I., Chittuluru, J., Kaganovich, a., Nguyen, L. T. T., Liao, J., Auclair, J. R., Johnson, D., Landeru, a., Simorellis, a. K., Ju, S., Cookson, M. R., Asturias, F. J., Agar, J. N., Webb, B. N., Kang, C., Ringe, D., Petsko, G. a., Pochapsky, T. C. & Hoang, Q. Q. (2011). A soluble -synuclein construct forms a dynamic tetramer. *Proceedings of the National Academy of Sciences*.
29. Binolfi, A., Theillet, F. X. & Selenko, P. (2012). Bacterial in-cell NMR of human alpha-synuclein: a disordered monomer by nature? *Biochemical Society Transactions* **40**, 950-U292.
30. Fauvet, B., Fares, M. B., Samuel, F., Dikiy, I., Tandon, A., Eliezer, D. & Lashuel, H. A. (2012). Characterization of Semisynthetic and Naturally N-alpha-Acetylated alpha-Synuclein in Vitro and in Intact Cells IMPLICATIONS FOR AGGREGATION AND CELLULAR PROPERTIES OF alpha-SYNUCLEIN. *Journal of Biological Chemistry* **287**, 28243-28262.
31. Fauvet, B., Mbefo, M. K., Fares, M.-B., Desobry, C., Michael, S., Ardah, M. T., Tsika, E., Coune, P., Prudent, M., Lion, N., Eliezer, D., Moore, D. J., Schneider, B., Aebischer, P., El-Agnaf, O. M., Masliah, E. & Lashuel, H. a. (2012). Alpha-synuclein in the central nervous system and from erythrocytes, mammalian cells and E. coli exists predominantly as a disordered monomer. *The Journal of biological chemistry* **287**, 15345-64.

32. Kang, L. J., Moriarty, G. M., Woods, L. A., Ashcroft, A. E., Radford, S. E. & Baum, J. (2012). N-terminal acetylation of alpha-synuclein induces increased transient helical propensity and decreased aggregation rates in the intrinsically disordered monomer. *Protein Science* **21**, 911-917.
33. Maltsev, A. S., Ying, J. F. & Bax, A. (2012). Impact of N-Terminal Acetylation of alpha-Synuclein on Its Random Coil and Lipid Binding Properties. *Biochemistry* **51**, 5004-5013.
34. Trexler, A. J. & Rhoades, E. (2012). N-terminal acetylation is critical for forming a-helical oligomer of a-synuclein. *Protein Science* **21**, 601-605.
35. Dettmer, U., Newman, A. J., Luth, E. S., Bartels, T. & Selkoe, D. (2013). In vivo crosslinking reveals principally oligomeric forms of alpha-synuclein and beta-synuclein in neurons and non-neural cells. *Journal of Biological Chemistry*.
36. Weinreb, P. H., Zhen, W., Poon, A. W., Conway, K. A. & Lansbury, P. T., Jr. (1996). NACP, a protein implicated in Alzheimer's disease and learning, is natively unfolded. *Biochemistry* **35**, 13709-15.
37. Bussell, R. & Eliezer, D. (2003). A structural and functional role for 11-mer repeats in alpha-synuclein and other exchangeable lipid binding proteins. *Journal of Molecular Biology* **329**, 763-778.
38. Uversky, V. N., Li, J. & Fink, A. L. (2001). Evidence for a partially folded intermediate in alpha-synuclein fibril formation. *Journal of Biological Chemistry* **276**, 10737-10744.
39. Munishkina, L. A., Fink, A. L. & Uversky, V. N. (2009). Accelerated Fibrillation of alpha-Synuclein Induced by the Combined Action of Macromolecular Crowding and Factors Inducing Partial Folding. *Current Alzheimer Research* **6**, 252-260.
40. Wu, K. P., Weinstock, D. S., Narayanan, C., Levy, R. M. & Baum, J. (2009). Structural Reorganization of alpha-Synuclein at Low pH Observed by NMR and REMD Simulations. *Journal of Molecular Biology* **391**, 784-796.
41. Hong, D.-P., Xiong, W., Chang, J.-Y. & Jiang, C. (2011). The role of the C-terminus of human α-synuclein: intra-disulfide bonds between the C-terminus and other regions stabilize non-fibrillar monomeric isomers. *FEBS letters* **585**, 561-6.
42. Park, S. M., Jung, H. Y., Kim, T. D., Park, J. H., Yang, C. H. & Kim, J. (2002). Distinct roles of the N-terminal-binding domain and the C-terminal-solubilizing domain of alpha-synuclein, a molecular chaperone. *J Biol Chem* **277**, 28512-20.
43. Weinreb, P. H., Zhen, W. G., Poon, A. W., Conway, K. A. & Lansbury, P. T. (1996). NACP, a protein implicated in Alzheimer's disease and learning, is natively unfolded. *Biochemistry* **35**, 13709-13715.
44. Giasson, B. I., Uryu, K., Trojanowski, J. Q. & Lee, V. M. Y. (1999). Mutant and wild type human alpha-synucleins assemble into elongated filaments with distinct morphologies in vitro. *Journal of Biological Chemistry* **274**, 7619-7622.
45. Soppa, J. (2010). Protein acetylation in archaea, bacteria, and eukaryotes. *Archaea (Vancouver, B.C.)* **2010**.
46. Uversky, V. N. (2002). Natively unfolded proteins : A point where biology waits for physics. *Protein science : a publication of the Protein Society* **11**, 739-56.
47. Uversky, V. N. (1993). Use of fast protein size-exclusion liquid chromatography to study the unfolding of proteins which denature through the molten globule. *Biochemistry* **32**, 13288-98.
48. Dunker, A. K., Lawson, J. D., Brown, C. J., Williams, R. M., Romero, P., Oh, J. S., Oldfield, C. J., Campen, A. M., Ratliff, C. R., Hipps, K. W., Ausio, J., Nissen, M. S., Reeves, R., Kang, C. H., Kissinger, C. R., Bailey, R. W., Griswold, M. D., Chiu, M., Garner, E. C. & Obradovic,

Z. (2001). Intrinsically disordered protein. *Journal of Molecular Graphics & Modelling* **19**, 26-59.

49. Eliezer, D., Kutluay, E., Bussell, R. & Browne, G. (2001). Conformational properties of alpha-synuclein in its free and lipid-associated states. *Journal of Molecular Biology* **307**, 1061-1073.
50. Allison, J. R., Varnai, P., Dobson, C. M. & Vendruscolo, M. (2009). Determination of the Free Energy Landscape of alpha-Synuclein Using Spin Label Nuclear Magnetic Resonance Measurements. *Journal of the American Chemical Society* **131**, 18314-18326.
51. Salmon, L., Nodet, G., Ozenne, V., Yin, G., Jensen, M. R., Zweckstetter, M. & Blackledge, M. (2010). NMR Characterization of Long-Range Order in Intrinsically Disordered Proteins. *Journal of the American Chemical Society* **132**, 8407-8418.
52. Bertoncini, C. W., Jung, Y. S., Fernandez, C. O., Hoyer, W., Griesinger, C., Jovin, T. M. & Zweckstetter, M. (2005). Release of long-range tertiary interactions potentiates aggregation of natively unstructured alpha-synuclein. *Proceedings of the National Academy of Sciences of the United States of America* **102**, 1430-1435.
53. Bernado, P., Bertoncini, C. W., Griesinger, C., Zweckstetter, M. & Blackledge, M. (2005). Defining long-range order and local disorder in native alpha-synuclein using residual dipolar couplings. *Journal of the American Chemical Society* **127**, 17968-17969.
54. Dedmon, M. M., Lindorff-Larsen, K., Christodoulou, J., Vendruscolo, M. & Dobson, C. M. (2005). Mapping long-range interactions in alpha-synuclein using spin-label NMR and ensemble molecular dynamics simulations. *Journal of the American Chemical Society* **127**, 476-7.
55. Cho, M. K., Kim, H. Y., Bernado, P., Fernandez, C. O., Blackledge, M. & Zweckstetter, M. (2007). Amino acid bulkiness defines the local conformations and dynamics of natively unfolded alpha-synuclein and tau. *Journal of the American Chemical Society* **129**, 3032-+.
56. Wu, K. P. & Baum, J. (2010). Detection of Transient Interchain Interactions in the Intrinsically Disordered Protein alpha-Synuclein by NMR Paramagnetic Relaxation Enhancement. *Journal of the American Chemical Society* **132**, 5546; PMCID: PMC3064441.
57. Kang, L., Wu, K.-P., Vendruscolo, M. & Baum, J. (2011). The A53T mutation is key in defining the differences in the aggregation kinetics of human and mouse α-synuclein. *Journal of the American Chemical Society* **133**, 13465-70.
58. Rao, J. N., Jao, C. C., Hegde, B. G., Langen, R. & Ulmer, T. S. (2010). A Combinatorial NMR and EPR Approach for Evaluating the Structural Ensemble of Partially Folded Proteins. *Journal of the American Chemical Society* **132**, 8657-8668.
59. Lee, J. C., Lai, B. T., Kozak, J. J., Gray, H. B. & Winkler, J. R. (2007). alpha-Synuclein tertiary contact dynamics. *Journal of Physical Chemistry B* **111**, 2107-2112.
60. Cho, M. K., Nodet, G., Kim, H. Y., Jensen, M. R., Bernado, P., Fernandez, C. O., Becker, S., Blackledge, M. & Zweckstetter, M. (2009). Structural characterization of alpha-synuclein in an aggregation prone state. *Protein Science* **18**, 1840-1846.
61. Bussell, R. & Eliezer, D. (2001). Residual structure and dynamics in Parkinson's disease-associated mutants of alpha-synuclein. *Journal of Biological Chemistry* **276**, 45996-46003.
62. Sung, Y.-H. & Eliezer, D. (2008). Residual structure, backbone dynamics, and interactions within the synuclein family. **372**, 689-707.
63. Narayanan, C., Weinstock, D. S., Wu, K. P., Baum, J. & Levy, R. M. (2012). Investigation of the Polymeric Properties of alpha-Synuclein and Comparison with NMR Experiments: A

Replica Exchange Molecular Dynamics Study. *Journal of Chemical Theory and Computation* **8**, 3929-3942.

64. Dyson, H. J. & Wright, P. E. (2005). Intrinsically unstructured proteins and their functions. *Nature Reviews Molecular Cell Biology* **6**, 197-208.
65. Hoyer, W., Cherny, D., Subramaniam, V. & Jovin, T. M. (2004). Impact of the acidic C-terminal region comprising amino acids 109-140 on alpha-synuclein aggregation in vitro. *Biochemistry* **43**, 16233-42.
66. Bertoncini, C. W., Jung, Y.-S., Fernandez, C. O., Hoyer, W., Griesinger, C., Jovin, T. M. & Zweckstetter, M. (2005). Release of long-range tertiary interactions potentiates aggregation of natively unstructured alpha-synuclein. *Proceedings of the National Academy of Sciences of the United States of America* **102**, 1430-5.
67. Yap, T. L., Pfefferkorn, C. M. & Lee, J. C. (2011). Residue-specific fluorescent probes of alpha-synuclein: detection of early events at the N- and C-termini during fibril assembly. *Biochemistry* **50**, 1963-5.
68. McClendon, S., Rospigliosi, C. C. & Eliezer, D. (2009). Charge neutralization and collapse of the C-terminal tail of alpha-synuclein at low pH. *Protein Science* **18**, 1531-1540.
69. Uversky, V. N., Li, J. & Fink, a. L. (2001). Evidence for a partially folded intermediate in alpha-synuclein fibril formation. *The Journal of biological chemistry* **276**, 10737-44.
70. Uversky, V. N., Li, J., Souillac, P., Millett, I. S., Doniach, S., Jakes, R., Goedert, M. & Fink, A. L. (2002). Biophysical properties of the synucleins and their propensities to fibrillate: inhibition of alpha-synuclein assembly by beta- and gamma-synucleins. *The Journal of biological chemistry* **277**, 11970-8.
71. Uversky, V. N., Lee, H.-J. J., Li, J., Fink, A. L. & Lee, S.-J. J. (2001). Stabilization of partially folded conformation during alpha-synuclein oligomerization in both purified and cytosolic preparations. *The Journal of biological chemistry* **276**, 43495-8.
72. Uversky, V. N., Li, J. & Fink, a. L. (2001). Metal-triggered structural transformations, aggregation, and fibrillation of human alpha-synuclein. A possible molecular NK between Parkinson's disease and heavy metal exposure. *The Journal of biological chemistry* **276**, 44284-96.
73. Uversky, V. N., Li, J. & Fink, A. L. (2001). Pesticides directly accelerate the rate of alpha-synuclein fibril formation: a possible factor in Parkinson's disease. *Febs Letters* **500**, 105-108.
74. Uversky, V. N., Li, J., Bower, K. & Fink, A. L. (2002). Synergistic effects of pesticides and metals on the fibrillation of alpha-synuclein: Implications for Parkinson's disease. *Neurotoxicology* **23**, 527-536.
75. Bertoncini, C. W., Fernandez, C. O., Griesinger, C., Jovin, T. M. & Zweckstetter, M. (2005). Familial mutants of alpha-synuclein with increased neurotoxicity have a destabilized conformation. *Journal of Biological Chemistry* **280**, 30649-30652.
76. Conway, K. A., Harper, J. D. & Lansbury, P. T. (1998). Accelerated in vitro fibril formation by a mutant alpha-synuclein linked to early-onset Parkinson disease. *Nature Medicine* **4**, 1318-1320.
77. Li, J., Uversky, V. N. & Fink, A. L. (2001). Effect of familial Parkinson's disease point mutations A30P and A53T on the structural properties, aggregation, and fibrillation of human alpha-synuclein. *Biochemistry* **40**, 11604-11613.
78. Li, J., Uversky, V. N. & Fink, A. L. (2002). Conformational behavior of human alpha-synuclein is modulated by familial Parkinson's disease point mutations A30P and A53T. *Neurotoxicology* **23**, 553-567.

79. El-Agnaf, O. M., Jakes, R., Curran, M. D. & Wallace, A. (1998). Effects of the mutations Ala30 to Pro and Ala53 to Thr on the physical and morphological properties of alpha-synuclein protein implicated in Parkinson's disease. *Febs Letters* **440**, 67-70.
80. Greenbaum, E. A., Graves, C. L., Mishizen-Eberz, A. J., Lupoli, M. A., Lynch, D. R., Englander, S. W., Axelsen, P. H. & Giasson, B. I. (2005). The E46K mutation in alpha-synuclein increases amyloid fibril formation. *Journal of Biological Chemistry* **280**, 7800-7807.
81. Wu, K. P., Kim, S., Fela, D. A. & Baum, J. (2008). Characterization of conformational and dynamic properties of natively unfolded human and mouse alpha-synuclein ensembles by NMR: Implication for aggregation. *Journal of Molecular Biology* **378**, 1104-1115.
82. Fredenburg, R. A., Rospigliosi, C., Meray, R. K., Kessler, J. C., Lashuel, H. A., Eliezer, D. & Lansbury, P. T. (2007). The impact of the E46K mutation on the properties of alpha-synuclein in its monomeric and oligomeric states. *Biochemistry* **46**, 7107-7118.
83. Rospigliosi, C. C., McClendon, S., Schmid, A. W., Ramlall, T. F., Barre, P., Lashuel, H. A. & Eliezer, D. (2009). E46K Parkinson's-Linked Mutation Enhances C-Terminal-to-N-Terminal Contacts in alpha-Synuclein. *Journal of Molecular Biology* **388**, 1022-1032.
84. Ulmer, T. S., Bax, A., Cole, N. B. & Nussbaum, R. L. (2005). Structure and dynamics of micelle-bound human alpha-synuclein. *The Journal of biological chemistry* **280**, 9595-603.
85. Eliezer, D., Kutluay, E., Bussell, R. & Browne, G. (2001). Conformational properties of alpha-synuclein in its free and lipid-associated states. *Journal of molecular biology* **307**, 1061-73.
86. Bartels, T., Ahlstrom, L. S., Leftin, A., Kamp, F., Haass, C., Brown, M. F. & Beyer, K. (2010). The N-terminus of the intrinsically disordered protein alpha-synuclein triggers membrane binding and helix folding. *Biophys J* **99**, 2116-24.
87. Eliezer, D., Kutluay, E., Bussell, R., Jr. & Browne, G. (2001). Conformational properties of alpha-synuclein in its free and lipid-associated states. *J Mol Biol* **307**, 1061-73.
88. Croke, R. L., Sallum, C. O., Watson, E., Watt, E. D. & Alexandrescu, A. T. (2008). Hydrogen exchange of monomeric alpha-synuclein shows unfolded structure persists at physiological temperature and is independent of molecular crowding in Escherichia coli. *Protein Sci* **17**, 1434-45.
89. Trexler, A. J. & Rhoades, E. (2009). alpha-Synuclein Binds Large Unilamellar Vesicles as an Extended Helix. *Biochemistry* **48**, 2304-2306.
90. Jao, C. C., Hegde, B. G., Chen, J., Haworth, I. S. & Langen, R. (2008). Structure of membrane-bound alpha-synuclein from site-directed spin labeling and computational refinement. *Proceedings of the National Academy of Sciences of the United States of America* **105**, 19666-19671.
91. Ulmer, T. S., Bax, A., Cole, N. B. & Nussbaum, R. L. (2005). Structure and dynamics of micelle-bound human alpha-synuclein. *Journal of Biological Chemistry* **280**, 9595-9603.
92. Bernstein, S. L., Liu, D. F., Wyttenbach, T., Bowers, M. T., Lee, J. C., Gray, H. B. & Winkler, J. R. (2004). alpha-synuclein: Stable compact and extended monomeric structures and pH dependence of dimer formation. *Journal of the American Society for Mass Spectrometry* **15**, 1435-1443.
93. Frimpong, A. K., Abzalimov, R. R., Uversky, V. N. & Kaltashov, I. A. (2010). Characterization of intrinsically disordered proteins with electrospray ionization mass spectrometry: conformational heterogeneity of alpha-synuclein. *Proteins-Structure Function and Bioinformatics* **78**, 714-22.

94. Pivato, M., De Franceschi, G., Tosatto, L., Frare, E., Kumar, D., Aioanei, D., Brucale, M., Tessari, I., Bisaglia, M., Samori, B., de Laureto, P. P. & Bubacco, L. (2012). Covalent α-Synuclein Dimers: Chemico-Physical and Aggregation Properties. *PloS one* **7**, e50027.
95. Celej, M. S., Sarroukh, R., Goormaghtigh, E., Fidelio, G. D., Ruysschaert, J. M. & Raussens, V. (2012). Toxic prefibrillar alpha-synuclein amyloid oligomers adopt a distinctive antiparallel beta-sheet structure. *Biochemical Journal* **443**, 719-26.
96. Uversky, V. N., Lee, H. J., Li, J., Fink, A. L. & Lee, S. J. (2001). Stabilization of partially folded conformation during alpha-synuclein oligomerization in both purified and cytosolic preparations. *Journal of Biological Chemistry* **276**, 43495-43498.
97. Zhou, W. & Freed, C. R. (2004). Tyrosine-to-cysteine modification of human alpha-synuclein enhances protein aggregation and cellular toxicity. *Journal of Biological Chemistry* **279**, 10128-35.
98. Goldberg, M. S. & Lansbury, P. T. (2000). Is there a cause-and-effect relationship between alpha-synuclein fibrillization and Parkinson's disease? *Nature Cell Biology* **2**, E115-E119.
99. Conway, K. A., Lee, S. J., Rochet, J. C., Ding, T. T., Harper, J. D., Williamson, R. E. & Lansbury, P. T. (2000). Accelerated oligomerization by Parkinson's disease linked alpha-synuclein mutants. *Molecular Basis of Dementia* **920**, 42-45.
100. Masliah, E., Rockenstein, E., Veinbergs, I., Mallory, M., Hashimoto, M., Takeda, A., Sagara, Y., Sisk, A. & Mucke, L. (2000). Dopaminergic loss and inclusion body formation in alpha-synuclein mice: Implications for neurodegenerative disorders. *Science* **287**, 1265-1269.
101. Amer, D. A. M., Irvine, G. B. & El-Agnaf, O. M. A. (2006). Inhibitors of alpha-synuclein oligomerization and toxicity: a future therapeutic strategy for Parkinson's disease and related disorders. *Experimental Brain Research* **173**, 223-233.
102. Kayed, R., Head, E., Thompson, J. L., McIntire, T. M., Milton, S. C., Cotman, C. W. & Glabe, C. G. (2003). Common structure of soluble amyloid oligomers implies common mechanism of pathogenesis. *Science* **300**, 486-489.
103. Wolfe, K. J. & Cyr, D. M. (2011). Amyloid in neurodegenerative diseases: friend or foe? *Semin Cell Dev Biol* **22**, 476-81.
104. Haass, C. & Selkoe, D. J. (2007). Soluble protein oligomers in neurodegeneration: lessons from the Alzheimer's amyloid beta-peptide. *Nat Rev Mol Cell Biol* **8**, 101-12.
105. Caughey, B. & Lansbury, P. T. (2003). Protofibrils, pores, fibrils, and neurodegeneration: Separating the responsible protein aggregates from the innocent bystanders. *Annual Review of Neuroscience* **26**, 267-298.
106. Dobson, C. M. (1999). Protein misfolding, evolution and disease. *Trends Biochem Sci* **24**, 329-32.
107. Lee, J., Culyba, E. K., Powers, E. T. & Kelly, J. W. (2011). Amyloid-β forms fibrils by nucleated conformational conversion of oligomers. *Nature chemical biology* **7**, 600-607.
108. Cremades, N., Cohen, S. I. A., Deas, E., Abramov, A. Y., Chen, A. Y., Orte, A., Sandal, M., Clarke, R. W., Dunne, P., Aprile, F. A., Bertoncini, C. W., Wood, N. W., Knowles, T. P. J., Dobson, C. M. & Klenerman, D. (2012). Direct Observation of the Interconversion of Normal and Toxic Forms of alpha-Synuclein. *Cell* **149**, 1048-1059.
109. Apetri, M. M., Maiti, N. C., Zagorski, M. G., Carey, P. R. & Anderson, V. E. (2006). Secondary structure of alpha-synuclein oligomers: characterization by raman and atomic force microscopy. *Journal of Molecular Biology* **355**, 63-71.

110. Lee, J.-H., Lee, I.-H., Choe, Y.-J., Kang, S., Kim, H. Y., Gai, W.-P., Hahn, J.-S. & Paik, S. R. (2009). Real-time analysis of amyloid fibril formation of alpha-synuclein using a fibrillation-state-specific fluorescent probe of JC-1. *The Biochemical journal* **418**, 311-23.
111. Gsponer, J., Haberthur, U. & Caflisch, A. (2003). The role of side-chain interactions in the early steps of aggregation: Molecular dynamics simulations of an amyloid-forming peptide from the yeast prion Sup35. *Proc Natl Acad Sci U S A* **100**, 5154-9.
112. Cheon, M., Chang, I., Mohanty, S., Luheshi, L. M., Dobson, C. M., Vendruscolo, M. & Favrin, G. (2007). Structural reorganisation and potential toxicity of oligomeric species formed during the assembly of amyloid fibrils. *PLoS Comput Biol* **3**, 1727-38.
113. Dusa, A., Kaylor, J., Edridge, S., Bodner, N., Hong, D. P. & Fink, A. L. (2006). Characterization of oligomers during alpha-synuclein aggregation using intrinsic tryptophan fluorescence. *Biochemistry* **45**, 2752-2760.
114. Bolognesi, B., Kumita, J. R., Barros, T. P., Esbjorner, E. K., Luheshi, L. M., Crowther, D. C., Wilson, M. R., Dobson, C. M., Favrin, G. & Yerbury, J. J. (2010). ANS binding reveals common features of cytotoxic amyloid species. *ACS Chem Biol* **5**, 735-40.
115. Outeiro, T. F., Putcha, P., Tetzlaff, J. E., Spoelgen, R., Koker, M., Carvalho, F., Hyman, B. T. & McLean, P. J. (2008). Formation of toxic oligomeric alpha-synuclein species in living cells. *PloS one* **3**, e1867.
116. Campioni, S., Mannini, B., Zampagni, M., Pensalfini, A., Parrini, C., Evangelisti, E., Relini, A., Stefani, M., Dobson, C. M., Cecchi, C. & Chiti, F. (2010). A causative link between the structure of aberrant protein oligomers and their toxicity. *Nat Chem Biol* **6**, 140-7.
117. Kim, H. Y., Cho, M. K., Kumar, A., Maier, E., Siebenhaar, C., Becker, S., Fernandez, C. O., Lashuel, H. A., Benz, R., Lange, A. & Zweckstetter, M. (2009). Structural Properties of Pore-Forming Oligomers of alpha-Synuclein. *Journal of the American Chemical Society* **131**, 17482-17489.
118. Tsigelny, I. F., Sharikov, Y., Wrasidlo, W., Gonzalez, T., Desplats, P. A., Crews, L., Spencer, B. & Masliah, E. (2012). Role of alpha-synuclein penetration into the membrane in the mechanisms of oligomer pore formation. *Febs Journal* **279**, 1000-1013.
119. Danzer, K. M., Haasen, D., Karow, A. R., Moussaud, S., Habeck, M., Giese, A., Kretzschmar, H., Hengerer, B. & Kostka, M. (2007). Different species of alpha-synuclein oligomers induce calcium influx and seeding. *Journal of Neuroscience* **27**, 9220-9232.
120. Cole, N. B., Murphy, D. D., Grider, T., Rueter, S., Brasaemle, D. & Nussbaum, R. L. (2002). Lipid droplet binding and oligomerization properties of the Parkinson's disease protein alpha-synuclein. *Journal of Biological Chemistry* **277**, 6344-6352.
121. Winner, B., Jappelli, R., Maji, S. K., Desplats, P. a., Boyer, L., Aigner, S., Hetzer, C., Loher, T., Vilar, M., Campioni, S., Tzitzilonis, C., Soragni, A., Jessberger, S., Mira, H., Consiglio, A., Pham, E., Masliah, E., Gage, F. H. & Riek, R. (2011). In vivo demonstration that alpha-synuclein oligomers are toxic. *Proceedings of the National Academy of Sciences of the United States of America* **108**, 4194-9.
122. Conway, K. A., Lee, S. J., Rochet, J. C., Ding, T. T., Harper, J. D., Williamson, R. E. & Lansbury, P. T., Jr. (2000). Accelerated oligomerization by Parkinson's disease linked alpha-synuclein mutants. *Ann N Y Acad Sci* **920**, 42-5.
123. Conway, K. A., Lee, S. J., Rochet, J. C., Ding, T. T., Williamson, R. E. & Lansbury, P. T., Jr. (2000). Acceleration of oligomerization, not fibrillization, is a shared property of both alpha-synuclein mutations linked to early-onset Parkinson's disease: implications for pathogenesis and therapy. *Proc Natl Acad Sci U S A* **97**, 571-6.

124. Lashuel, H. A., Petre, B. M., Wall, J., Simon, M., Nowak, R. J., Walz, T. & Lansbury, P. T. (2002). alpha-synuclein, especially the Parkinson's disease-associated mutants, forms pore-like annular and tubular protofibrils. *Journal of Molecular Biology* **322**, 1089-1102.
125. Kaylor, J., Bodner, N., Edridge, S., Yamin, G., Hong, D.-p. & Fink, A. L. (2005). Characterization of Oligomeric Intermediates in a-Synuclein Fibrillation : FRET Studies of Y125W/Y133F/Y136F alpha-synuclein. *Journal of Molecular Biology* **353**, 357-372.
126. Ding, T. T., Lee, S. J., Rochet, J. C. & Lansbury, P. T. (2002). Annular alpha-synuclein protofibrils are produced when spherical protofibrils are incubated in solution or bound to brain-derived membranes. *Biochemistry* **41**, 10209-10217.
127. Pountney, D. L., Voelcker, N. H. & Gai, W. P. (2005). Annular alpha-synuclein oligomers are potentially toxic agents in alpha-synucleinopathy. Hypothesis. *Neurotoxicity Research* **7**, 59-67.
128. Zerovnik, E. (2011). Oligomerization preceding amyloid fibril formation: a process in common to intrinsically disordered and globular proteins. *Network* **22**, 154-61.
129. Munishkina, L. A., Phelan, C., Uversky, V. N. & Fink, A. L. (2003). Conformational behavior and aggregation of alpha-synuclein in organic solvents: modeling the effects of membranes. *Biochemistry* **42**, 2720-30.
130. Souza, J. M., Giasson, B. I., Chen, Q. P., Lee, V. M. Y. & Ischiropoulos, H. (2000). Dityrosine cross-linking promotes formation of stable alpha-synuclein polymers - Implication of nitrative and oxidative stress in the pathogenesis of neurodegenerative synucleinopathies. *Journal of Biological Chemistry* **275**, 18344-18349.
131. Krishnan, S., Chi, E. Y., Wood, S. J., Kendrick, B. S., Li, C., Garzon-Rodriguez, W., Wypych, J., Randolph, T. W., Narhi, L. O., Biere, A. L., Citron, M. & Carpenter, J. F. (2003). Oxidative dimer formation is the critical rate-limiting step for Parkinson's disease alpha-synuclein fibrillogenesis. *Biochemistry* **42**, 829-37.
132. Norris, E. H., Giasson, B. I., Ischiropoulos, H. & Lee, V. M. Y. (2003). Effects of oxidative and nitrative challenges on alpha-synuclein fibrillogenesis involve distinct mechanisms of protein modifications. *Journal of Biological Chemistry* **278**, 27230-27240.
133. Hodara, R., Norris, E. H., Giasson, B. I., Mishizen-Eberz, A. J., Lynch, D. R., Lee, V. M.-Y. M.-Y. & Ischiropoulos, H. (2004). Functional consequences of alpha-synuclein tyrosine nitration: diminished binding to lipid vesicles and increased fibril formation. *The Journal of biological chemistry* **279**, 47746-53.
134. Yamin, G., Glaser, C. B., Uversky, V. N. & Fink, A. L. (2003). Certain metals trigger fibrillation of methionine-oxidized alpha-synuclein. *Journal of Biological Chemistry* **278**, 27630-27635.
135. Jo, E. J., McLaurin, J., Yip, C. M., St George-Hyslop, P. & Fraser, P. E. (2000). alpha-synuclein membrane interactions and lipid specificity. *Journal of Biological Chemistry* **275**, 34328-34334.
136. Lee, H. J., Choi, C. & Lee, S. J. (2002). Membrane-bound alpha-synuclein has a high aggregation propensity and the ability to seed the aggregation of the cytosolic form. *Journal of Biological Chemistry* **277**, 671-678.
137. Wright, J. A., Wang, X. & Brown, D. R. (2009). Unique copper-induced oligomers mediate alpha-synuclein toxicity. *Faseb Journal* **23**, 2384-2393.
138. Haque, F., Pandey, A. P., Cambrea, L. R., Rochet, J.-C. & Hovis, J. S. (2010). Adsorption of alpha-Synuclein on Lipid Bilayers: Modulating the Structure and Stability ofProtein Assemblies. *Journal of Physical Chemistry B* **114**, 4070-4081.

139. Munishkina, L. A., Fink, A. L. & Uversky, V. N. (2008). Concerted Action of Metals and Macromolecular Crowding on the Fibrillation of alpha-Synuclein. *Protein and Peptide Letters* **15**, 1079-1085.
140. Uversky, V. N., Li, J. & Fink, A. L. (2001). Metal-triggered structural transformations, aggregation, and fibrillation of human alpha-synuclein - A possible molecular link between Parkinson's disease and heavy metal exposure. *Journal of Biological Chemistry* **276**, 44284-44296.
141. Santner, A. & Uversky, V. N. (2010). Metalloproteomics and metal toxicology of alpha-synuclein. *Metallomics* **2**, 378-392.
142. Lowe, R., Pountney, D. L., Jensen, P. H. & Gai, W. E. I. P. (2004). Calcium (II) selectively induces ⎵ -synuclein annular oligomers via interaction with the C-terminal domain. 3245-3252.
143. Uversky, V. N., Yamin, G., Souillac, P. O., Goers, J., Glaser, C. B. & Fink, A. L. (2002). Methionine oxidation inhibits fibrillation of human alpha-synuclein in vitro. *Febs Letters* **517**, 239-244.
144. Glaser, C. B., Yamin, G., Uversky, V. N. & Fink, A. L. (2005). Methionine oxidation, alpha-synuclein and Parkinson's disease. *Biochimica Et Biophysica Acta-Proteins and Proteomics* **1703**, 157-169.
145. Zhou, W., Long, C., Reaney, S. H., Di Monte, D. A., Fink, A. L. & Uversky, V. N. (2010). Methionine oxidation stabilizes non-toxic oligomers of alpha-synuclein through strengthening the auto-inhibitory intra-molecular long-range interactions. *Biochimica Et Biophysica Acta-Molecular Basis of Disease* **1802**, 322-330.
146. Hong, D. P., Fink, A. L. & Uversky, V. N. (2008). Structural Characteristics of alpha-Synuclein Oligomers Stabilized by the Flavonoid Baicalein. *Journal of Molecular Biology* **383**, 214-223.
147. Lee, K. W., Chen, W., Junn, E., Im, J. Y., Grosso, H., Sonsalla, P. K., Feng, X. Y., Ray, N., Fernandez, J. R., Chao, Y., Masliah, E., Voronkov, M., Braithwaite, S. P., Stock, J. B. & Mouradian, M. M. (2011). Enhanced Phosphatase Activity Attenuates alpha-Synucleinopathy in a Mouse Model. *Journal of Neuroscience* **31**, 6963-6971.
148. Ohrfelt, A., Zetterberg, H., Andersson, K., Persson, R., Secic, D., Brinkmalm, G., Wallin, A., Mulugeta, E., Francis, P. T., Vanmechelen, E., Aarsland, D., Ballard, C., Blennow, K. & Westman-Brinkmalm, A. (2011). Identification of Novel α-Synuclein Isoforms in Human Brain Tissue by using an Online NanoLC-ESI-FTICR-MS Method. *Neurochemical research*.
149. Anderson, J. P., Walker, D. E., Goldstein, J. M., de Laat, R., Banducci, K., Caccavello, R. J., Barbour, R., Huang, J. P., Kling, K., Lee, M., Diep, L., Keim, P. S., Shen, X. F., Chataway, T., Schlossmacher, M. G., Seubert, P., Schenk, D., Sinha, S., Gai, W. P. & Chilcote, T. J. (2006). Phosphorylation of Ser-129 is the dominant pathological modification of alpha-synuclein in familial and sporadic Lewy body disease. *Journal of Biological Chemistry* **281**, 29739-29752.
150. Polevoda, B., Norbeck, J., Takakura, H., Blomberg, a. & Sherman, F. (1999). Identification and specificities of N-terminal acetyltransferases from Saccharomyces cerevisiae. *The EMBO journal* **18**, 6155-68.
151. Polevoda, B. & Sherman, F. (2003). N-terminal Acetyltransferases and Sequence Requirements for N-terminal Acetylation of Eukaryotic Proteins. *Journal of Molecular Biology* **325**, 595-622.
152. Starheim, K. K., Gromyko, D., Velde, R., Varhaug, J. E. & Arnesen, T. (2009). Composition and biological significance of the human Nalpha-terminal acetyltransferases. *BMC Proc* **3 Suppl 6**, S3.

153. Van Damme, P., Arnesen, T. & Gevaert, K. (2011). Protein alpha-N-acetylation studied by N-terminomics. *The FEBS journal* **278**, 3822-34.
154. Helbig, A. O., Gauci, S., Raijmakers, R., van Breukelen, B., Slijper, M., Mohammed, S. & Heck, A. J. R. (2010). Profiling of N-acetylated protein termini provides in-depth insights into the N-terminal nature of the proteome. *Molecular & cellular proteomics : MCP* **9**, 928-39.
155. Zabrocki, P., Bastiaens, I., Delay, C., Bammens, T., Ghillebert, R., Pellens, K., De Virgilio, C., Van Leuven, F. & Winderickx, J. (2008). Phosphorylation, lipid raft interaction and traffic of alpha-synuclein in a yeast model for Parkinson. *Biochimica et biophysica acta* **1783**, 1767-80.
156. Arnesen, T. (2011). Towards a functional understanding of protein N-terminal acetylation. *PLoS biology* **9**, e1001074.
157. Forte, G. M., Pool, M. R. & Stirling, C. J. (2011). N-terminal acetylation inhibits protein targeting to the endoplasmic reticulum. *PLoS Biol* **9**, e1001073.
158. Hwang, C.-S., Shemorry, A. & Varshavsky, A. (2010). N-terminal acetylation of cellular proteins creates specific degradation signals. *Science (New York, N.Y.)* **327**, 973-7.
159. Jornvall, H. (1975). Acetylation of Protein N-terminal amino groups structural observations on alpha-amino acetylated proteins. *J Theor Biol* **55**, 1-12.
160. Helbig, A. O., Rosati, S., Pijnappel, P. W. W. M., van Breukelen, B., Timmers, M. H. T. H., Mohammed, S., Slijper, M. & Heck, A. J. R. (2010). Perturbation of the yeast N-acetyltransferase NatB induces elevation of protein phosphorylation levels. *BMC genomics* **11**, 685.
161. Greenfield, N. J., Stafford, W. F. & Hitchcock-DeGregori, S. E. (1994). The effect of N-terminal acetylation on the structure of an N-terminal tropomyosin peptide and alpha alpha-tropomyosin. *Protein science : a publication of the Protein Society* **3**, 402-10.
162. Gast, K. & Fiedler, C. (2012). Dynamic and static light scattering of intrinsically disordered proteins. *Methods Mol Biol* **896**, 137-61.
163. El-Agnaf, O. M. A., Salem, S. A., Paleologou, K. E., Curran, M. D., Gibson, M. J., Court, J. A., Schlossmacher, M. G. & Allsop, D. (2006). Detection of oligomeric forms of alpha-synuclein protein in human plasma as a potential biomarker for Parkinson's disease. *Faseb Journal* **20**, 419-425.
164. Aurora, R. & Rose, G. D. (1998). Helix capping. *Protein Science* **7**, 21-38.
165. Chakrabartty, A., Doig, A. J. & Baldwin, R. L. (1993). Helix Capping Propensities in Peptides Parallel Those in Proteins. *Proceedings of the National Academy of Sciences of the United States of America* **90**, 11332-11336.
166. George, J. M. (2002). The synucleins. *Genome Biology* **3**, REVIEWS3002.
167. Uversky, V. N., Li, J., Souillac, P., Millett, I. S., Doniach, S., Jakes, R., Goedert, M. & Fink, A. L. (2002). Biophysical properties of the synucleins and their propensities to fibrillate: inhibition of alpha-synuclein assembly by beta- and gamma-synucleins. *Journal of Biological Chemistry* **277**, 11970-8.
168. Lee, D., Paik, S. R. & Choi, K. Y. (2004). Beta-synuclein exhibits chaperone activity more efficiently than alpha-synuclein. *Febs Letters* **576**, 256-60.
169. Rockenstein, E., Hansen, L. A., Mallory, M., Trojanowski, J. Q., Galasko, D. & Masliah, E. (2001). Altered expression of the synuclein family mRNA in Lewy body and Alzheimer's disease. *Brain Research* **914**, 48-56.
170. Beyer, K., Domingo-Sabat, M., Santos, C., Tolosa, E., Ferrer, I. & Ariza, A. (2010). The decrease of beta-synuclein in cortical brain areas defines a molecular subgroup of dementia with Lewy bodies. *Brain* **133**, 3724-33.

171. Beyer, K., Ispierto, L., Latorre, P., Tolosa, E. & Ariza, A. (2011). Alpha- and beta-synuclein expression in Parkinson disease with and without dementia. *Journal of the Neurological Sciences* **310**, 112-7.
172. Hashimoto, M., Rockenstein, E., Mante, M., Mallory, M. & Masliah, E. (2001). beta-Synuclein inhibits alpha-synuclein aggregation: a possible role as an anti-parkinsonian factor. *Neuron* **32**, 213-23.
173. Fan, Y., Limprasert, P., Murray, I. V. J., Smith, A. C., Lee, V. M. Y., Trojanowski, J. Q., Sopher, B. L. & La Spada, A. R. (2006). beta-synuclein modulates alpha-synuclein neurotoxicity by reducing alpha-synuclein protein expression. *Human Molecular Genetics* **15**, 3002-3011.
174. Hashimoto, M., Rockenstein, E., Mante, M., Crews, L., Bar-On, P., Gage, F. H., Marr, R. & Masliah, E. (2004). An antiaggregation gene therapy strategy for Lewy body disease utilizing beta-synuclein lentivirus in a transgenic model. *Gene Therapy* **11**, 1713-23.
175. Park, J. Y. & Lansbury, P. T., Jr. (2003). Beta-synuclein inhibits formation of alpha-synuclein protofibrils: a possible therapeutic strategy against Parkinson's disease. *Biochemistry* **42**, 3696-700.
176. Israeli, E. & Sharon, R. (2009). Beta-synuclein occurs in vivo in lipid-associated oligomers and forms hetero-oligomers with alpha-synuclein. *Journal of Neurochemistry* **108**, 465-74.
177. Tsigelny, I. F., Bar-On, P., Sharikov, Y., Crews, L., Hashimoto, M., Miller, M. A., Keller, S. H., Platoshyn, O., Yuan, J. X. & Masliah, E. (2007). Dynamics of alpha-synuclein aggregation and inhibition of pore-like oligomer development by beta-synuclein. *Febs Journal* **274**, 1862-77.
178. Singleton, A. B., Farrer, M., Johnson, J., Singleton, A., Hague, S., Kachergus, J., Hulihan, M., Peuralinna, T., Dutra, A., Nussbaum, R., Lincoln, S., Crawley, A., Hanson, M., Maraganore, D., Adler, C., Cookson, M. R., Muenter, M., Baptista, M., Miller, D., Blancato, J., Hardy, J. & Gwinn-Hardy, K. (2003). alpha-synuclein locus triplication causes Parkinson's disease. *Science* **302**, 841-841.
179. Hashimoto, M., Takenouchi, T., Rockenstein, E. & Masliah, E. (2003). alpha-Synuclein up-regulates expression of caveolin-1 and down-regulates extracellular signal-regulated kinase activity in B103 neuroblastoma cells: role in the pathogenesis of Parkinson's disease. *Journal of Neurochemistry* **85**, 1468-1479.
180. Seo, J. H., Rah, J. C., Choi, S. H., Shin, J. K., Min, K., Kim, H. S., Park, C. H., Kim, S., Kim, E. M., Lee, S. H., Lee, S., Suh, S. W. & Suh, Y. H. (2002). alpha-Synuclein regulates neuronal survival via Bcl-2 family expression and PI3/Akt kinase pathway. *Faseb Journal* **16**, 1826-+.
181. Hashimoto, M., Bar-on, P., Ho, G., Takenouchi, T., Rockenstein, E., Crews, L. & Masliah, E. (2004). beta-synuclein regulates Akt activity in neuronal cells - A possible mechanism for neuroprotection in Parkinson's disease. *Journal of Biological Chemistry* **279**, 23622-23629.
182. Snyder, H., Mensah, K., Hsu, C., Hashimoto, M., Surgucheva, I. G., Festoff, B., Surguchov, A., Masliah, E., Matouschek, A. & Wolozin, B. (2005). beta-Synuclein reduces proteasomal inhibition by alpha-synuclein but not gamma-synuclein. *Journal of Biological Chemistry* **280**, 7562-9.
183. Vigneswara, V., Cass, S., Wayne, D., Bolt, E. L., Ray, D. E. & Carter, W. G. (2013). Molecular ageing of alpha- and Beta-synucleins: protein damage and repair mechanisms. *Plos One* **8**, e61442.

184. da Costa, C. A., Masliah, E. & Checler, F. (2003). Beta-synuclein displays an antiapoptotic p53-dependent phenotype and protects neurons from 6-hydroxydopamine-induced caspase 3 activation: cross-talk with alpha-synuclein and implication for Parkinson's disease. *Journal of Biological Chemistry* **278**, 37330-5.
185. Chandra, S., Fornai, F., Kwon, H. B., Yazdani, U., Atasoy, D., Liu, X. R., Hammer, R. E., Battaglia, G., German, D. C., Castillo, P. E. & Sudhof, T. C. (2004). Double-knockout mice for alpha- and beta-synucleins: Effect on synaptic functions. *Proceedings of the National Academy of Sciences of the United States of America* **101**, 14966-14971.
186. Anwar, S., Peters, O., Millership, S., Ninkina, N., Doig, N., Connor-Robson, N., Threlfell, S., Kooner, G., Deacon, R. M., Bannerman, D. M., Bolam, J. P., Chandra, S. S., Cragg, S. J., Wade-Martins, R. & Buchman, V. L. (2011). Functional alterations to the nigrostriatal system in mice lacking all three members of the synuclein family. *Journal of Neuroscience* **31**, 7264-74.
187. Greten-Harrison, B., Polydoro, M., Morimoto-Tomita, M., Diao, L., Williams, A. M., Nie, E. H., Makani, S., Tian, N., Castillo, P. E., Buchman, V. L. & Chandra, S. S. (2010). alphabetagamma-Synuclein triple knockout mice reveal age-dependent neuronal dysfunction. *Proc Natl Acad Sci U S A* **107**, 19573-8.
188. Taschenberger, G., Toloe, J., Tereshchenko, J., Akerboom, J., Wales, P., Benz, R., Becker, S., Outeiro, T., Looger, L., Bahr, M., Zweckstetter, M. & Kugler, S. (2013). Bs-synuclein aggregates and induces neurodegeneration in dopaminergic neurons. *Annals of Neurology*.
189. Galvin, J. E., Uryu, K., Lee, V. M. & Trojanowski, J. Q. (1999). Axon pathology in Parkinson's disease and Lewy body dementia hippocampus contains alpha-, beta-, and gamma-synuclein. *Proc Natl Acad Sci U S A* **96**, 13450-5.
190. Ohtake, H., Limprasert, P., Fan, Y., Onodera, O., Kakita, A., Takahashi, H., Bonner, L. T., Tsuang, D. W., Murray, I. V., Lee, V. M., Trojanowski, J. Q., Ishikawa, A., Idezuka, J., Murata, M., Toda, T., Bird, T. D., Leverenz, J. B., Tsuji, S. & La Spada, A. R. (2004). Beta-synuclein gene alterations in dementia with Lewy bodies. *Neurology* **63**, 805-11.
191. Wei, J., Fujita, M., Nakai, M., Waragai, M., Watabe, K., Akatsu, H., Rockenstein, E., Masliah, E. & Hashimoto, M. (2007). Enhanced lysosomal pathology caused by beta-synuclein mutants linked to dementia with Lewy bodies. *Journal of Biological Chemistry* **282**, 28904-28914.
192. Fujita, M., Sugama, S., Sekiyama, K., Sekigawa, A., Tsukui, T., Nakai, M., Waragai, M., Takenouchi, T., Takamatsu, Y., Wei, J., Rockenstein, E., Laspada, A. R., Masliah, E., Inoue, S. & Hashimoto, M. (2010). A beta-synuclein mutation linked to dementia produces neurodegeneration when expressed in mouse brain. *Nature Communications* **1**, 110.
193. Rivers, R. C., Kumita, J. R., Tartaglia, G. G., Dedmon, M. M., Pawar, A., Vendruscolo, M., Dobson, C. M. & Christodoulou, J. (2008). Molecular determinants of the aggregation behavior of alpha- and beta-synuclein. *Protein Science* **17**, 887-98.
194. Sung, Y. H. & Eliezer, D. (2007). Residual structure, backbone dynamics, and interactions within the synuclein family. *Journal of Molecular Biology* **372**, 689-707.
195. Hoffman-Zacharska, D., Koziorowski, D., Ross, O. A., Milewski, M., Poznanski, J., Jurek, M., Wszolek, Z. K., Soto-Ortolaza, A., Slawek, J., Janik, P., Jamrozik, Z., Potulska-Chromik, A., Jasinska-Myga, B., Opala, G., Krygowska-Wajs, A., Czyzewski, K., Dickson, D. W., Bal, J. & Friedman, A. (2013). Novel A18T and pA29S substitutions in alpha-synuclein may be associated with sporadic Parkinson's disease. *Parkinsonism & Related Disorders* **19**, 1057-1060.

196. Appel-Cresswell, S., Vilarino-Guell, C., Encarnacion, M., Sherman, H., Yu, I., Shah, B., Weir, D., Thompson, C., Szu-Tu, C., Trinh, J., Aasly, J. O., Rajput, A., Rajput, A. H., Stoessl, A. J. & Farrer, M. J. (2013). Alpha-synuclein p.H50Q, a novel pathogenic mutation for Parkinson's disease. *Movement Disorders* **28**, 811-813.
197. Lesage, S., Anheim, M., Letournel, F., Bousset, L., Honore, A., Rozas, N., Pieri, L., Madiona, K., Durr, A., Melki, R., Verny, C., Brice, A. & Study, F. P. D. G. (2013). G51D alpha-Synuclein mutation causes a novel Parkinsonian-pyramidal syndrome. *Annals of Neurology* **73**, 459-471.
198. Giasson, B. I., Murray, I. V., Trojanowski, J. Q. & Lee, V. M. (2001). A hydrophobic stretch of 12 amino acid residues in the middle of alpha-synuclein is essential for filament assembly. *Journal of Biological Chemistry* **276**, 2380-6.
199. Zibaee, S., Jakes, R., Fraser, G., Serpell, L. C., Crowther, R. A. & Goedert, M. (2007). Sequence determinants for amyloid fibrillogenesis of human alpha-synuclein. *Journal of Molecular Biology* **374**, 454-464.
200. Roodveldt, C., Andersson, A., De Genst, E. J., Labrador-Garrido, A., Buell, A. K., Dobson, C. M., Tartaglia, G. G. & Vendruscolo, M. (2012). A Rationally Designed Six-Residue Swap Generates Comparability in the Aggregation Behavior of alpha-Synuclein and beta-Synuclein. *Biochemistry* **51**, 8771-8778.
201. Zibaee, S., Fraser, G., Jakes, R., Owen, D., Serpell, L. C., Crowther, R. A. & Goedert, M. (2010). Human beta-synuclein rendered fibrillogenic by designed mutations. *Journal of Biological Chemistry* **285**, 38555-67.
202. Yamin, G., Munishkina, L. A., Karymov, M. A., Lyubchenko, Y. L., Uversky, V. N. & Fink, A. L. (2005). Forcing nonamyloidogenic beta-synuclein to fibrillate. *Biochemistry* **44**, 9096-9107.
203. Knowles, T. P. J., Vendruscolo, M. & Dobson, C. M. (2014). The amyloid state and its association with protein misfolding diseases. *Nature Reviews Molecular Cell Biology* **15**, 384-396.
204. Lee, E. N., Cho, H. J., Lee, C. H., Lee, D., Chung, K. C. & Paik, S. R. (2004). Phthalocyanine tetrasulfonates affect the amyloid formation and cytotoxicity of alpha-synuclein. *Biochemistry* **43**, 3704-3715.
205. Lamberto, G. R., Binolfi, A., Orcellet, M. L., Bertoncini, C. W., Zweckstetter, M., Griesinger, C. & Fernandez, C. O. (2009). Structural and mechanistic basis behind the inhibitory interaction of PcTS on alpha-synuclein amyloid fibril formation. *Proceedings of the National Academy of Sciences of the United States of America* **106**, 21057-21062.
206. Lamberto, G. R., Torres-Monserrat, V., Bertoncini, C. W., Salvatella, X., Zweckstetter, M., Griesinger, C. & Fernandez, C. O. (2011). Toward the Discovery of Effective Polycyclic Inhibitors of alpha-Synuclein Amyloid Assembly. *Journal of Biological Chemistry* **286**, 32036-32044.
207. Mirecka, E. A., Shaykhalishahi, H., Gauhar, A., Akgul, S., Lecher, J., Willbold, D., Stoldt, M. & Hoyer, W. (2014). Sequestration of a beta-Hairpin for Control of alpha-Synuclein Aggregation. *Angewandte Chemie-International Edition* **53**, 4227-4230.
208. Cheruvara, H., Allen-Baume, V. L., Kad, N. M. & Mason, J. M. (2015). Intracellular Screening of a Peptide Library to Derive a Potent Peptide Inhibitor of alpha-Synuclein Aggregation. *Journal of Biological Chemistry* **290**, 7426-7435.
209. Norris, E. H., Giasson, B. I., Hodara, R., Xu, S. H., Trojanowski, J. Q., Ischiropoulos, H. & Lee, V. M. Y. (2005). Reversible inhibition of alpha-synuclein fibrillization by dopaminochrome-mediated conformational alterations. *Journal of Biological Chemistry* **280**, 21212-21219.

210. Lorenzen, N., Nielsen, S. B., Yoshimura, Y., Vad, B. S., Andersen, C. B., Betzer, C., Kaspersen, J. D., Christiansen, G., Pedersen, J. S., Jensen, P. H., Mulder, F. A. A. & Otzen, D. E. (2014). How Epigallocatechin Gallate Can Inhibit alpha-Synuclein Oligomer Toxicity in Vitro. *Journal of Biological Chemistry* **289**, 21299-21310.

211. Shaltiel-Karyo, R., Frenkel-Pinter, M., Egoz-Matia, N., Frydman-Marom, A., Shalev, D. E., Segal, D. & Gazit, E. (2010). Inhibiting alpha-synuclein oligomerization by stable cell-penetrating beta-synuclein fragments recovers phenotype of Parkinson's disease model flies. *Plos One* **5**, e13863.

212. Mougenot, A. L., Nicot, S., Bencsik, A., Morignat, E., Verchere, J., Lakhdar, L., Legastelois, S. & Baron, T. (2012). Prion-like acceleration of a synucleinopathy in a transgenic mouse model. *Neurobiology of Aging* **33**, 2225-8.

213. Desplats, P., Lee, H.-J., Bae, E.-J., Patrick, C., Rockenstein, E., Crews, L., Spencer, B., Masliah, E. & Lee, S.-J. (2009). Inclusion formation and neuronal cell death through neuron-to-neuron transmission of alpha-synuclein. *Proceedings of the National Academy of Sciences of the United States of America* **106**, 13010-13015.

214. Kordower, J. H., Dodiya, H. B., Kordower, A. M., Terpstra, B., Paumier, K., Madhavan, L., Sortwell, C., Steece-Collier, K. & Collier, T. J. (2011). Transfer of host-derived alpha synuclein to grafted dopaminergic neurons in rat. *Neurobiology of Disease* **43**, 552-7.

215. Kordower, J. H., Chu, Y., Hauser, R. A., Freeman, T. B. & Olanow, C. W. (2008). Lewy body-like pathology in long-term embryonic nigral transplants in Parkinson's disease. *Nature Medicine* **14**, 504-506.

216. Li, J. Y., Englund, E., Holton, J. L., Soulet, D., Hagell, P., Lees, A. J., Lashley, T., Quinn, N. P., Rehncrona, S., Bjorklund, A., Widner, H., Revesz, T., Lindvall, O. & Brundin, P. (2008). Lewy bodies in grafted neurons in subjects with Parkinson's disease suggest host-to-graft disease propagation. *Nature Medicine* **14**, 501-3.

217. Volpicelli-Daley, L. A., Luk, K. C., Patel, T. P., Tanik, S. A., Riddle, D. M., Stieber, A., Meaney, D. F., Trojanowski, J. Q. & Lee, V. M. Y. (2011). Exogenous alpha-Synuclein Fibrils Induce Lewy Body Pathology Leading to Synaptic Dysfunction and Neuron Death. *Neuron* **72**, 57-71.

218. Luk, K. C., Kehm, V. M., Zhang, B., O'Brien, P., Trojanowski, J. Q. & Lee, V. M. Y. (2012). Intracerebral inoculation of pathological alpha-synuclein initiates a rapidly progressive neurodegenerative alpha-synucleinopathy in mice. *Journal of Experimental Medicine* **209**, 975-986.

219. Luk, K. C., Kehm, V., Carroll, J., Zhang, B., O'Brien, P., Trojanowski, J. Q. & Lee, V. M. Y. (2012). Pathological alpha-Synuclein Transmission Initiates Parkinson-like Neurodegeneration in Nontransgenic Mice. *Science* **338**, 949-953.

220. Masliah, E., Rockenstein, E., Veinbergs, I., Sagara, Y., Mallory, M., Hashimoto, M. & Mucke, L. (2001). beta-Amyloid peptides enhance alpha-synuclein accumulation and neuronal deficits in a transgenic mouse model linking Alzheimer's disease and Parkinson's disease. *Proceedings of the National Academy of Sciences of the United States of America* **98**, 12245-12250.

221. Mandal, P. K., Pettegrew, J. W., Masliah, E., Hamilton, R. L. & Mandal, R. (2006). Interaction between A beta peptide and alpha synuclein: Molecular mechanisms in overlapping pathology of Alzheimer's and Parkinson's in dementia with Lewy body disease. *Neurochemical Research* **31**, 1153-1162.

222. Clinton, L. K., Blurton-Jones, M., Myczek, K., Trojanowski, J. Q. & LaFerla, F. M. (2010). Synergistic Interactions between A beta, Tau, and alpha-Synuclein: Acceleration of Neuropathology and Cognitive Decline. *Journal of Neuroscience* **30**, 7281-7289.

223. Biere, A. L., Wood, S. J., Wypych, J., Steavenson, S., Jiang, Y., Anafi, D., Jacobsen, F. W., Jarosinski, M. A., Wu, G. M., Louis, J. C., Martin, F., Narhi, L. O. & Citron, M. (2000). Parkinson's disease-associated alpha-synuclein is more fibrillogenic than beta- and gamma-synuclein and cannot cross-seed its homologs. *Journal of Biological Chemistry* **275**, 34574-9.
224. Windisch, M., Hutter-Paier, B., Schreiner, E. & Wronski, R. (2004). Beta-Synuclein-derived peptides with neuroprotective activity: an alternative treatment of neurodegenerative disorders? *Journal of Molecular Neuroscience* **24**, 155-65.
225. Ono, K., Takahashi, R., Ikeda, T. & Yamada, M. (2012). Cross-seeding effects of amyloid beta-protein and alpha-synuclein. *Journal of Neurochemistry* **122**, 883-890.
226. Giasson, B. I., Forman, M. S., Higuchi, M., Golbe, L. I., Graves, C. L., Kotzbauer, P. T., Trojanowski, J. Q. & Lee, V. M. Y. (2003). Initiation and synergistic fibrillization of tau and alpha-synuclein. *Science* **300**, 636-640.
227. Kang, L. J., Moriarty, G. M., Woods, L. A., Ashcroft, A. E., Radford, S. E. & Baum, J. (2012). N-terminal acetylation of alpha-synuclein induces increased transient helical propensity and decreased aggregation rates in the intrinsically disordered monomer. *Protein Science* **21**, 911-917; PMCID; PMC3403430.
228. Kang, L. J., Wu, K. P., Vendruscolo, M. & Baum, J. (2011). The A53T Mutation is Key in Defining the Differences in the Aggregation Kinetics of Human and Mouse alpha-Synuclein. *Journal of the American Chemical Society* **133**, 13465-13470.
229. Donaldson, L. W., Skrynnikov, N. R., Choy, W. Y., Muhandiram, D. R., Sarkar, B., Forman-Kay, J. D. & Kay, L. E. (2001). Structural characterization of proteins with an attached ATCUN motif by paramagnetic relaxation enhancement NMR spectroscopy. *Journal of the American Chemical Society* **123**, 9843-9847.
230. Clore, G. M. & Iwahara, J. (2009). Theory, practice, and applications of paramagnetic relaxation enhancement for the characterization of transient low-population states of biological macromolecules and their complexes. *Chem Rev* **109**, 4108-39.
231. Delaglio, F., Grzesiek, S., Vuister, G. W., Zhu, G., Pfeifer, J. & Bax, A. (1995). Nmrpipe - a Multidimensional Spectral Processing System Based on Unix Pipes. *Journal of Biomolecular Nmr* **6**, 277-293.
232. Goddard, T. D., Kneller, D. G. SPARKY 3.
233. Fawzi, N. L., Doucleff, M., Suh, J. Y. & Clore, G. M. (2010). Mechanistic details of a protein-protein association pathway revealed by paramagnetic relaxation enhancement titration measurements. *Proceedings of the National Academy of Sciences of the United States of America* **107**, 1379-1384.
234. Fitzkee, N. C., Masse, J. E., Shen, Y., Davies, D. R. & Bax, A. (2010). Solution Conformation and Dynamics of the HIV-1 Integrase Core Domain. *Journal of Biological Chemistry* **285**, 18072-18084.
235. Elzhov, T. M., Katharine M.; Spiess Andrej-Nikolai; Bolker, B. (2013). minpack.lm: R interface to the Levenberg-Marquardt nonlinear least-squares algorithm found in MINPACK, plus support for bounds.
236. Tang, J., Orlicky, S., Mittag, T., Willems, A., Chen, G., Mercurio, F., Shilton, B., Forman-Kay, J., Sicheri, F. & Tyers, M. (2007). SCF ubiquitin ligase mechanics: multisite substrate recognition and higher order structure. *Febs Journal* **274**, 4-4.
237. Marsh, J. A., Singh, V. K., Jia, Z. C. & Forman-Kay, J. D. (2006). Sensitivity of secondary structure propensities to sequence differences between alpha- and gamma-synuclein: Implications for fibrillation. *Protein Science* **15**, 2795-2804.

238. Ruckert, M. & Otting, G. (2000). Alignment of biological macromolecules in novel nonionic liquid crystalline media for NMR experiments. *Journal of the American Chemical Society* **122**, 7793-7797.
239. Ottiger, M., Delaglio, F., Marquardt, J. L., Tjandra, N. & Bax, A. (1998). Measurement of dipolar couplings for methylene and methyl sites in weakly oriented macromolecules and their use in structure determination. *Journal of Magnetic Resonance* **134**, 365-369.
240. Farrow, N. A., Muhandiram, R., Singer, A. U., Pascal, S. M., Kay, C. M., Gish, G., Shoelson, S. E., Pawson, T., Formankay, J. D. & Kay, L. E. (1994). Backbone Dynamics of a Free and a Phosphopeptide-Complexed Src Homology-2 Domain Studied by N-15 Nmr Relaxation. *Biochemistry* **33**, 5984-6003.
241. Moriarty, G. M., Minetti, C. A., Remeta, D. P. & Baum, J. (2014). A revised picture of the Cu(II)-alpha-synuclein complex: the role of N-terminal acetylation. *Biochemistry* **53**, 2815-7.
242. Horne, R. W. & Cockayne, D. J. H. (1991). Negative Staining. *Micron and Microscopica Acta* **22**, 319-319.
243. Altenbach, C., Marti, T., Khorana, H. G. & Hubbell, W. L. (1990). Transmembrane Protein-Structure - Spin Labeling of Bacteriorhodopsin Mutants. *Science* **248**, 1088-1092.
244. Poluektov, O. G., Utschig, L. M., Dalosto, S. & Thurnauer, M. C. (2003). Probing local dynamics of the photosynthetic bacterial reaction center with a cysteine specific spin label. *Journal of Physical Chemistry B* **107**, 6239-6244.
245. Berliner, L. J., Grunwald, J., Hankovszky, H. O. & Hideg, K. (1982). A Novel Reversible Thiol-Specific Spin Label - Papain Active-Site Labeling and Inhibition. *Analytical Biochemistry* **119**, 450-455.
246. Battiste, J. L. & Wagner, G. (2000). Utilization of site-directed spin labeling and high-resolution heteronuclear nuclear magnetic resonance for global fold determination of large proteins with limited nuclear overhauser effect data. *Biochemistry* **39**, 5355-5365.
247. Eliezer, D. (2012). Distance information for disordered proteins from NMR and ESR measurements using paramagnetic spin labels. *Methods Mol Biol* **895**, 127-38.
248. Koehler, J. & Meiler, J. (2011). Expanding the utility of NMR restraints with paramagnetic compounds: Background and practical aspects. *Progress in Nuclear Magnetic Resonance Spectroscopy* **59**, 360-389.
249. Tang, C., Ghirlando, R. & Clore, G. M. (2008). Visualization of transient ultra-weak protein self-association in solution using paramagnetic relaxation enhancement. *Journal of the American Chemical Society* **130**, 4048-4056.
250. Anthis, N. J. & Clore, M. (2011). Intrinsic Dynamics Prime Calmodulin for Peptide Binding: Characterizing Lowly Populated States by Paramagnetic Relaxation Enhancement. *Biophysical Journal* **100**, 604-604.
251. Bobko, A. A., Kirilyuk, I. A., Grigor'ev, I. A., Zweier, J. L. & Khramtsov, V. V. (2007). Reversible reduction of nitroxides to hydroxylamines: Roles for ascorbate and glutathione. *Free Radical Biology and Medicine* **42**, 404-412.
252. Iwahara, J., Tang, C. & Clore, G. M. (2007). Practical aspects of (1)H transverse paramagnetic relaxation enhancement measurements on macromolecules. *Journal of Magnetic Resonance* **184**, 185-195.
253. Silvestre-Ryan, J., Bertoncini, C. W., Fenwick, R. B., Esteban-Martin, S. & Salvatella, X. (2013). Average Conformations Determined from PRE Data Provide High-Resolution Maps of Transient Tertiary Interactions in Disordered Proteins. *Biophysical Journal* **104**, 1740-1751.

254. Marsh, J. A. & Forman-Kay, J. D. (2012). Ensemble modeling of protein disordered states: Experimental restraint contributions and validation. *Proteins-Structure Function and Bioinformatics* **80**, 556-572.
255. Ganguly, D. & Chen, J. H. (2009). Structural Interpretation of Paramagnetic Relaxation Enhancement-Derived Distances for Disordered Protein States. *Journal of Molecular Biology* **390**, 467-477.
256. Gillespie, J. R. & Shortle, D. (1997). Characterization of long-range structure in the denatured state of staphylococcal nuclease .2. Distance restraints from paramagnetic relaxation and calculation of an ensemble of structures. *Journal of Molecular Biology* **268**, 170-184.
257. Polevoda, B. & Sherman, F. (2002). The diversity of acetylated proteins. *Genome Biology* **3**, reviews0006.
258. Uversky, V. N., Li, J., Souillac, P., Millett, I. S., Doniach, S., Jakes, R., Goedert, M. & Fink, A. L. (2002). Biophysical properties of the synucleins and their propensities to fibrillate - Inhibition of alpha-synuclein assembly by beta- and gamma-synucleins. *Journal of Biological Chemistry* **277**, 11970-11978.
259. Yamin, G., Munishkina, L. A., Karymov, M. A., Lyubchenko, Y. L., Uversky, V. N. & Fink, A. L. (2005). Forcing nonamyloidogenic beta-synuclein to fibrillate. *Biochemistry* **44**, 9096-107.
260. Bertoncini, C. W., Rasia, R. M., Lamberto, G. R., Binolfi, A., Zweckstetter, M., Griesinger, C. & Fernandez, C. O. (2007). Structural characterization of the intrinsically unfolded protein beta-synuclein, a natural negative regulator of alpha-synuclein aggregation. *Journal of Molecular Biology* **372**, 708-22.
261. Maltsev, A. S., Ying, J. & Bax, A. (2012). Impact of N-terminal acetylation of α-synuclein on its random coil and lipid binding properties. *Biochemistry* **51**, 5004-13.
262. Spillantini, M. G., Schmidt, M. L., Lee, V. M. Y., Trojanowski, J. Q., Jakes, R. & Goedert, M. (1997). alpha-synuclein in Lewy bodies. *Nature* **388**, 839-840.
263. Goedert, M. (2001). Parkinson's disease and other alpha-synucleinopathies. *Clinical Chemistry and Laboratory Medicine* **39**, 308-312.
264. Nakajo, S., Shioda, S., Nakai, Y. & Nakaya, K. (1994). Localization of phosphoneuroprotein 14 (PNP 14) and its mRNA expression in rat brain determined by immunocytochemistry and in situ hybridization. *Brain Res Mol Brain Res* **27**, 81-6.
265. Fujita, M., Sekigawa, A., Sekiyama, K., Sugama, S. & Hashimoto, M. (2009). Neurotoxic conversion of beta-synuclein: a novel approach to generate a transgenic mouse model of synucleinopathies? *Journal of Neurology* **256 Suppl 3**, 286-92.
266. Masliah, E. & Hashimoto, M. (2002). Development of new treatments for Parkinson's disease in transgenic animal models: A role for beta-synuclein. *Neurotoxicology* **23**, 461-468.
267. Fan, Y., Limprasert, P., Murray, I. V., Smith, A. C., Lee, V. M., Trojanowski, J. Q., Sopher, B. L. & La Spada, A. R. (2006). Beta-synuclein modulates alpha-synuclein neurotoxicity by reducing alpha-synuclein protein expression. *Human Molecular Genetics* **15**, 3002-11.
268. Ferreon, A. C. M., Moosa, M. M., Gambin, Y. & Deniz, A. A. (2012). Counteracting chemical chaperone effects on the single-molecule alpha-synuclein structural landscape. *Proceedings of the National Academy of Sciences of the United States of America* **109**, 17826-17831.
269. Park, S. M., Jung, H. Y., Kim, T. D., Park, J. H., Yang, C. H. & Kim, J. (2002). Distinct roles of the N-terminal-binding domain and the C-terminal-solubilizing domain of alpha-synuclein, a molecular chaperone. *Journal of Biological Chemistry* **277**, 28512-28520.

270. Sung, Y. H. & Eliezer, D. (2006). Secondary structure and dynamics of micelle bound beta- and gamma-synuclein. *Protein Science* **15**, 1162-1174.
271. Fernandez, C. O., Hoyer, W., Zweckstetter, M., Jares-Erijman, E. A., Subramaniam, V., Griesinger, C. & Jovin, T. M. (2004). NMR of alpha-synuclein-polyamine complexes elucidates the mechanism and kinetics of induced aggregation. *Embo Journal* **23**, 2039-2046.
272. Meuvis, J., Gerard, M., Desender, L., Baekelandt, V. & Engelborghs, Y. (2010). The Conformation and the Aggregation Kinetics of alpha-Synuclein Depend on the Proline Residues in Its C-Terminal Region. *Biochemistry* **49**, 9345-9352.
273. McLean, P. J. & Hyman, B. T. (2002). An alternatively spliced form of rodent alpha-synuclein forms intracellular inclusions in vitro: role of the carboxy-terminus in alpha-synuclein aggregation. *Neuroscience Letters* **323**, 219-223.
274. Izawa, Y., Tateno, H., Kameda, H., Hirakawa, K., Hato, K., Yagi, H., Hongo, K., Mizobata, T. & Kawata, Y. (2012). Role of C-terminal negative charges and tyrosine residues in fibril formation of alpha-synuclein. *Brain and Behavior* **2**, 595-605.
275. Ulrih, N. P., Barry, C. H. & Fink, A. L. (2008). Impact of Tyr to Ala mutations on alpha-synuclein fibrillation and structural properties. *Biochimica Et Biophysica Acta-Molecular Basis of Disease* **1782**, 581-585.
276. Kang, L., Janowska, M. K., Moriarty, G. M. & Baum, J. (2013). Mechanistic insight into the relationship between N-terminal acetylation of alpha-synuclein and fibril formation rates by NMR and fluorescence. *Plos One* **8**, e75018.
277. Altschul, S. F., Madden, T. L., Schaffer, A. A., Zhang, J. H., Zhang, Z., Miller, W. & Lipman, D. J. (1997). Gapped BLAST and PSI-BLAST: a new generation of protein database search programs. *Nucleic Acids Research* **25**, 3389-3402.
278. Humphrey, W., Dalke, A. & Schulten, K. (1996). VMD: visual molecular dynamics. *J Mol Graph* **14**, 33-8, 27-8.
279. Case, D. A., Berryman, J. T., Betz, R. M., Cerutti, D. S., Cheatham, I. T. E., Darden, T. A., Duke, R. E., Giese, T. J., Gohlke, H., Goetz, A. H., Homeyer, N., Izadi, S., Janowski, P., Kaus, J., Kovalenko, A., Lee, T. S., LeGrand, S., Li, P., Luchko, T., Luo, R., Madej, B., Merz, K. M., Monard, G., Needham, P., Nguyen, H., Nguyen, H. T., Omelyan, I., Onufriev, A., Roe, D. R., Roitberg, A., Salomon-Ferrer, R., Simmerling, C. L., Smith, W., Swails, J., Walker, R. C., Wang, J., Wolf, R. M., Wu, X., M., Y. D. & Kollman, P. M. (2015). AMBER 2015. *University of California, San Francisco*.
280. Lovell, S. C., Davis, I. W., Adrendall, W. B., de Bakker, P. I. W., Word, J. M., Prisant, M. G., Richardson, J. S. & Richardson, D. C. (2003). Structure validation by C alpha geometry: phi,psi and C beta deviation. *Proteins-Structure Function and Genetics* **50**, 437-450.
281. Giasson, B. I., Murray, I. V. J., Trojanowski, J. Q. & Lee, V. M. Y. (2001). A hydrophobic stretch of 12 amino acid residues in the middle of alpha-synuclein is essential for filament assembly. *Journal of Biological Chemistry* **276**, 2380-2386.
282. Soto, C. (2003). Unfolding the role of protein misfolding in neurodegenerative diseases. *Nature Reviews Neuroscience* **4**, 49-60.
283. Uversky, V. N., Oldfield, C. J. & Dunker, A. K. (2008). Intrinsically disordered proteins in human diseases: Introducing the D(2) concept. *Annual Review of Biophysics* **37**, 215-246.
284. de Lau, L. M. & Breteler, M. M. (2006). Epidemiology of Parkinson's disease. *Lancet Neurology* **5**, 525-35.
285. Cooper, A. A., Gitler, A. D., Cashikar, A., Haynes, C. M., Hill, K. J., Bhullar, B., Liu, K., Xu, K., Strathearn, K. E., Liu, F., Cao, S., Caldwell, K. A., Caldwell, G. A., Marsischky, G., Kolodner, R. D., Labaer, J., Rochet, J. C., Bonini, N. M. & Lindquist, S. (2006). Alpha-

synuclein blocks ER-Golgi traffic and Rab1 rescues neuron loss in Parkinson's models. *Science* **313**, 324-8.

286. Burre, J., Sharma, M., Tsetsenis, T., Buchman, V., Etherton, M. R. & Sudhof, T. C. (2010). alpha-Synuclein Promotes SNARE-Complex Assembly in Vivo and in Vitro. *Science* **329**, 1663-1667.
287. Burre, J., Sharma, M. & Sudhof, T. C. (2014). alpha-Synuclein assembles into higher-order multimers upon membrane binding to promote SNARE complex formation. *Proc Natl Acad Sci U S A*.
288. Murphy, D. D., Rueter, S. M., Trojanowski, J. Q. & Lee, V. M. (2000). Synucleins are developmentally expressed, and alpha-synuclein regulates the size of the presynaptic vesicular pool in primary hippocampal neurons. *Journal of Neuroscience* **20**, 3214-20.
289. Wang, L., Das, U., Scott, D. A., Tang, Y., McLean, P. J. & Roy, S. (2014). alpha-Synuclein Multimers Cluster Synaptic Vesicles and Attenuate Recycling. *Current Biology*.
290. Jiang, Z., de Messieres, M. & Lee, J. C. (2013). Membrane remodeling by alpha-synuclein and effects on amyloid formation. *Journal of the American Chemical Society* **135**, 15970-3.
291. Varkey, J., Mizuno, N., Hegde, B. G., Cheng, N., Steven, A. C. & Langen, R. (2013). alpha-Synuclein oligomers with broken helical conformation form lipoprotein nanoparticles. *Journal of Biological Chemistry* **288**, 17620-30.
292. Meng, X. Y., Munishkina, L. A., Fink, A. L. & Uversky, V. N. (2009). Molecular Mechanisms Underlying the Flavonoid-Induced Inhibition of alpha-Synuclein Fibrillation. *Biochemistry* **48**, 8206-8224.
293. Rao, J. N., Dua, V. & Ulmer, T. S. (2008). Characterization of alpha-synuclein interactions with selected aggregation-inhibiting small molecules. *Biochemistry* **47**, 4651-6.
294. Lendel, C., Bertoncini, C. W., Cremades, N., Waudby, C. A., Vendruscolo, M., Dobson, C. M., Schenk, D., Christodoulou, J. & Toth, G. (2009). On the Mechanism of Nonspecific Inhibitors of Protein Aggregation: Dissecting the Interactions of alpha-Synuclein with Congo Red and Lacmoid. *Biochemistry* **48**, 8322-8334.
295. Horvath, I., Weise, C. F., Andersson, E. K., Chorell, E., Sellstedt, M., Bengtsson, C., Olofsson, A., Hultgren, S. J., Chapman, M., Wolf-Watz, M., Almqvist, F. & Wittung-Stafshede, P. (2012). Mechanisms of protein oligomerization: inhibitor of functional amyloids templates alpha-synuclein fibrillation. *Journal of the American Chemical Society* **134**, 3439-44.
296. Jones, D. R., Moussaud, S. & McLean, P. (2014). Targeting heat shock proteins to modulate alpha-synuclein toxicity. *Ther Adv Neurol Disord* **7**, 33-51.
297. Breydo, L., Wu, J. W. & Uversky, V. N. (2012). alpha-Synuclein misfolding and Parkinson's disease. *Biochimica Et Biophysica Acta-Molecular Basis of Disease* **1822**, 261-285.
298. Hashimoto, M., Bar-On, P., Ho, G., Takenouchi, T., Rockenstein, E., Crews, L. & Masliah, E. (2004). Beta-synuclein regulates Akt activity in neuronal cells. A possible mechanism for neuroprotection in Parkinson's disease. *Journal of Biological Chemistry* **279**, 23622-9.
299. Beyer, K., Ispierto, L., Latorre, P., Tolosa, E. & Ariza, A. (2011). Alpha- and beta-synuclein expression in Parkinson disease with and without dementia. *Journal of the Neurological Sciences* **310**, 112-117.
300. Rivers, R. C., Kumita, J. R., Tartaglia, G. G., Dedmon, M. M., Pawar, A., Vendruscolo, M., Dobson, C. M. & Christodoulou, J. (2008). Molecular determinants of the aggregation behavior of alpha- and beta-synuclein. *Protein Science* **17**, 887-898.

301. Sevcsik, E., Trexler, A. J., Dunn, J. M. & Rhoades, E. (2011). Allostery in a Disordered Protein: Oxidative Modifications to alpha-Synuclein Act Distally To Regulate Membrane Binding. *Journal of the American Chemical Society* **133**, 7152-7158.
302. Bertoncini, C. W., Rasia, R. M., Lamberto, G. R., Binolfi, A., Zweckstetter, M., Griesinger, C. & Fernandez, C. O. (2007). Structural characterization of the intrinsically unfolded protein beta-synuclein, a natural negative regulator of alpha-synuclein aggregation. *Journal of Molecular Biology* **372**, 708-722.
303. Bourhim, M., Kruzel, M., Srikrishnan, T. & Nicotera, T. (2007). Linear quantitation of Abeta aggregation using Thioflavin T: reduction in fibril formation by colostrinin. *J Neurosci Methods* **160**, 264-8.
304. Groenning, M., Norrman, M., Flink, J. M., van de Weert, M., Bukrinsky, J. T., Schluckebier, G. & Frokjaer, S. (2007). Binding mode of Thioflavin T in insulin amyloid fibrils. *Journal of Structural Biology* **159**, 483-97.
305. Peterson, D. W., Zhou, H. J., Dahlquist, F. W. & Lew, J. (2008). A soluble oligomer of tau associated with fiber formation analyzed by NMR. *Biochemistry* **47**, 7393-7404.
306. Vilar, M., Chou, H.-T., Luehrs, T., Maji, S. K., Riek-Loher, D., Verel, R., Manning, G., Stahlberg, H. & Riek, R. (2008). The fold of alpha-synuclein fibrils. *Proceedings of the National Academy of Sciences of the United States of America* **105**, 8637-8642.
307. Comellas, G., Lemkau, L. R., Nieuwkoop, A. J., Kloepper, K. D., Ladror, D. T., Ebisu, R., Woods, W. S., Lipton, A. S., George, J. M. & Rienstra, C. M. (2011). Structured Regions of alpha-Synuclein Fibrils Include the Early-Onset Parkinson's Disease Mutation Sites. *Journal of Molecular Biology* **411**, 881-895.
308. Karamanos, T. K., Kalverda, A. P., Thompson, G. S. & Radford, S. E. (2014). Visualization of Transient Protein-Protein Interactions that Promote or Inhibit Amyloid Assembly. *Molecular Cell* **55**, 214-226.
309. Marsh, J. A., Teichmann, S. A. & Forman-Kay, J. D. (2012). Probing the diverse landscape of protein flexibility and binding. *Current Opinion in Structural Biology* **22**, 643-650.
310. Sivanesam, K., Byrne, A., Bisaglia, M., Bubacco, L. & Andersen, N. (2015). Binding Interactions of Agents That Alter alpha-Synuclein Aggregation. *RSC Adv* **5**, 11577-11590.
311. Fonseca-Ornelas, L., Eisbach, S. E., Paulat, M., Giller, K., Fernandez, C. O., Outeiro, T. F., Becker, S. & Zweckstetter, M. (2014). Small molecule-mediated stabilization of vesicle-associated helical alpha-synuclein inhibits pathogenic misfolding and aggregation. *Nature Communications* **5**.
312. Guo, J. L. & Lee, V. M. Y. (2014). Cell-to-cell transmission of pathogenic proteins in neurodegenerative diseases. *Nature Medicine* **20**, 130-138.
313. Irwin, D. J., Lee, V. M. Y. & Trojanowski, J. Q. (2013). Parkinson's disease dementia: convergence of alpha-synuclein, tau and amyloid-beta pathologies. *Nature Reviews Neuroscience* **14**, 626-636.
314. Kurosinski, P., Guggisberg, M. & Gotz, J. (2002). Alzheimer's and Parkinson's disease - overlapping or synergistic pathologies? *Trends in Molecular Medicine* **8**, 3-5.
315. Haass, C. & Selkoe, D. J. (2007). Soluble protein oligomers in neurodegeneration: lessons from the Alzheimer's amyloid beta-peptide. *Nature Reviews Molecular Cell Biology* **8**, 101-112.
316. Cremades, N., Cohen, S. I. A., Chen, A. Y., Orte, A., Sandal, M., Clarke, R. W., Dunne, P., Aprile, F. A., Bertoncini, C. W., Knowles, T. P. J., Dobson, C. M. & Klenerman, D. (2011). Direct observation of the interconversion of normal and pathogenic forms of alpha-synuclein. *European Biophysics Journal with Biophysics Letters* **40**, 215-216.

317. Roberts, H. L. & Brown, D. R. (2015). Seeking a mechanism for the toxicity of oligomeric alpha-synuclein. *Biomolecules* **5**, 282-305.
318. Zhu, M., Han, S. B., Zhou, F. M., Carter, S. A. & Fink, A. L. (2004). Annular oligomeric amyloid intermediates observed by in situ atomic force microscopy. *Journal of Biological Chemistry* **279**, 24452-24459.
319. Hoyer, W., Antony, T., Cherny, D., Heim, G., Jovin, T. M. & Subramaniam, V. (2002). Dependence of alpha-synuclein aggregate morphology on solution conditions. *Journal of Molecular Biology* **322**, 383-393.
320. Gallea, J. I. & Celej, M. S. (2014). Structural insights into amyloid oligomers of the Parkinson disease related protein alpha-synuclein. *Journal of Biological Chemistry*.
321. Paslawski, W., Mysling, S., Thomsen, K., Jorgensen, T. J. D. & Otzen, D. E. (2014). Co-existence of Two Different alpha-Synuclein Oligomers with Different Core Structures Determined by Hydrogen/Deuterium Exchange Mass Spectrometry. *Angewandte Chemie-International Edition* **53**, 7560-7563.
322. Kaylor, J., Bodner, N., Edridge, S., Yamin, G., Hong, D. P. & Fink, A. L. (2005). Characterization of oligomeric intermediates in alpha-synuclein fibrillation: FRET studies of Y125W/Y133F/Y136F alpha-synuclein. *Journal of Molecular Biology* **353**, 357-372.
323. Taschenberger, G., Garrido, M., Tereshchenko, Y., Bahr, M., Zweckstetter, M. & Kugler, S. (2012). Aggregation of alpha Synuclein promotes progressive in vivo neurotoxicity in adult rat dopaminergic neurons. *Acta Neuropathologica* **123**, 671-683.
324. Wan, O. W. & Chung, K. K. K. (2012). The Role of Alpha-Synuclein Oligomerization and Aggregation in Cellular and Animal Models of Parkinson's Disease. *Plos One* **7**.
325. Colla, E., Jensen, P. H., Pletnikova, O., Troncoso, J. C., Glabe, C. & Lee, M. K. (2012). Accumulation of Toxic alpha-Synuclein Oligomer within Endoplasmic Reticulum Occurs in alpha-Synucleinopathy In Vivo. *Journal of Neuroscience* **32**, 3301-3305.
326. Lorenzen, N., Nielsen, S. B., Buell, A. K., Kaspersen, J. D., Arosio, P., Vad, B. S., Paslawski, W., Christiansen, G., Valnickova-Hansen, Z., Andreasen, M., Enghild, J. J., Pedersen, J. S., Dobson, C. M., Knowles, T. P. J. & Otzen, D. E. (2014). The Role of Stable alpha-Synuclein Oligomers in the Molecular Events Underlying Amyloid Formation. *Journal of the American Chemical Society* **136**, 3859-3868.
327. Zhou, W., Milder, J. B. & Freed, C. R. (2008). Transgenic mice overexpressing tyrosine-to-cysteine mutant human alpha-synuclein: a progressive neurodegenerative model of diffuse Lewy body disease. *J Biol Chem* **283**, 9863-70.